U-PB GEOCHRONOMETRY AND REGIONAL GEOLOGY OF THE SOUTHERN OKANAGAN VALLEY, BRITISH COLUMBIA: THE WESTERN BOUNDARY OF A METAMORPHIC CORE COMPLEX

by

DAVID LAMON PARKINSON

B.A. UNIVERSITY OF CALIFORNIA, SANTA BARBARA, 1981

A THESIS SUBMITTED IN PARTIAL FULFILMENT OF

THE REQUIREMENTS FOR THE DEGREE OF

MASTER OF SCIENCE

in

THE FACULTY OF GRADUATE STUDIES

Geological Sciences

We accept this thesis as conforming

to the required standard

THE UNIVERSITY OF BRITISH COLUMBIA

August, 1985

9c

In presenting this thesis in partial fulfilment of the requirements for an advanced degree at the The University of British Columbia, I agree that the Library shall make it freely available for reference and study. I further agree that permission for extensive copying of this thesis for scholarly purposes may be granted by the Head of my Department or by his or her representatives. It is understood that copying or publication of this thesis for financial gain shall not be allowed without my written permission.

Geological Sciences

The University of British Columbia
2075 Wesbrook Place
Vancouver, Canada
V6T 1W5

Date: August, 1985

ABSTRACT

The Okanagan Valley is the boundary between the Okanagan Metamorphic and Plutonic Complex of the Omenica Belt to the east and the Intermontane Belt to the west. The Okanagan Metamorphic and Plutonic Complex consists of greenschist to amphibolite grade paragneiss and large areas of massive, gneissic, and mylonitic granitic rock. The Intermontane Belt consists of tectonically scrambled late Paleozoic to Triassic eugeosynclinal rocks, intruded by large Jurassic plutons and locally by plutons of mid-Cretaceous age. These are overlain by Eocene non-marine volcanic and sedimentary rocks, capped by fanglomerate breccias and gravity slide megabreccias.

The thesis area contains all of these elements. In particular, the mid-Jurassic Oliver pluton is composed of three separate intrusive phases. The oldest phase is a heterogeneous biotite-hornblende diorite, which was intruded by the most extensive phase: a porphyritic biotite granite. The youngest phase is a garnet-muscovite granite. The intrusion of this last phase created the porphyritic biotite granite from an originally more mafic, hornblende bearing granodiorite. The mineralogy of the garnet-muscovite granite suggests that it might be of S-type. Several geochemical plots contradict this and suggests it is a highly evolved I-type magma.

Previous geochronometry indicates that the tectonic boundary between the Okanagan Metamorphic and Plutonic Complex and the Intermontane Belt separates: 1) gneisses on the east that consistantly yield K-Ar dates of 40-60 Ma, typically 51 Ma for hornblende and 48-50 Ma for biotite, from 2) intrusive rocks on the west that yield Jurassic K-Ar and Rb-Sr dates and Eocene volcanic rocks, erupted largely between 53 and 45 Ma.

U-Pb dating of zircons indicates the presence of early Jurassic to mid-Jurassic plutons both east (granite of Anarchist Mtn., 160Ma; gneiss of Osoyoos, 201Ma;

deformed) and west (Similkameen granodiorite, 170Ma; Olalla Syenite, 180–190Ma; undeformed) of the Okanagan Valley. East of the Okanagan Valley there are also mylonitic gneisses of Cretaceous age (gneiss of Skaha Lake, 105–120Ma; gneissic sill of Vaseaux Lake, 97Ma), as well as metamorphosed and deformed Eocene intrusives (Rhomb Porphyry, 51Ma). The interpretation is that, although there are Jurassic plutons and early Mesozoic deformation in both the Okanagan Metamorphic and Plutonic Complex and the Intermontane Belt, there are also Cretaceous and Tertiary intrusive bodies within the Okanagan Metamorphic and Plutonic Complex that have been highly deformed in late Cretaceous to early Tertiary time. Regional geochronometry summarized on time versus blocking temperature graphs emphasizes the large (10 km) and rapid (1–4 mm/yr) unroofing needed to bring the gneisses east of the Okanagan Valley to near surface temperatures in Eocene time. Field evidence for a low angle west dipping detachment fault (Okanagan Valley fault) which juxtaposes brittle disrupted Eocene and older rocks against unannealed mylonitic rocks with Eocene K–Ar dates justifies comparison of the Okanagan Metamorphic and Plutonic Complex with other Cordilleran metamorphic core complexes.

Table of Contents

LIST OF FIGURES AND PLATES vi
LIST OF TABLES viii

I. INTRODUCTION 1
Location of Study Area 1
Previous Field Work 3
Acknowledgements 5

II. REGIONAL GEOLOGIC SETTING 6
Okanagan Metamorphic and Plutonic Complex 6
Eugeosynclinal Formations of the Okanagan Valley Region 12
Plutonic Rocks West of the Okanagan Valley 16
Tertiary Formations 18

III. DESCRIPTION OF MAP UNITS/STRATIGRAPHY 22
Paragneisses 22
Leucogneiss 25
Cretaceous or Jurassic gniessic granitic rocks 28
Late Paleozoic–Triassic Eugeosynclinal Rocks 28
Oliver Pluton 29
Diorite 31
Porphyritic Biotite Granite 33
Garnet-Muscovite Granite 39
Discussion of Geochemistry 41
Eocene Strata 54
Eocene Dikes 55

IV. GEOCHRONOMETRY 61
Geochronometry - Previous Work 61
Geochronometry - This Study 78
West of the Okanagan Valley 78
Samples from the Okanagan Metamorphic and Plutonic Complex 82
Summary of Geochronometry 89
Discussion 90

V. STRUCTURE 94
Upper Plate 94
Okanagan Valley Fault and Related Fault Rocks 98
Lower Plate 102
Timing of Brittle and Ductile Deformation 108
Discussion and Regional Implications 109
Conclusions 111

VI. GEOLOGIC HISTORY OF THE SOUTHERN OKANAGAN REGION 113

REFERENCES CITED 116

APPENDIX A - WHOLE ROCK SAMPLE LOCALITIES AND DESCRIPTIONS 127

APPENDIX B - U-PB ANALYTICAL PROCEDURE AND DATA 128

APPENDIX C - RB/SR ANALYTICAL TECHNIQUES 149

LIST OF FIGURES AND PLATES

Figure 1: Location Map..2
Figure 2: Geologic Map and Legend...7
Figure 3: Outcrop of gneisses...9
Figure 4: Stereonet of poles to fractures................................19
Figure 5: Mylonitic gneisses...21
Figure 6: Foliated leucogneiss...24
Figure 7: Photomicrographs of leucogneiss................................27
Figure 8: Isoclinal fold in lPz-Tr.......................................30
Figure 9: Boudins in lPz-Tr..30
Figure 10: Agmatite..32
Figure 11: Contact between Jpgr and Jgr..................................32
Figure 12: Diorite...34
Figure 13: Pegmatitic Diorite..34
Figure 14: Photomicrograph of Diorite....................................35
Figure 15: General character of Jpgr.....................................35
Figure 16: Photomicrograph of Jpgr.......................................37
Figure 17: Photomicrograph of Jpgr.......................................37
Figure 18: Photomicrograph of Jpgr.......................................38
Figure 19: Photomicrograph of Jgr..38
Figure 20: Photomicrograph of Jgr..40
Figure 21: Major element variation diagram...............................42
Figure 22: AFM diagram...43
Figure 23: Normative Q-Or-Plag diagram...................................44
Figure 24: MgO vs CaO..45
Figure 25: Sr and Rb vs SiO_2..47
Figure 26: Zr and Ba vs SiO_2..50
Figure 27: Normative Q-Ab-Or...52
Figure 28: C and Di vs SiO_2...53
Figure 29: Molar $Al_2O_3/(CaO+Na_2O+K_2O)$ vs Rb/Sr......................56
Figure 30: Skaha Formation...57
Figure 31: Photomicrograph of Eocene dike................................57
Figure 32: Photomicrograph of Eocene dike................................59
Figure 33: Foliated, lineated rhomb porphyry.............................59
Figure 34: Photomicrographs of rhomb porphyry............................60
Figure 35: Location map for previous K-Ar dates..........................62
Figure 36: White Lake Basin Chronology...................................66
Figure 37: K-Ar histograms...67
Figure 38: Rb-Sr diagram for Osoyoos area plutons........................68
Figure 39: Rb-Sr diagram for leucogneiss.................................69
Figure 40: U-Pb location Map...70
Figure 41: Concordia diagram: 150-225 Ma.................................84
Figure 42: Photomicrograph of gneissic sill of Vaseaux Lake..............85
Figure 43: Concordia diagram: 25-150 Ma..................................87
Figure 44: U-Pb sample locality for gneiss of Skaha Lake.................85

Figure 45: Closure temperature vs time....................................91
Figure 46: Approximate uplift rates..92
Figure 47: Fractured Oliver pluton...95
Figure 48: Stereonet of poles to fractures and dikes.......................96
Figure 49: Low angle faults and fractures..................................97
Figure 50: Map of Mahoney Lake area..99
Figure 51: Photomicrographs of mylonitic pgn..............................101
Figure 52: Photomicrographs of brecciated mylonite.........................103
Figure 53: Photomicrographs of mylonites..................................104
Figure 54: Asymmetric fabric in rhomb porphyry.............................105
Figure 55: Stereonet of poles to foliations...............................107
Figure 56: Lineations in leucogneiss......................................107
Figure 57: Stereonet of lineations..110
Figure 58: Cross Section White Lake - Vaseaux Lake area...................112

PLATE 1...~~in pocket~~ See Special Collections

LIST OF TABLES

Table 1: Vaseaux Formation..11
Table 2: Structural succession from Ryan (1973).......................13
Table 3: Eugeosynclinal Formations....................................15
Table 4: Stratigraphy of White Lake Basin.............................17
Table 5: Whole Rock Chemistry...48
Table 6: Previous K-Ar data...63
Table 7: Previous and present study Rb-Sr data........................72
Table 8: Previous U-Pb data...79
Table 9: U-Pb data..80
Table 10: Structural elements in the Vaseaux Formation...............106

I. INTRODUCTION

This study focuses on the boundary between the Intermontane and Omineca Belts of the Canadian Cordillera. In southern British Columbia this boundary is coincident with the Okanagan Valley, east of which is the Okanagan Metamorphic and Plutonic Complex (Okulitch et al., 1977; Okulitch, 1984) of the Omineca Belt, and west of which are Carboniferous to Triassic eugeosynclinal formations, Jurassic intrusives and Eocene volcanic and sedimentary rocks of the Intermontane Belt.

The Okanagan Valley and adjacent uplands have been under geologic study for more than a century, and most recently the site of many University of British Columbia Ph.D. theses (Church, 1967; Okulitch, 1969; Christie, 1973; and Ryan, 1973). The purpose of the present study has been to map an area connecting these four thesis maps (Fig. 1), to study the Oliver pluton with its mixed S- and I-type characteristics, and to carry out a regional U-Pb geochronologic reconnaissance. The result is a geologic synthesis of the southern Okanagan Valley region.

Several conventions will be used throughout, these are: a) the time scale used is that of Palmer (1983); b) decay constants used for age calculations are from Steiger and Jager (1977); c) plutonic rock names are from Strekeisen (1976).

Location of Study Area

One reason for the continued geologic work in the Okanagan Valley is its accessibility. Highway 97 runs the length of the valley and is connected to Vancouver by Highway 3 at its southern end, near the U.S.-Canada border (Fig. 1), and by Highway 1 at its northern end, near Vernon. Within the study area there are many secondary or lower class roads.

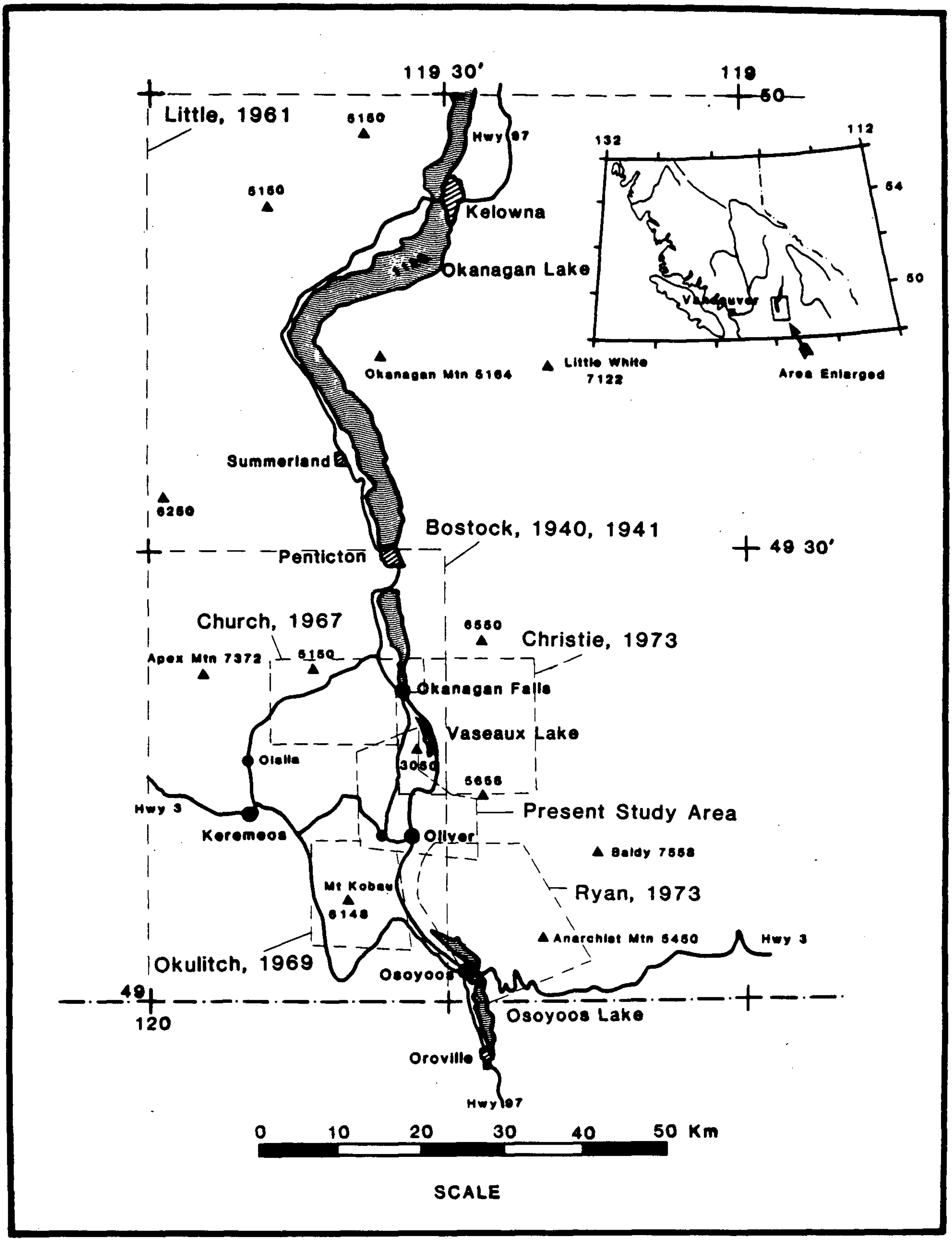

Figure 1: Location map of the study area; also shown are areas mapped for Ph.D. theses and by the G.S.C..

An area of 80 km^2 extending 12 km north, and 4 km east and west, of the town of Oliver (latitude 49° 11′, longitude 119° 33′) was mapped from June to August 1983. Mapping was done on 1:16,000 scale topographic maps enlarged from 1:50,000 NTS maps 82E/1,2,5,6 sheets, supplemented by air photographs (series 7580–82,7602 B.C. Ministry of Environment) and 1:5,000 scale topographic maps of series 72–6T (B.C. Ministry of Environment). Field observations were compiled onto a final 1:25,000 scale base (Plate 1).

Previous Field Work

Field work in the Okanagan Valley began in the 1860's with a reconnaissance by G.M. Dawson (1877). This work was followed by the International Boundary Survey (Daly, 1906 and 1912), and then by Brock (1934), who studied the metamorphic rocks of the southern Okanagan. The first systematic detailed mapping of the southern Okanagan Valley was done by Bostock from 1927–1930 (Maps 341A, 1940; 627A, 1941a; 628A, 1941b), and Cairnes in 1934 (Maps 37–21, 1937; 538A, 1947) for the Geological Survey of Canada. This work was revised and incorporated by H.W. Little in 1958–1959 in his map of the west half of the Kettle River Sheet (Map 15–1961) (Fig. 1). A new Geological Survey of Canada 1:250,000 scale map of the Penticton Sheet was begun in 1983 by D. Templeman-Kluit.

Metamorphic and plutonic rocks east of the Okanagan Valley were studied by J.V. Ross and his students (Ross, 1973, 1974, 1981; Ryan, 1973; Christie, 1973; Medford, 1975, 1973; Ross and Christie, 1979).

The abundant granitic rock in the Okanagan area was noted by Daly (1906), and by Brock (1934), who attributed metamorphism of the Shuswap rocks to the emplacement of these granitic bodies. Waters and Krauskopf's (1941) study of the Colville batholith, just south of the U.S.-Canada border, is the classic on protoclastic borders of granitic plutons. The Colville batholith has since been restudied and reinterpreted by Snook (1965), Fox et al. (1976), and Cheney (1980). Hibbard (1971) mapped a large area in northern Washington state, primarily within the plutonic granitic rocks of the Okanogan Range.

Work on granitic rocks north of the border has been directed to the west of Okanagan Valley. Petö (1973 and 1979) and Petö and Armstrong (1976) published papers on the petrology and geochronology of the Pennask Batholith. The Oliver pluton has been the subject of many U.B.C. B.Sc. theses because of its proximity to the U.B.C. field camp, and to its petrologic diversity (Matsen, 1960; Lammle, 1962; Cannon, 1966; Richards, 1968; Moore, 1970; Holtby, 1972). These were supervised by W.H. White and A.J. Sinclair and some results have been published (White et al., 1968; Sinclair, et al., 1983).

The Intermontane Belt lower grade rocks of Carboniferous–Permian to Triassic age have been the subject of two theses (Okulitch, 1969; Milford, 1984) (Fig. 1). Other work on these rocks include those by Ross and Barnes (1972), Barnes and Ross (1975) and Read and Okulitch (1977).

The Tertiary sedimentary and volcanic rocks of the White Lake Basin were studied by Church (1967) (Fig. 1). He has continued to work on these and other Tertiary outliers in and around the Okanagan Valley (Church, 1972, 1973, 1975, 1977, 1978, 1979a, 1979b, 1980a, 1980b, 1980c, 1980d, 1980e, 1981a, 1981b, 1982, 1985; Church and Johnson, 1978; Church et al., 1983). W.H. Mathews has investigated the relationship between the Tertiary volcanics and the underlying metamorphic rocks (Mathews, 1981).

Acknowledgements

The author would like to thank R. L. Armstrong, thesis supervisor, for providing support, supervision, advice and enthusiasm throughout the project.

Thanks are also due to R. Parrish for suggesting the map area and for continued guidance, insight, and enthusiasm. P. Van der Heyden, K. Scott and S. Horsky provided laboratory assistance. J. Mortensen is thanked for his guidance, and healthy dose of paranoia, in U-Pb techniques and interpretation. Assistance from members of the staff at the Department of Geology, University of British Columbia, most notably E. Montgomery, also merits recognition.

This study benefited greatly from discussions with R. Parrish, J. Mortensen, W. H. Mathews, J. Monger, D. Templeman-Kluit, J. Montgomery, J. Fillipone, J. Logan, I. Moffat, M. Bloodgood, L. Erdman, K. McColl, and R. Friedman.

Finally the writer would like to thank J. Rublee for patience and encouragement, and M. Stockton, F. Borah and M. Honer for unique insights, postcards and financing his education.

Natural Sciences and Engineering Research Council of Canada grant number 67-8841 to R. L. Armstrong provided support throughout the project.

II. REGIONAL GEOLOGIC SETTING

The rocks in the Southern Okanagan can be divided into four "packages": The Okanagan Metamorphic and Plutonic Complex, which is mainly east of the Okanagan Valley; late Paleozoic to Triassic eugeosynclinal formations found both east and west of the Okanagan Valley; undeformed Jurassic (and a few Cretaceous) plutons which occur mainly west of the Okanagan Valley; and finally Eocene sedimentary and volcanic rocks of White Lake Basin, also largely west of the Okanagan Valley (Fig. 2).

Okanagan Metamorphic and Plutonic Complex

The Okanagan Metamorphic and Plutonic Complex, in the southern Okanagan, consists primarily of granitic orthogneiss (K–Jg on Fig. 2); only locally does amphibolite–grade paragneiss predominate (pgn on Fig. 2). The best exposures of paragneiss are around Vaseaux Lake where they comprise the Vaseaux Formation defined by Bostock (1941a). These feldspathic gneisses, with minor mica schist, calc–silicate rocks and amphibolite, crop out over an area of 200 km^2. Throughout the Vaseaux Formation there are also voluminous discordant to concordant foliated granitic bodies (Fig. 3). The Vaseaux Formation is in fault contact everywhere along its northwest, west and southwest limits with rocks of the Intermontane Belt. To the northeast, east and southeast, the Vaseaux is in intrusive(?) contact with gneissic granites (Christie, 1973; Little, 1961). Christie (1973) defined five paragneiss units within the Vaseaux Formation, (Table 1) from structurally lowest numbered 1, to highest numbered 5. In addition he defined two intrusive units, designated A and B. (A sample of Christie's unit A, leucogneiss of this study, was collected for U–Pb analysis).

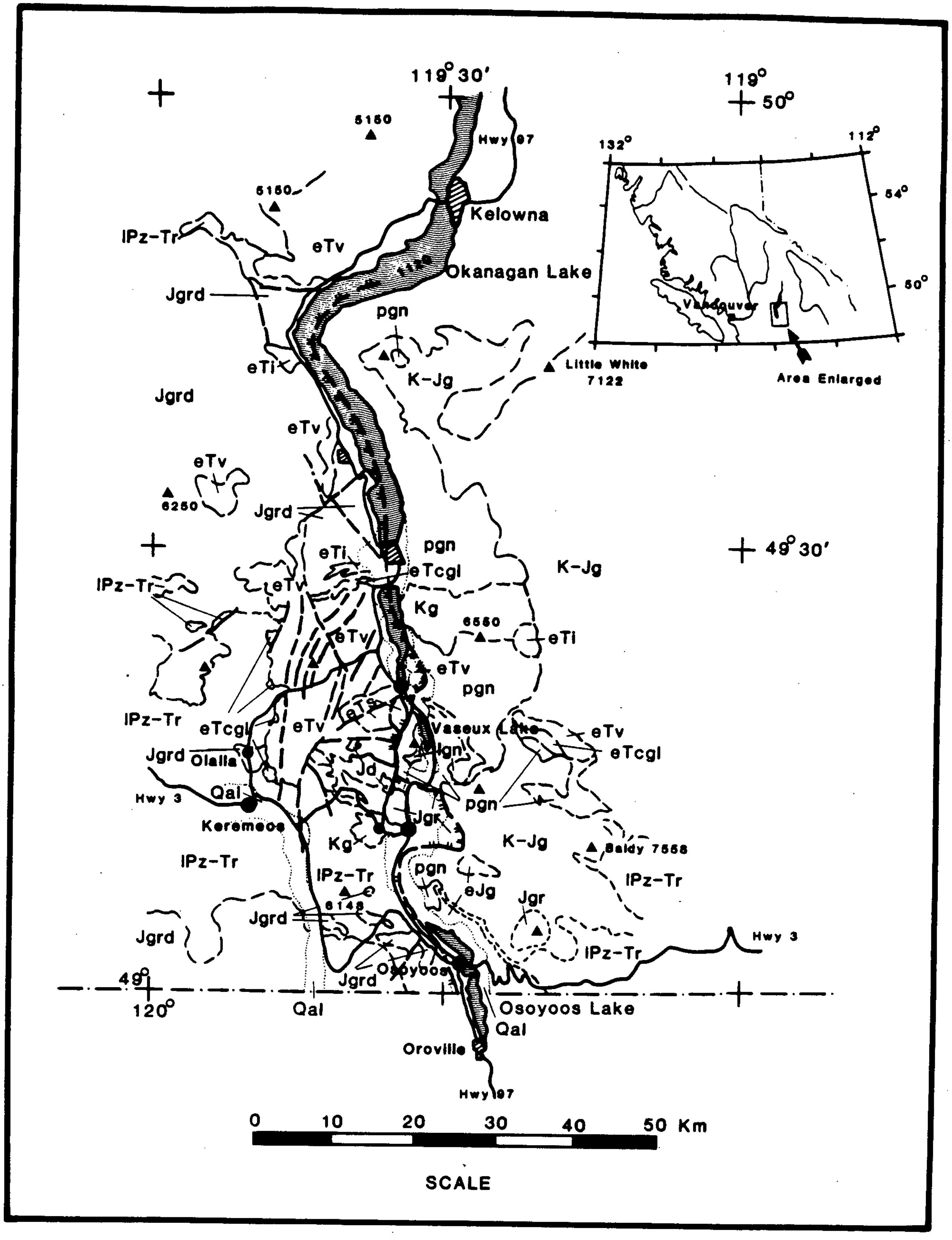

Figure 2: Geologic map and legend of the southern Okanagan area.

LEGEND

Stratified Rocks

	Qal	Alluvium
Tertiary	eTs	Eocene sediments; non-marine ss & shales
	eTcgl	Eocene conglomerate
	eTbr	Eocene breccia
	eTv	Eocene volcanic rocks; trachyte, dacite trachyandesite, andesite, basaltic andesite
late Paleozoic -Triassic	lPz-Tr	late Paleozoic-Triassic; greenstones, chert limestone, argillites, minor greywacke; includes: Old Tom, Shoemaker, Kobau, Anarchist, and Nicola formations
age uncertain	pgn	paragneiss; amphibolite, feldspathic gneiss, semipelitic gneiss, calc-silicates, marble, schist; locally with up to and more than 50% granitic injections

Intrusive Rocks

age uncertain	lgn	leucogneiss; concordant with foliation in surrounding pgn, possible J-K age
Tertiary	eTi	Eocene intrusive; syenitic to granitic
Cretaceous	Kg	Cretaceous intrusives; gneissic granodiorite of Skaha Lake, and possibly Fairview granodiorite
Cretaceous / Jurassic	K-Jg	Cretaceous or Jurassic (?) granodioritic to granitic gneiss; most highly deformed adjacent to Okanagan Valley
Jurassic	Jgrd,Jgr,Jd	Jurassic hb granodiorite (Similkameen batholith and probable satellites);Jurassic granite, foliated east of Okanagan Valley;Jurassic hb-bi diorite
	eJg	Early Jurassic granodioritic gneiss

Fault; known, assumed; hachure on upper plate

Contact; known, assumed

Figure 3: Photograph of outcrop of gneisses in roadcut on east shore of Vaseaux Lake, showing xenoliths of Vaseaux paragneiss in fóliated granitic gneiss.

Christie identified and described five phases of deformation. He interpreted the first three to be pre-mid-Pennsylvanian by structural correlation with the Kobau Formation (Okulitch, 1973). Unit A was interpreted by Christie to have been intruded during phase 2 deformation, and unit B during or prior to phase 3. He considered phases 4 and 5, namely very broad warping on two trends and vertical joints, to be of Tertiary age. The protolith for the Vaseaux Formation was inferred to be a sequence of greywacke, argillite, minor ultramafic rock, mafic volcanic rock, and minor limestone (Christie, 1973).

To the south, and east of Osoyoos Lake, Ryan (1973) studied paragneisses (Table 2) which he mapped as high-grade equivalents of, and traceable into, the Anarchist Group of the eugeosynclinal package east of the Okanagan Valley. Ryan also mapped five intrusive bodies, which display varying degrees of deformation. Five phases of deformation were identified, the first 3 interpreted as pre-mid-Pennsylvanian, based on structural correlation with Old Tom and Shoemaker formations (Ross and Barnes, 1972; Read and Okulitch, 1977), and the latter two as Tertiary. The earliest intrusive body (gneiss of Osoyoos; collected for U-Pb analysis) was interpreted by Ryan as being either pre- or syn-phase 1 deformation. Two of the remaining four intrusives were interpreted as post-phase 2 but pre-phase 3, a relatively late one as syn-phase 3 (Anarchist Mtn. granite; collected for U-Pb analysis) and the latest (the Oliver pluton; 152 Ma by U-Pb by R.L. Armstrong and B. Ryan, unpublished) as post-phase 3. Ryan's Rb-Sr work indicated that most intermediate and late intrusives were of Jurassic age. The Anarchist Group consists of greywacke, argillite, chert, mafic volcanic, and minor limestone; it contains lenses of ultramafic rock (Rinehart and Fox, 1972; Ryan, 1973). Krauskopf (1941) identified mid-Permian fossils from the middle and upper divisions of the Anarchist Group, as mapped in northern Washington (which continues north into Ryan's thesis area). Ryan chose to disregard the fossil and Rb-Sr data to reach his conclusions on the ages of the deformation based on structural

Table 1 - Description of Vaseaux Formation
(from Christie, 1973)

Unit B - Foliated and unfoliated syn-, to post-F_3 granitic intrusives.

Unit A - Syn-F_2 leucocratic granitic intrusive.

Unit 5 - Biotite granulite;
Hornblende granulites;
Amphibolite layers common.

——— Sheared Contact

Unit 4b- Laminated and massive amphibolites.

——— Sheared Contact

Unit 4a- Laminated amphibolites;
Basal granulites;
Minor impure quartzite, calc-silicate and marble.

——— Sheared Contact

Unit 3 - Semi-pelitic granulites, hornblende greater than biotite;
thin biotite schist layers.

——— Sheared Contact

Unit 2 - Biotite-muscovite schists with interlayered semi-pelitic granulite;
Minor marble, calc-silicate, quartzite.

——— Sheared Contact

Unit 1 - Biotite semi-pelitic granulite;
Biotite schist layers characteristic;
with associated ultramafic lenses.

correlations of the three early deformation episodes (using attitude, style, and ages assigned elsewhere by other workers).

Studies on granitic rocks within the Okanagan Metamorphic and Plutonic Complex generally have been related to structural geometry (Christie, 1973; Ryan, 1973; Medford, 1973). Little (1961) distinguished two major phases: Nelson type - generally more mafic and petrographically similar to the Nelson Batholith to the east, and Valhalla type - more felsic and younger than the Nelson intrusives. Recent work, east of the study area, in the Valhalla Dome (Parrish, 1984; Parrish et al., 1985) has shown that in the type area for the Valhalla Intrusives identified by Little, the rocks are in part Eocene in age. This suggests that regional petrologic correlations may be misleading.

Eugeosynclinal Formations of the Okanagan Valley Region

The eugeosynclinal rocks (lPz-Tr on Fig. 2) adjacent to the Okanagan Valley have various formation and group names (Table 3). Because of structural complexity, poor exposure, scarcity of fossils, and lack of distinctive stratigraphic horizons, no complete, or consistent stratigraphic picture has emerged.

Okulitch (1973) interpreted the highly deformed Kobau Formation to be pre-mid-Pennsylvanian on structural correlations with metamorphic rocks of the Okanagan Metamorphic and Plutonic Complex to the east, and on its relationship to the undeformed Blind Creek limestone to the north. The Blind Creek limestone was originally interpreted to be Upper Mississippian to Lower Permian in age (Barnes and Ross, 1975) but has since been reinterpreted as Late Triassic in age (Read and Okulitch, 1977). Ryan (1973) interpreted the Anarchist Group to be older than the Kobau and equivalent to the Vaseaux Formation on structural grounds. Both of these correlations disregard mid-Permian fossils identified from the Anarchist Group in

Table 2 - Description of Structural Succession
from an area east of Osoyoos
(B. Ryan, 1973)

Unit IX - Oliver pluton (unfoliated) post-F_3

Unit VIII - Garnet-biotite granite, syn-F_3;
(Anarchist Mtn. granite of this study).

Unit VII - Muscovite-biotite granite.

Unit VI - Biotite granite.

Unit V - Biotite-hornblende granodiorite, syn-, or pre-F_1.
(Osoyoos gneiss of this study).

Unit IV - Amphibolite.

Unit III - Pelite - argillite, phyllite, schist.

Unit II - Quartzite - probable metachert.

Unit I - Amphibolite - high grade area;
greenstone - low grade area.

northern Washington (Krauskopf, 1941). Rinehart and Fox, (1972), and Fox et al. (1977) have mapped both Anarchist and Kobau equivalents in northern Washington and have also concluded that the Anarchist Group is older and the Kobau Formation lies unconformably or disconformably upon Anarchist. Peatfield (1978) attempted to correlate eugeosynclinal formations between Rossland B.C. on the east and the Okanagan area. His correlations, at least those pertaining to the Okanagan area, follow Okulitch (1973).

Read and Okulitch (1977) documented a regional Triassic unconformity and also attempted a correlation of eugeosynclinal formations. This unconformity is exposed near Olalla, 20 km northwest of the study area. Read and Okulitch (1977) recognized there a pre–Late Triassic deformation that affected late Paleozoic rocks (Old Tom and Shoemaker Formations of Little, 1961). This deformed eugeosynclinal sequence (limestone pods, greenstone, ultramafic lenses, ribbon chert, and argillite) is overlain by relatively undeformed Upper Triassic Nicola Group equivalents (chert pebble conglomerate, bedded limestone, and siltstone). Milford (1984) has found fossils that show the Apex Mountain Group (formerly Old Tom and Shoemaker Formations) ranges in age from mid–Carboniferous on the east near Olalla to mid–Triassic on the west. This sequence was intruded by the Olalla Syenite, a zoned mafic alkalic complex (Sturdevant, 1963) (collected for U–Pb analysis by R.L. Armstrong), and Similkameen batholith to the south (Fox et al., 1977; collected for U–Pb analysis).

The lithologic similarity of these different formations (Kobau Formation, Anarchist Group, Apex Mountain Group) is noteworthy and, with the exception of intermediate volcanic rocks and greywackes in the Anarchist, they appear to be nearly identical. On this basis, and on lack of contradictory fossil evidence, these formations are, in the present report, lumped together as a single mid–Carboniferous to Triassic eugeosynclinal package. They represent a complex of marine basin environments (either ocean floor or interarc or back arc basin; Monger, 1977) that was deformed in Triassic time, then eroded, and subsequently overlain by the Late Triassic Nicola

Table 3 - Eugeosynclinal Formations

Late Triassic		<u>Nicola Group at Olalla</u> (Read and Okulitch, 1977) -massive limestone -chert granule limestone -chert breccia -minor sandstone -shale, limestone	
mid-Carboniferous to Early Triassic	<u>Apex Mtn. Group</u> (Milford, 1984) Formerly Old Tom and Shoemaker formations. -chert -greenstone -chert conglomerate -argillite -limestone	<u>Kobau Formation</u> (Okulitch, 1973) -chert -greenstone -argillite -limestone	<u>Anarchist Group</u> (Fox et al., 1977) -greenstone -chert conglomerate -chert -argillite -greywacke -limestone

Group (Read and Okulitch, 1977). This is admittedly a broad interpretation but based on existing data, or its inadequacy, little more can be said.

Plutonic Rocks West of the Okanagan Valley

Since the pioneering study of Daly (1912), petrologic work on granitic rocks in the southern Okanagan, north of the U.S.-Canada border, has been restricted to study of the Jurassic Pennask batholith (Jgrd on Fig. 2) between Princeton, Penticton and Kelowna (Petö, 1973, 1973a, 1974, and 1979; Petö and Armstrong, 1976). The Pennask batholith is zoned with mafic intrusives at the border and younger felsic intrusives more abundant towards the center. Petö argues, on chemical grounds, that the felsic intrusives could be derived from the mafic intrusives through magmatic differentiation (Petö, 1973) and that the chemical data is consistent with the interpretation that the mafic (and felsic differentiates) could be derived from partial fusion of the Triassic Nicola Group basalts (Petö, 1979). He argues against the batholith being derived from Shuswap gneisses of the Okanagan Metamorphic and Plutonic Complex to the east of Okanagan Lake on the basis of higher $^{87}Sr/^{86}Sr$ ratios in the gneisses (Petö and Armstrong, 1976). The wide range in ages makes a single magmatic series unlikely.

The other major batholith in the Southern Okanagan is the Similkameen (Jgrd on Fig. 2). Rinehart and Fox (1972) and Fox et al. (1976, 1977) have studied this complex in some detail in Washington. It is zoned from an older, mafic and alkalic border phase (Kruger Complex) to a more felsic core (Fox et al., 1977). K-Ar dates on Similkameen biotite and hornblende are discordant but the oldest K-Ar dates of 171 and 177 Ma are inferred to be the intrusive age (Engels et al., 1976).

Table 4 - Stratigraphy of White Lake Basin
(Church, 1973)

SHAHA FORMATION

Upper Member: Fanglomerate.

Lower Member: Slide breccias, some intercalated conglomerate and tephrite (augite porphyry).

WHITE LAKE FORMATION

Upper Member: Pyroclastic rocks, volcanic breccia, sedimentary rocks and tephrite.

Lower and Middle Members: Volcanic sandstone, conglomerate and some coal; feldspar porphyry lavas, lahars, pyroclasitc rocks.

MARAMA FORMATION

Rhyolite, rhyodacite, pyroclastics, basal conglomerate.

MARRON FORMATION

Park Rill Member: Merocrystalline and glassy andesite.

Nimpit Lake Member: Trachyte and trachyandesite lavas.

Kearns Creek Member: Pyroxene rich vesicular basaltic andesite lava.

Kitley Lake Member: Trachyte and trachyandesite lavas.

Yellow Lake Member: Anorthoclase lava, augite porphyry lavas, and pyroclastic rocks.

SPRINGBROOK FORMATION

Boulder conglomerate.

Tertiary Formations

The largest and best studied section of Tertiary rocks is the White Lake Basin section (Fig. 2). Church (1973) divided this section into five formations (Table 4). The following summary is taken from Church, (1973).

The maximum thickness of this section is 2400 m. Volcanic rocks comprise most of the lower half, and volcaniclastic to coarse clastic sediments comprise the upper half of the section. A relatively thin (0–60 m) conglomerate (Springbrook Formation) is the basal unit. This is followed by voluminous basaltic, andesitic, and trachyandesitic Marron Formation, deposited with slight angular unconformity upon the conglomerate. A second slight angular unconformity marks the base of the Marama Formation, composed of rhyodacite, rhyolite lava and pyroclastic rock and a basal conglomerate. The first significant angular unconformity marks the base of the White Lake Formation comprised of volcaniclastic to arkosic sediments, pyroclastic rocks, and rare lavas. The Skaha Formation overlies a second major angular unconformity. The Lower Skaha is mainly coarse conglomerate (fanglomerate) and megabreccias. These megabreccias include large (1 km^2), intact "rafted slabs" of Old Tom Formation, Shoemaker Formation, and granite – probably Oliver pluton (Church, 1973). The upper Skaha Formation is a poorly-bedded coarse conglomerate interpreted to be shed from a high terrain to the southeast. The clasts within this conglomerate are chert, greenstone, granite, arkose, Tertiary augite porphyry, and phyllite.

The rocks of White Lake Basin are folded, ruptured and ultimately become chaotic along the eastern boundary of the basin. Along the western border the lower units dip eastward only moderately (0–10°) but eastward and stratigraphically upward, the successive formations dip increasingly to the east. In addition, all formation boundaries are at least slight angular unconformities, becoming increasingly angular for younger formations. Normal faulting appears to have been active throughout deposition

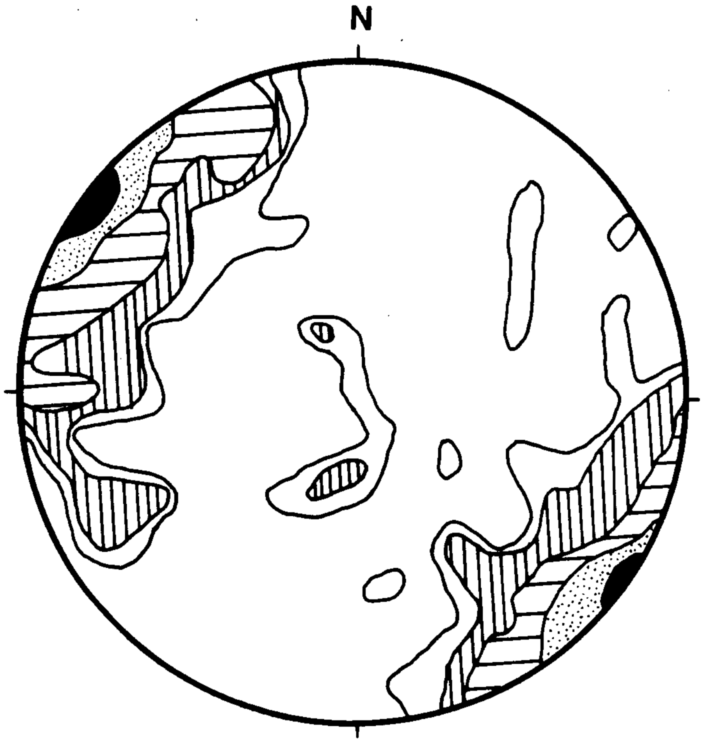

Figure 4: Stereonet of poles to fractures/cleavages from the eastern border of White Lake Basin (from Church, 1973); contour intervals are >7%, 5–7%, 2–5%, 1–2%, 0.5–1.0% and <0.5%.

of the basin but especially at the time of deposition of White Lake sediments, and culminating during deposition of Skaha Formation. Along the eastern boundary, where the deformation is greatest, Church did a detailed study of slickenside, and fracture orientation (Fig. 4), which shows that the predominant fracture/cleavage orientation is NNE, dipping steeply both west and east. The slickensides point to both normal – NW side down and slightly obliquely normal – NNW side down movement.

There are several known intrusives of Eocene age in the southern Okanagan. A few were described and dated by Armstrong and Petö (1981) and Medford et al. (1983). The Shingle Creek porphyry (Bostock, 1966) was dated by K–Ar as 52.4 Ma (Church, 1979b). These intrusives are calc–alkaline to alkaline, potassic, rhyolite to syenite. They are probably related to rhyolite in the Marama Formation (Church, 1973).

Figure 5: Photograph of outcrop of mylonitic gneisses on old railway cut west of Vaseaux Lake.

III. DESCRIPTION OF MAP UNITS/STRATIGRAPHY

Using the broad subdivision of rock types developed for the regional geology, the stratigraphy of the thesis area can be divided into four parts: metamorphic rocks of the Okanagan Metamorphic and Plutonic Complex (pgn and lgn); chert, limestone, minor argillite, greenstone, and greywacke of probable late Paleozoic to Triassic age (lPz–Tr); intrusive plutonic rocks of Jurassic age (Jgr, Jgrd, Jd); and Tertiary volcanic, sedimentary, and intrusive rocks (eTv, eTs, eTd). This section will deal with distribution, relationship to other units, lithology, chemical composition of the intrusive units, and finally age and correlations (Plate 1).

Paragneisses (pgn)

As mentioned in the previous chapter the paragneisses within the study area were named the Vaseaux Formation by Bostock (1941a). They were studied structurally by Christie (1973) who defined five lithologic units in a structural succession (Table 1). In the present study these were grouped into one unit - pgn. The area of pgn mapped extends from Mahoney Lake in the west to the cliffs west of Vaseaux Lake in the east, and from Covert Farms in the south to Green Lake in the north. Unit pgn has been intruded by unit lgn, but is in low–angle fault contact with all adjacent map units (lPz–Tr, eTv, eTs, Jd and Jpgr) to the west.

Within the study area the paragneisses are predominantly banded to massive amphibolite and biotite– or hornblende–plagioclase gneiss with minor mica schist and rare calc–silicate and diopside marble lenses.

The amphibolites range in mineralogy from biotite–plagioclase–hornblende to plagioclase–hornblende amphibolites, both contain garnet. The grain size is also variable from fine (0.5–1 mm) to medium (2–4 mm). These rocks predominate in the mapped area of pgn and are more abundant in the western and northern half of pgn exposure. Schist is subordinate to amphibolite and tends to follow the outline of the leucogneiss (lgn) body which is interpreted by Christie (1973) as intruding the core of a phase 2 antiform. Minor and discontinuous pods of calc–silicate and diopside marble are found within the schist unit.

The schist consists predominantly of biotite, quartz, plagioclase, and garnet, but muscovite is commonly present "in highly sheared portions of the unit" (Christie, 1973). The schist is also interlayered with what Christie (1973) has called semi–pelitic granulite or simply biotite–quartz–feldspar gneiss. Gneissic granitic sheets or sills are common as lit–par–lit injections into the schist and amphibolite. Studying the metamorphic grade of these gneisses is, as stated by Christie, unrewarding, mainly because of lack of variation of mineral assemblages within the area. Most of the area is at the same metamorphic grade: middle to upper amphibolite facies. Christie (1973) states that sillimanite is only locally developed at the contacts with intrusive granitic bodies.

The paragneisses have a well developed foliation which dips gently westward. Throughout the pgn unit variable shear is evident, with locally developed mylonitic fabrics (Fig. 5). The amount of mylonite within pgn generally increases structurally and topographically upward and is most intensely developed directly below eTv and eTs at Mahoney Lake. Also at this locality are exposures of very siliceous mylonites and banded quartzites (metachert?). At high structural and topographic levels (again in particular at Mahoney Lake but continuing southward from there to Meyers Flat) the paragneisses are increasingly altered to chlorite and epidote with very late pyrite. This chlorite alteration is both synchronous with the latest mylonites (epidote and chlorite deformed in highest level mylonites) as well as post–mylonite (pyrite cubes and chlorite breccias with mylonite clasts). These structurally highest zones of mylonite and

Figure 6: Photograph of foliated leucogneiss, from north of Covert Farms.

associated chlorite alteration are spatially related to fault breccias, also chloritized , and faulted eTv and eTs. The contact between these Tertiary units and underlying mylonitic pgn has been mapped in the present study as a low-angle (10°-20°) west-dipping fault zone.

The stratigraphy of the paragneisses is not distinctive enough to make any lithologic correlations. The age of the paragneisses is only known to be older than Jurassic (based on Rb-Sr data of Armstrong on lgn). The abundance of amphibolite, and associated metamorphosed ultramafics (and lack of quartzite or well bedded, continuous carbonate) suggests to the author that these gneisses can be correlated with the lower grade Anarchist Group, Kobau Group, and Apex Mountain Group found locally. Ryan (1973), working east of Osoyoos, traced greenschist grade Anarchist Group rocks northward into amphibolite grade paragneisses which are identical to, but not continuous with, paragneisses in the Vaseaux area. Whole-rock Rb-Sr dating of schists within the Vaseaux Formation, in contrast, suggests a Precambrian age (Ryan and Armstrong, unpublished).

Leucogneiss (lgn)

Within the pgn unit, and containing all but the earliest fabric present in the pgn, is a granitic intrusion: leucogneiss. At the southwestern end of exposure of lgn near Covert Farms it is easily demonstrated that the lgn/pgn contact is intrusive. This contact is commonly marked by leucocratic pegmatite and the intrusive body is here (Covert Farms area) relatively leucocratic (hence the name). This intrusion is now sill-like with respect to the foliation and compositional layering in pgn. The lgn unit can be easily traced on both sides of Vaseaux Lake and defines a broad, domal structure (phases 4 and 5 of Christie, 1973) within the metamorphic complex. Farther to the north and east, across Okanagan Valley, this unit becomes richer in biotite.

The overall textural character of the lgn unit is variable and ranges from weak development of gneissic foliation (Fig. 6) to well developed horizons of lineated and foliated mylonite. Overall the body is a homogeneous biotite granite to granodiorite with lighter colored pegmatitic borders. The large volume of small granitic sills within the pgn unit are both texturally and lithologically similar to lgn, and apparently are injections from this intrusive.

The lgn unit is a medium-grained equigranular biotite granodiorite. In thin section quartz is ubiquitously strained, variably recrystallized, and elongated parallel to the foliation. Plagioclase and K-feldspar are rounded and commonly broken due to deformation (Fig. 7). The plagioclase (An_{5-10}) (all plagioclase compositions determined optically) is commonly zoned (normal to complex). The only mafic mineral is biotite (or chlorite after biotite) which defines the foliation and is generally intergranular to plagioclase and K-feldspar, rarely occuring as inclusions in K-feldspar. The pegmatitic and most leucocratic phases contain muscovite, gray quartz, white plagioclase, potassium feldspar, and red garnet. At the structurally uppermost exposures of the leucogneiss it is commonly altered: chloritized biotite, minor epidote, and allanite.

The age and correlation of lgn are debatable. U-Pb results are ambiguous. The interpretation, although not unique, is that the leucogneiss was intruded in the Jurassic and has since been subjected to a later event(s) of Cretaceous or younger age. Part of the reason for suggesting a Jurassic intrusive age is that there are no known older plutons in the southern Okanagan area. In addition a whole-rock Rb-Sr errorchron (Armstrong, unpublished) based on a fairly large sample suite is Jurassic - likely a maximum age.

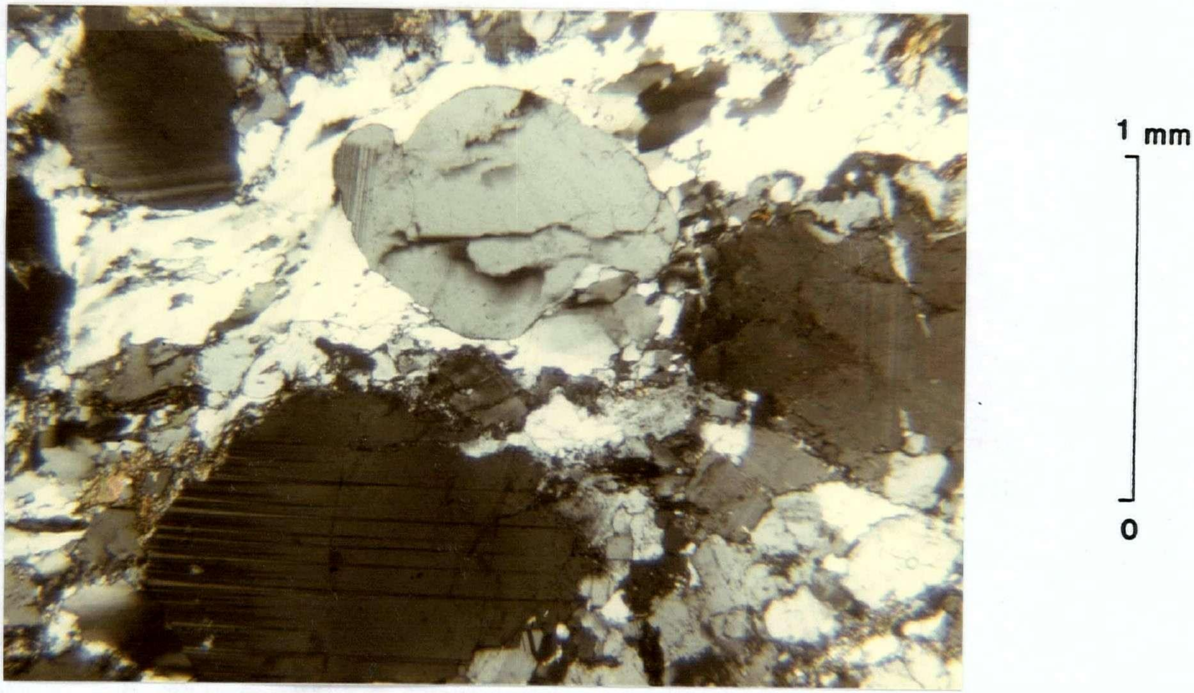

Figure 7: Photomicrograph of leucogneiss showing extensive deformation.

Cretaceous or Jurassic gneissic granitic rocks (K-Jgr)

Foliated and lineated granitic rocks were mapped on the southeastern margin of the study area. Christie (1973) mapped this as his unit B, and Ryan (1973) as his units VI and VII. Little (1961) mapped this unit as continuous with much of the granitic rocks to the east. This unit is in the footwall of the Okanagan Valley fault which is its western boundary. K-Jgr comprises only a minor portion of the study area and therefore was not examined in any detail. Its composition is biotite granodiorite to quartz monzonite. The presence or absence of K-feldspar porphyroclasts is the main variation within this unit.

Both Christie and Ryan interpreted this unit to have intruded post F_2 and pre- or syn-F_3, although the trend of the lineations for both of these phases is coaxial. Little correlated, on the basis of petrology, the K-Jgr with Valhalla intrusives to the east. The only age determination on this unit is a K-Ar biotite date of 56 Ma (Armstrong and Mathews, unpublished), which more than likely represents thermal resetting.

Late Paleozoic-Triassic Eugeosynclinal Rocks (lPz-Tr)

Exposures of lPz-Tr are restricted to south and north of the Oliver pluton along the western margin of the field area. This unit is in fault contact to the north with the Tertiary White Lake Basin sequence (Bostock, 1941a; Little, 1961) and in partial fault contact with dioritic rocks of the northern Oliver pluton. The southern contact of the Oliver pluton is intrusive into the Kobau Formation, and at the upper reaches of Orofino Creek the Oliver pluton again appears to have intruded lPz-Tr.

Because this unit is sporadically exposed, as well as lacking any distinctive or continuous stratigraphy, only the bounding structures were mapped. No attempt was made to decipher its internal structure, although this is known to be complex (Fig. 8; Okulitch, 1973). This unit is composed of chert or metachert, greenstone, carbonate, and minor greywacke.

The metachert ranges from 90 to 98 percent quartz with very rare plagioclase, and rare to common biotite, white mica, and chlorite. The texture of the quartz is also variable, with the development of both 120° and sutured grain boundaries. The grain size is generally fine (0.5 mm or less) but ranges to medium (0.5–1 mm).

Carbonates are discontinuous along strike and are commonly found as pods: 10 meters or less in strike length and, 5 meters or less in thickness. Locally these carbonate pods are metamorphosed to calc-silicates adjacent to the Oliver pluton, and show extensive deformation (Fig. 9).

The greywacke is restricted to the northeasternmost exposures of the map area. It is fault bounded. The greywacke is an immature, medium grained, well-sorted sediment with angular clasts of mono-crystalline quartz, plagioclase, and K-feldspar.

Oliver Pluton (Jd, Jpgr, Jgr)

The Oliver pluton is a composite, very heterogeneous intrusive body. The heterogeneity is defined by both compositional differences and textural variations between three distinct phases. The northern third of the pluton is predominantly diorite, becoming agmatitic southward towards the contact with the main body of porphyritic biotite granite. This biotite granite is in turn intruded by a garnet-muscovite granite. The pluton is not neatly concentrically zoned but there is a mafic outer zone and a felsic core. Three distinct magmatic intrusive episodes are inferred but they are not necessarily separated by long time periods.

The outer contact relationships of the Oliver pluton vary considerably. As stated in the previous section intrusive contacts into lPz-Tr unit are found on the southern

Figure 8: Photograph of isoclinal fold in chert unit of lPz–Tr.

Figure 9: Photograph of calc–silicate boudins in lPz–Tr unit.

border of the Oliver. Contacts to the north with lPz–Tr, to the northeast with pgn, and to the east with gneissic granite have all been mapped as faults. Nowhere can the Oliver pluton be seen to intrude the metamorphic rocks to the east. The internal contacts between the three phases vary from a broad agmatitic zone between Jd and Jpgr (Fig. 10) to a knife sharp contact between Jpgr and Jgr (Fig. 11).

The three phases (Jd, Jpgr, Jgr) will be described in order of decreasing relative age.

Diorite (Jd)

The dioritic phase of the northern third of the Oliver pluton is also exposed on the western edge of the map area, west of Burnell Lake (Plate 1). The diorite is observed in various stages of disaggregation and assimilation (Fig. 12) in a broad agmatitic zone at the contact with the porphyritic biotite granite. This assimilation is the cause for the porphyritic biotite granite being more mafic adjacent to and within this agmatite zone. There are various types of agmatite: angular, rounded, and sheared; mostly diorite, or mostly granitic.

Near its northern contact the diorite becomes increasingly foliated. Just north of Orofino Creek highly deformed, mylonitic, metasediments of lPz–Tr are exposed. Northward in the metasediments this deformation decreases. These observations suggest that this contact is a fault, dipping gently ($<30^\circ$) to the north.

The presence of a large inclusion of lPz–Tr within the diorite is evidence that the diorite does in fact intrude the metasediments. Supporting evidence is the development of higher-grade calc-silicates adjacent to the diorite in the northwestern part of the area.

Internally the diorite is extremely heterogeneous. It is difficult to discern how much of this heterogeneity is original and how much is superimposed by the later

Figure 10: Photograph of agmatite defining border between Jpgr and Jd.

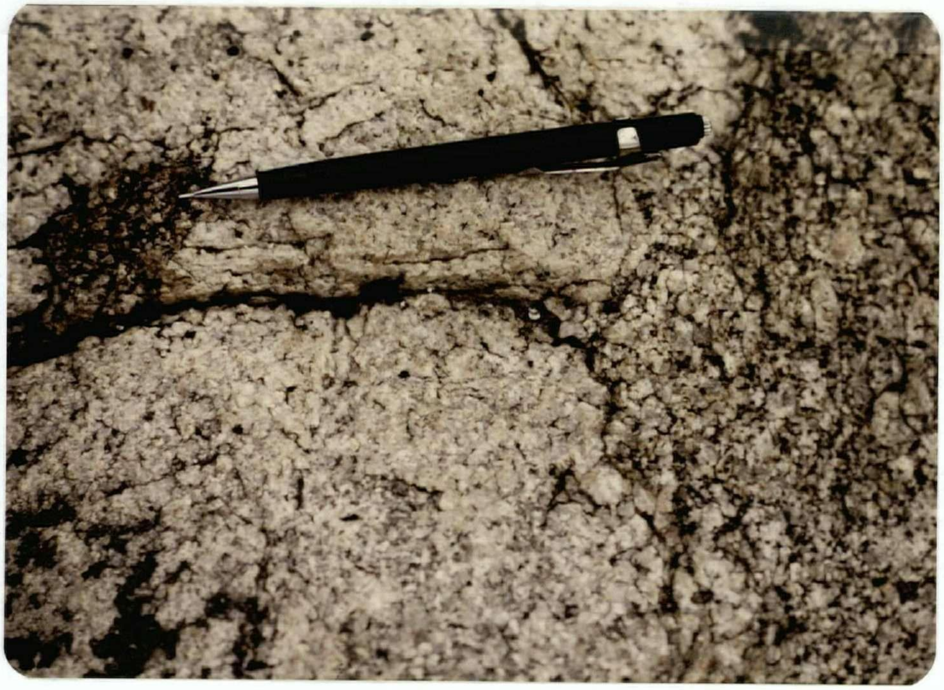

Figure 11: Photograph of sharp contact between Jpgr (on right) and Jgr (on left).

intrusion of Jpgr and Jgr. Texturally the diorite ranges from agmatite to gneiss. Within a single outcrop grain size ranges from fine and medium to pegmatitic (Fig. 13).

Hornblende diorite is the most comon composition but can change within meters, to biotite diorite. This heterogeneity may be original or superimposed. In thin section the diorite is variably but ubiquitously altered with the development of chlorite, epidote, and sericite. Hornblende is invariably euhedral, plagioclase (An_{35-45}) ranges from euhedral, in plagioclase rich samples, to anhedral and interstitial in rocks which contain 80 percent or more hornblende (Fig. 14). Biotite content ranges from zero to generally about 10 percent and rarely reaches 40 percent. Opaques are common and are in part secondary pyrite.

The age, based on field relationships, is well bracketed between Triassic (youngest age of lPz–Tr unit that it intrudes) and mid–Jurassic (age of Jgr that intrudes it). The origin and correlation is more of a problem. It may be an intrusive equivalent to Late Triassic Nicola volcanic rocks. More likely, it represents an early mafic phase of the Early to Mid–Jurassic intrusions.

Porphyritic Biotite Granite (Jpgr)

The main phase of the Oliver pluton is a porphyritic K–feldspar granite (Fig. 15). This phase clearly intruded the diorite. The Jpgr also intruded lPz–Tr along the southern border of the pluton and is itself intruded by Jgr in the central part of the map area, northwest of the town of Oliver. A west–dipping low angle fault is the contact between the gneissic granites of the Okanagan Metamorphic and Plutonic Complex, to the east, and Jpgr.

The mineralogy of the Jpgr is consistently biotite–plagioclase (An_{20}) –quartz–porhyritic K–feldspar (1 cm). Biotite is the main mafic mineral and, for most of the area, the only original one present. The southern border of the Jpgr, the only

Figure 12: Photograph of diorite in various stages of assimilation.

Figure 13: Photograph of pegmatitc Jd.

Figure 14: Photomicrographs of Jd, showing euhedral hornblende and subhedral to anhedral plagioclase.

Figure 15: Photograph showing the general character of Jpgr unit.

area where hornblende is identified as a component (Fig. 16), is more mafic. In addition the biotites display a deep brown pleochroism and striking pleochroic haloes (Fig. 17). Elsewhere in the Jpgr the biotites are green and show very small or no pleochroic haloes (Fig. 18). In the southern exposures plagioclase (25 percent, An_{25}) is euhedral to subhedral and lath shaped; K-feldspar (25 percent, microcline microperthite) is not as porphyritic as elsewhere in this unit but is still coarse (0.5 cm); quartz (25 percent) is anhedral and strained but not recrystallized - as it very commonly is elsewhere in the unit. Sphene, zircon, and apatite are accessory minerals, the latter two being responsible for the well-developed pleochroic haloes in biotite. This mineralogy puts the southern part of the Jpgr unit (in Strekeisens, 1976 IUGS classification) on the border between granodiorite and granite. The alteration in the southern Jpgr is limited to minor saussurite development in plagioclase, minor chlorite and epidote. The majority of Jpgr exposures lack hornblende and contain chlorite, epidote, saussurite/white mica$\pm$calcite as common alteration products - locally making up to 5-10 percent of the rock.

The rocks with green biotite + alteration products are interpreted to be an altered equivalent of the hornblende-biotite granite exposed in the southern part of the Jpgr. This alteration is spatially related to the later intruding Jgr, which is more felsic, potassic and sodic.

Another explanation for the mafic character of the southern border of the Oliver was proposed by Richards (1968). He called on the assimilation of Kobau formation as the cause. Lack of Kobau Formation inclusions along this contact and the unsuitable composition of the Kobau (chert, limestone, and rare greenstone) argue against this hypothesis. For the Jpgr unit as a whole, it appears that alteration of an original hornblende-biotite granite/granodiorite to a biotite granite by the later intruding Jgr is the most satisfactory explanation for the limited preservation of hornblende.

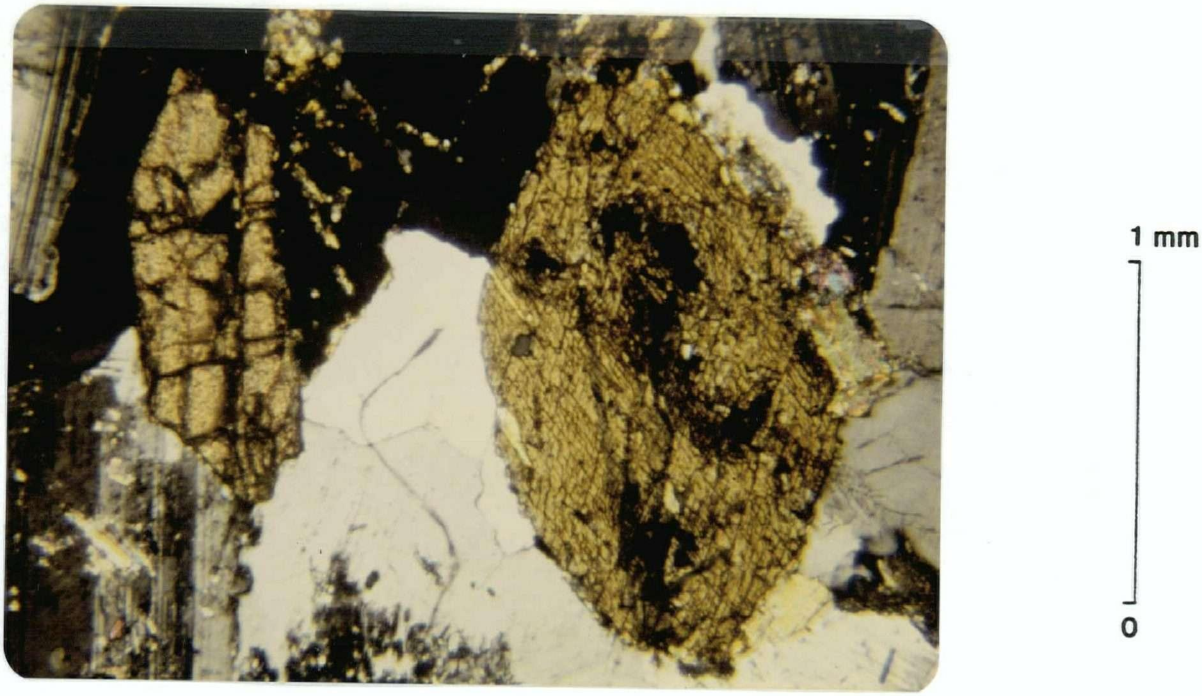

Figure 16: Photomicrograph of hornblende in southern Jpgr.

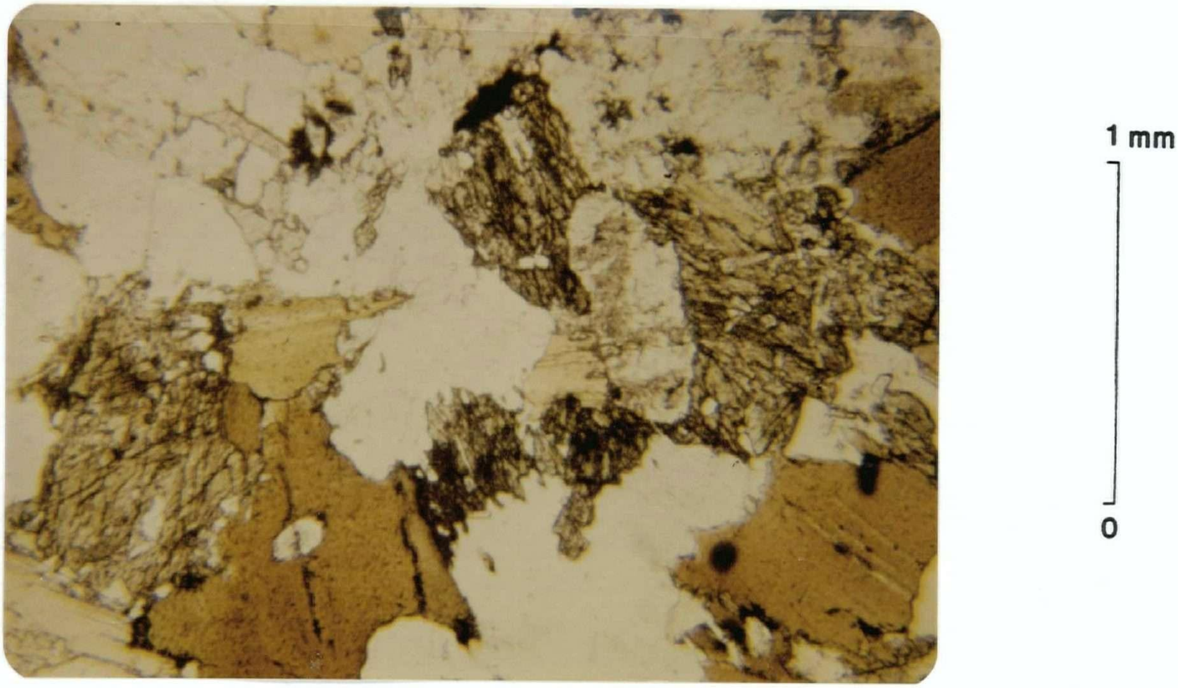

Figure 17: Photomicrograph of brown biotite from southern Jpgr, with pleochroic haloes.

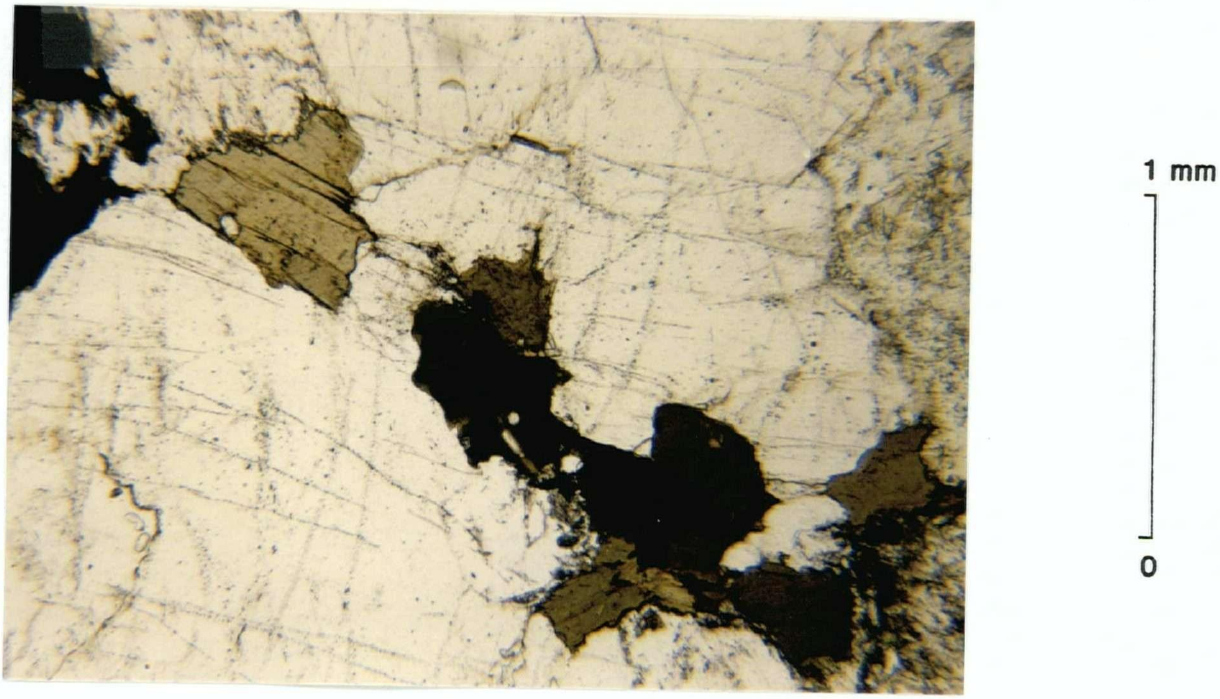

Figure 18: Photomicrograph of altered Jpgr showing green biotite.

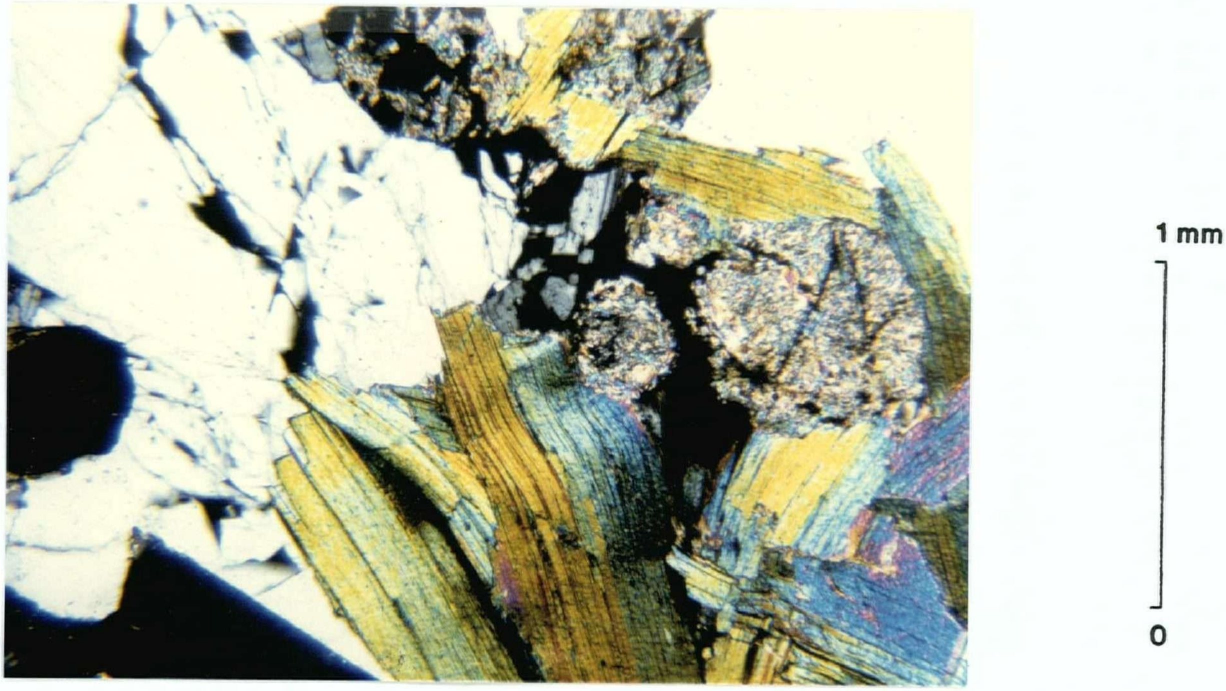

Figure 19: Photomicrograph of Jgr muscovite, and altered garnets.

The Jpgr unit is older than Jgr unit, which gives a 152 Ma concordant U–Pb zircon date (Ryan and Armstrong, unpublished), and younger than the lPz–Tr unit which it intrudes.

Garnet-Muscovite Granite (Jgr)

The youngest phase of the Oliver pluton is a leucocratic garnet–muscovite granite. Sharp intrusive contacts are observed with the Jpgr unit. The Jgr is the least voluminous of the three phases. It is restricted to an exposure with the shape of a large half circle, northwest of the town of Oliver. The only other exposures are small circular outcrops, two of which are of mappable scale. The field exposures, and contact relationships suggest a very viscous, nearly solid intrusion. The highly felsic nature of this unit supports this interpretation. The only rocks that cut the Jgr are Eocene rhomb porphyry and lamprophere dikes.

The Jgr unit is extremely homogeneous. It does not change texturally or lithologically across its exposure. The only variability is amount of manganese stain along fractures.

The mineralogy of the granite is plagioclase (An_{0-2}) = quartz = K–feldspar (microcline, with minor microperthite) > muscovite > garnet (Fig. 19). The quartz, plagioclase, and K–feldspar are equigranular and give the unit its characteristic gray–white color. The muscovite is magmatic, and euhedral (Fig. 19) (Best et al, 1974; Anderson and Rowley, 1981; Miller et al., 1981) The garnet is red in hand specimen and commonly 0.2 mm in size. Garnets range from nearly euhedral with minor alteration or reaction rims to completely replaced by white mica pseudomorphs (Fig. 20).

This unit has given a concordant U–Pb zircon date of 152± 3 Ma and a Rb–Sr whole rock date of 157± 8 Ma (Armstrong and Ryan, unpublished).

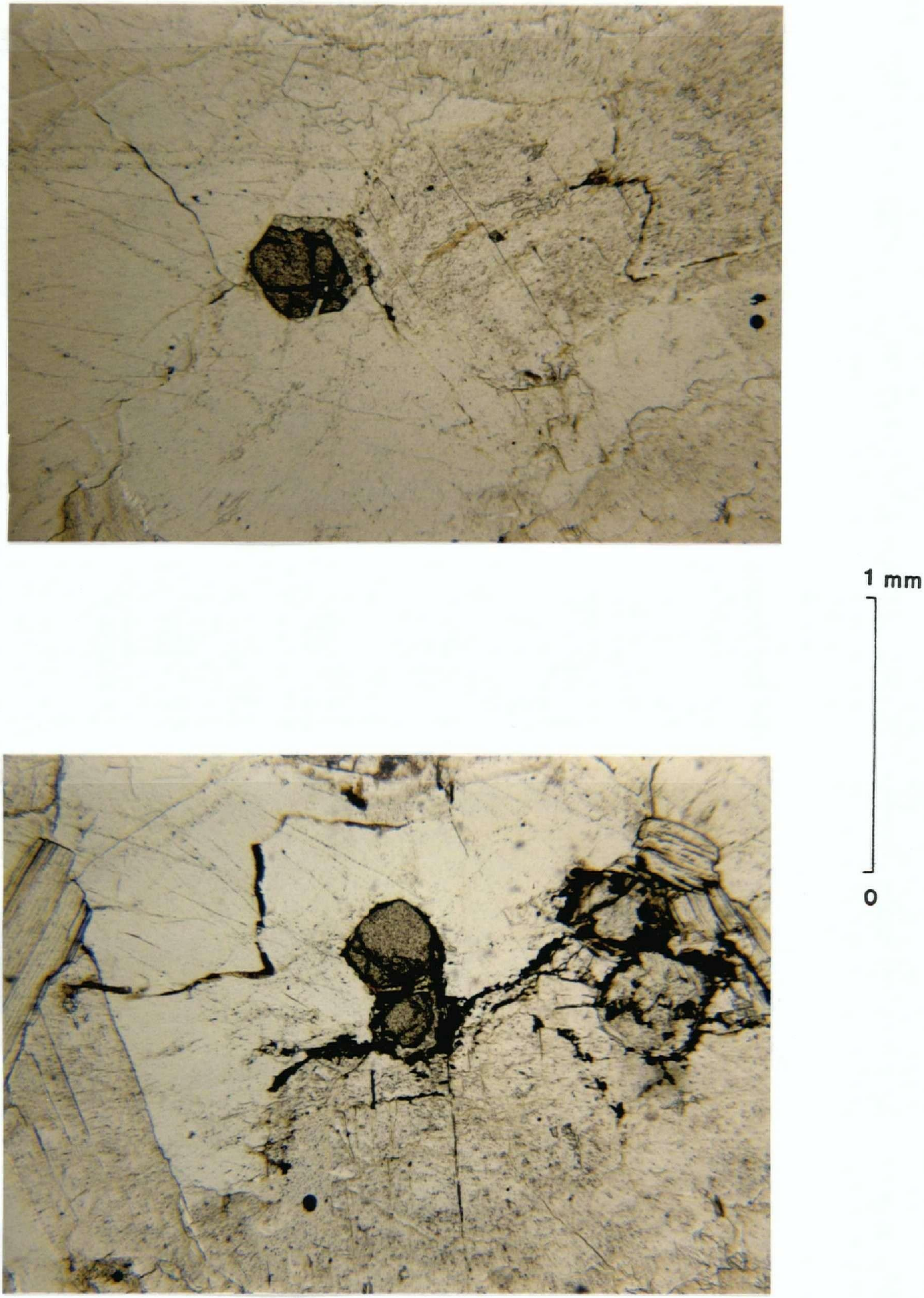

Figure 20: Photomicrograph from Jgr showing partly altered garnets (top) and unaltered and completely altered garnets (bottom).

Discussion of Geochemistry

Whole rock XRF major element analyses, using pressed powder pellet technique of Van der Heyden, Horsky and Fletcher (1982), were done on a total of 26 samples. Two analyses were duplicated. Trace elements were measured on 11 samples, and Rb and Sr concentrations on 20 samples. The results are given in Table 5. The discussion of the whole rock chemistry will be broken into three parts 1) general characteristics, 2) differences between Jpgr and Jgr and, 3) investigation of S- and I-type classifications. It should be stated, however, that because some samples are both intrusive and altered, in some cases highly altered, the data should only be used for discerning general trends and associations and should not be used for detailed petrogenetic models and calculations.

1) General Characteristics

General characteristics are: A - the scattered nature of the diorites on the Harker diagram and AFM plot (Fig. 21 and 22) which confirms the textural and lithologic heterogeneity seen in the field and thin section. B - the highly felsic nature of the Jgr unit - 75 to 78 percent SiO_2 and virtually no iron or magnesium, and C - the spread in Jpgr samples from moderate to higher silica values and lower Fe, Mg and Ca. On an AFM diagram (Fig. 22) the three units, in particular Jpgr and Jgr, plot within the trend for calc-alkaline rocks (Kuno, 1968; Irvine and Baragar, 1971).

On a normative Q-Or-Plag diagram (Fig. 23) the Jpgr straddles the granodiorite/granite fields and Jgr plots mostly within the granite field.

2) Geochemical Comparison of Jpgr and Jgr.

The spread in values in the Jpgr is interpreted to be due to alteration affects caused by the intrusion of Jgr. The samples of Jpgr which are at the lower silica end of this trend are the least altered in thin section. Those samples with values approaching Jgr are increasingly altered - as well as spatially closer to Jgr. On a

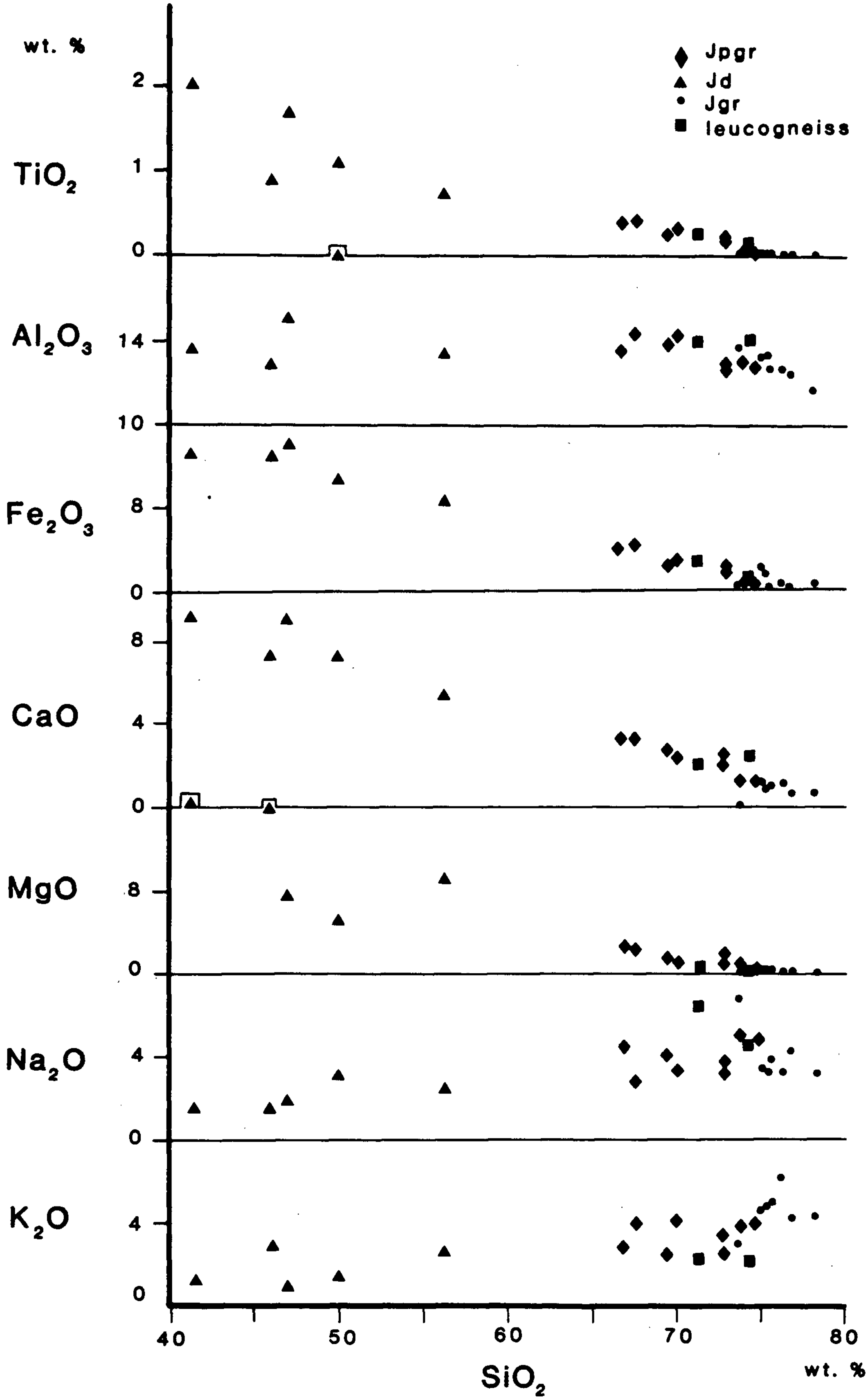

Figure 21: Major element variation diagram for different phases of Oliver pluton. Also shown are two analyses from the leucogneiss.

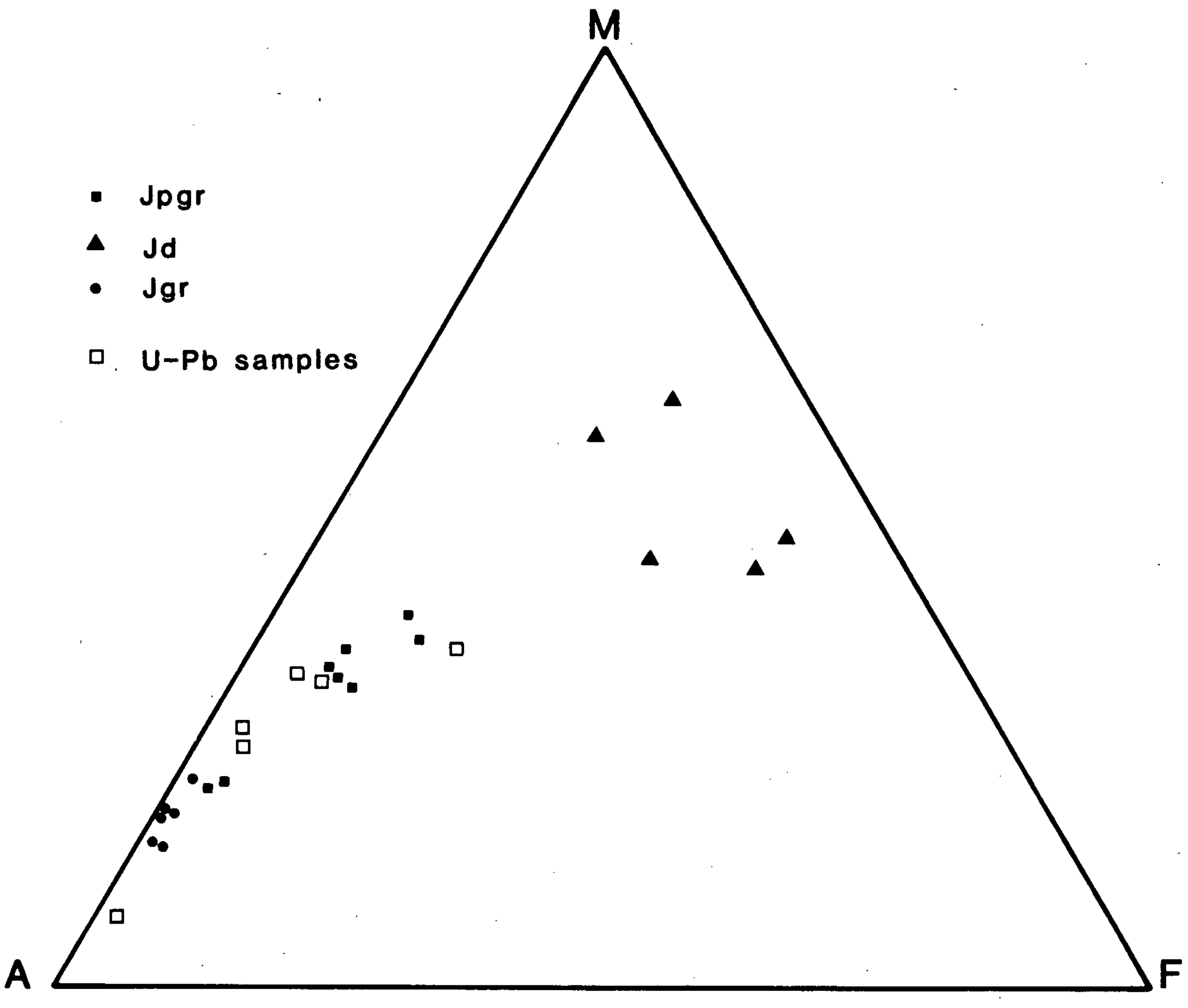

Figure 22: AFM diagram for samlpes from Oliver pluton; note symbol change for Jpgr unit. Also plotted are U-Pb samples.

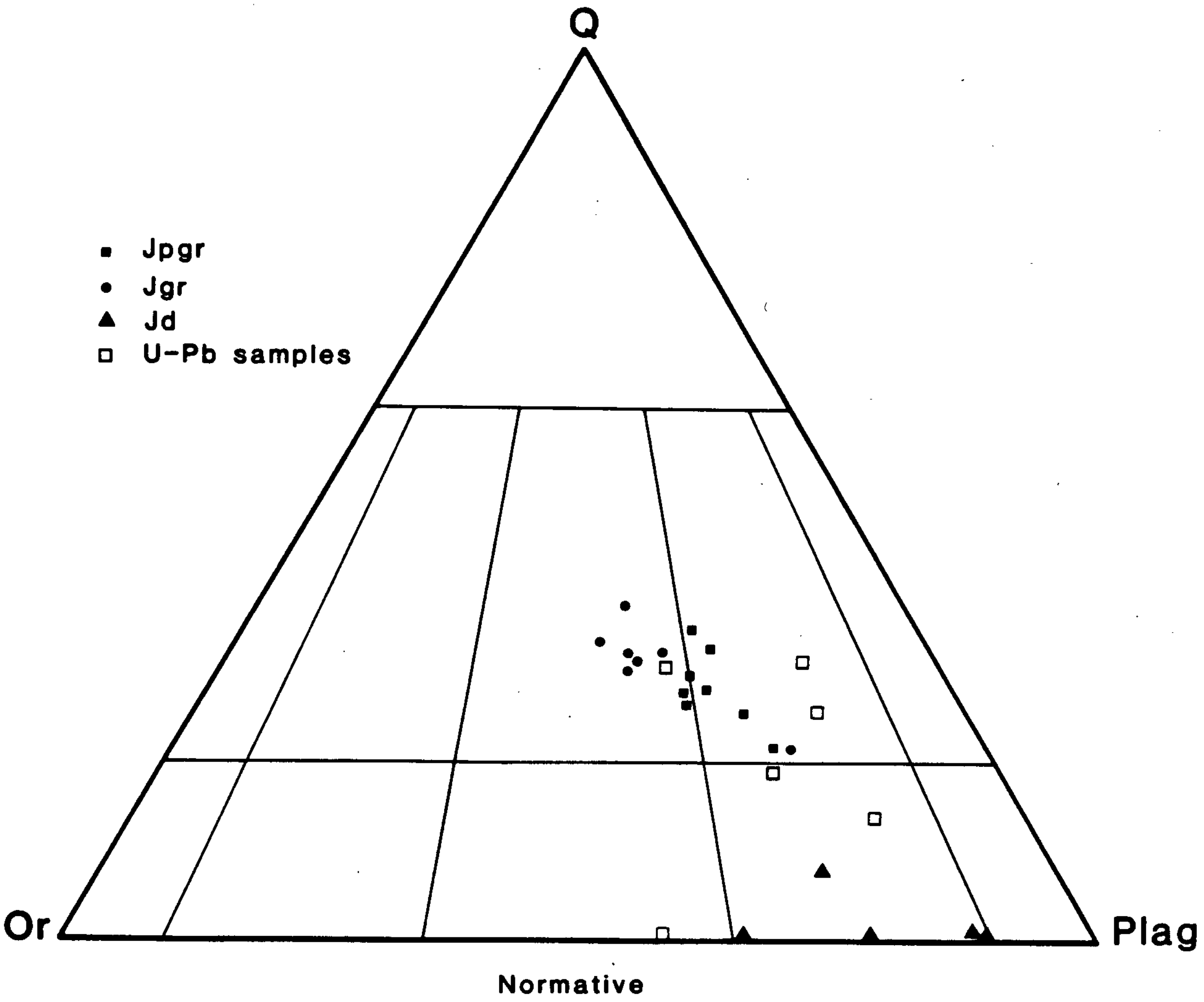

Figure 23: Q–Or–Plag diagram showing most Jgr plotting in the granite field, most Jpgr plotting on boundary between granite and granodiorite fields.

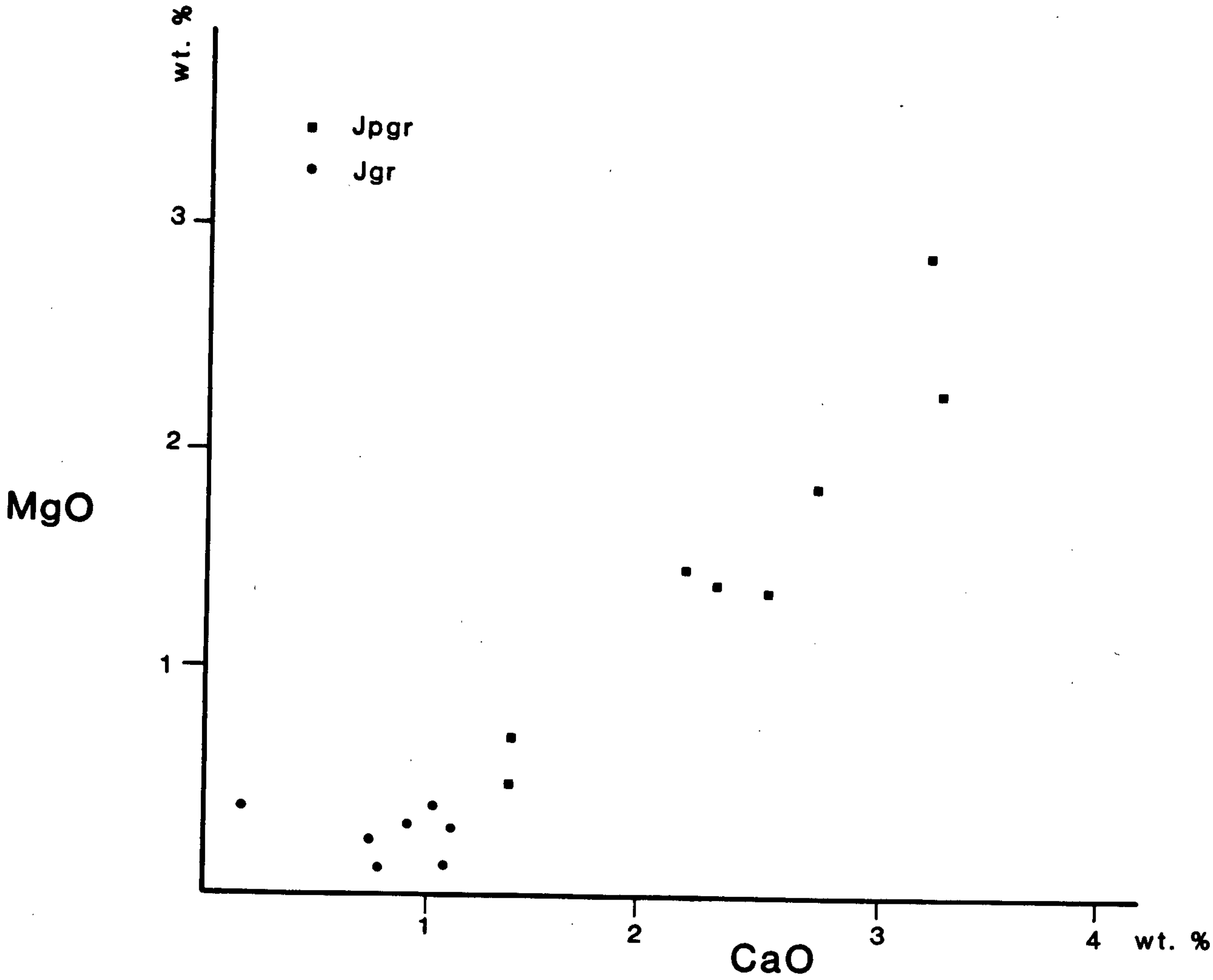

Figure 24: Mgo vs CaO plot for Jpgr and Jgr samples.

MgO vs CaO diagram (Fig. 24) these two units plot even more distinctly apart with only two Jpgr values close to the Jgr cluster. These two samples are again the most highly altered. This separation of units on geochemical characteristics also can be seen on trace element plots (Fig. 25 and 26) (Sr, Rb, Ba, and Zr vs SiO_2). Of these Zr and Sr seem to show the most distinct separation. The interpretation of this, as suggested above, is that the Jpgr values which plot away from Jgr represent the original composition of this unit (that of a Hb–Bi granodiorite), which was altered when the Jgr unit intruded. These two units are not an in situ differentation sequence and may have separate origins.

In support of this is the normative Q–Ab–Or projection (Fig. 27; "Petrogeny's Residua System") on which the Jpgr and Jgr plot in or approaching the thermal trough at the experimentally determined minima for low pressure conditions (Tuttle and Bowen, 1958). Taking normative An into account would shift the minimum towards Q, for a particular P_t (Strong, 1979; Hyndman, 1984). In general the Jpgr samples plot to the Ab side of the fractionation curve which separates liquids which become more potassic as cooling continues from those which become more sodic with continued cooling (Carmichael et al., 1974). The Jgr samples generally plot on the Or side of this fractionation line. This, from petrographic evidence, is to be expected. Plagioclase was clearly a liquidus mineral for the Jpgr unit and alkali–feldspar is euhedral to sub–hedral in Jgr samples, suggesting it was a liquidus mineral.

3) Comparison with S– and I–Type Granites

In recent years work on granites has focused on whether the source rock was of sedimentary (S) or igneous (I) origin (Chappell and White, 1974). The Jgr unit (containing both garnet and muscovite, as well as having very high silica composition) appears to fit into the S category. In an effort to substantiate the petrographic observations several plots were made which demonstrate the S or I character of a granitic rock. These plots show: A – degree of alumina saturation with respect to

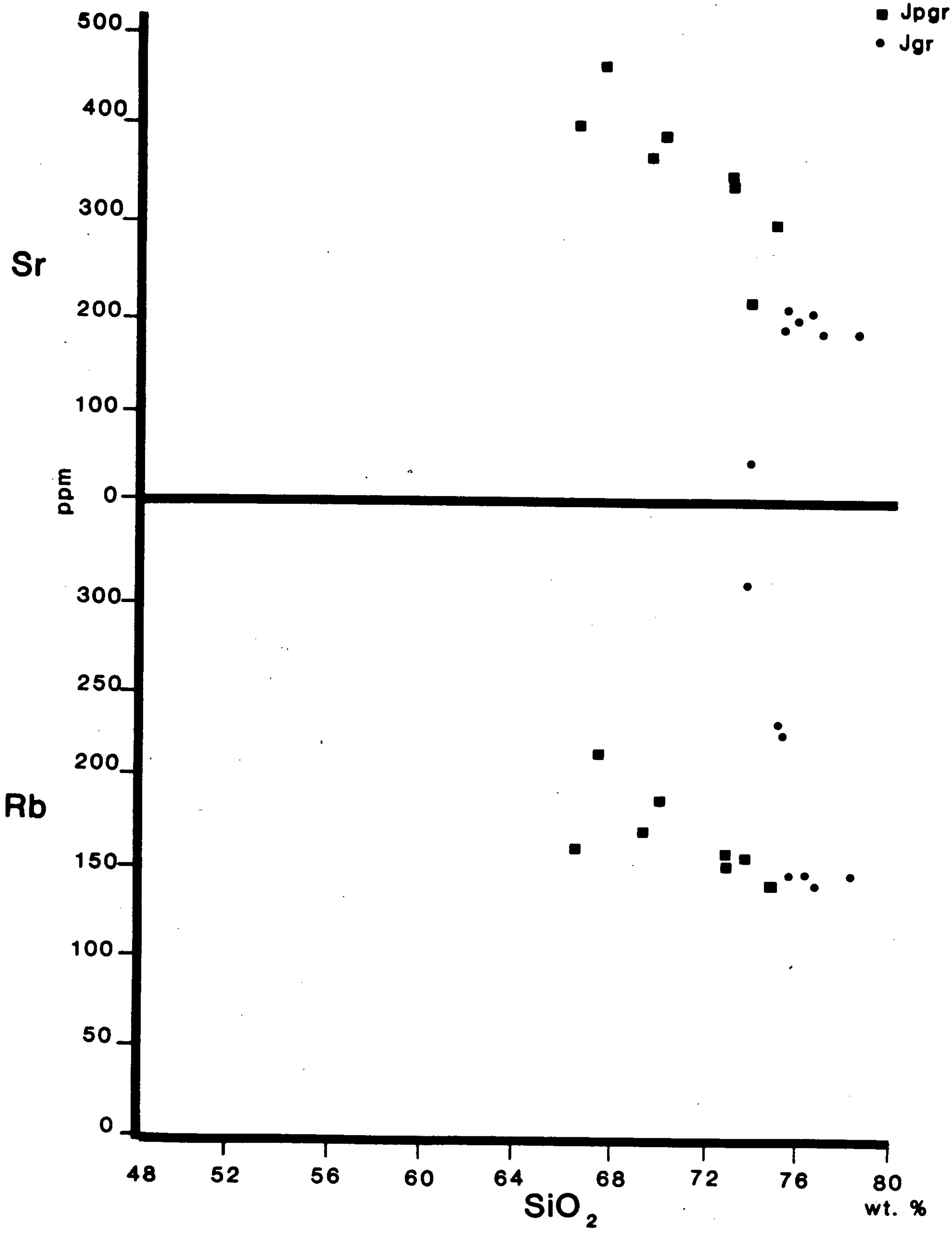

Figure 25: Sr and Rb vs SiO_2 for Jpgr and Jgr samples.

Table 5

(See Appendix A for procedures and error estimates).

WHOLE ROCK DATA FOR PORHYRITIC BIOTITE GRANITE

SAMPLE#	227	205	275.1	275.2	205	203	71	245
SiO2	73.74	72.87	69.45	66.66	72.74	70.05	74.64	67.47
TiO2	0.10	0.25	0.28	0.39	0.27	0.31	0.07	0.46
Al2O3	13.18	12.97	13.90	13.73	13.02	14.35	12.83	14.49
Fe2O3	1.38	2.67	2.95	4.37	3.05	3.18	1.31	4.45
MnO	0.17	0.16	0.17	0.18	0.06	0.06	0.12	0.17
MgO	0.69	1.44	1.83	2.88	1.38	1.35	0.47	2.25
CaO	1.37	2.15	2.74	3.22	2.27	2.51	1.37	3.27
Na2O	4.59	3.64	4.15	4.24	3.19	3.43	4.43	2.85
K2O	3.77	3.26	3.23	2.99	3.38	4.04	3.97	3.93
P2O5	0.07	0.10	0.11	0.16	0.14	0.16	0.06	0.20
H2O	0.93	0.49	1.19	1.19	0.49	0.56	0.73	0.46

CATION NORMS

Q	27.40	32.66	23.51	18.56	30.91	25.87	28.87	23.68
OR	22.51	20.39	19.36	17.90	19.57	24.25	23.71	23.66
AB	41.73	29.30	38.11	38.88	33.28	31.32	40.28	26.12
AN	4.24	10.57	9.76	9.58	9.54	11.59	3.41	15.20
DI	1.74	-	2.65	4.44	0.51	-	2.46	-
HY	1.06	4.18	4.11	7.77	3.79	4.12	0.08	8.10
MT	0.19	1.88	1.87	1.98	1.82	1.91	0.14	2.08
IL	0.14	0.38	0.40	0.55	0.35	0.44	0.10	0.65
HM	0.84	-	-	-	0.02	-	0.83	-
AP	0.15	0.30	0.23	0.34	0.21	0.34	0.13	0.43
C	-	0.35	-	-	-	0.16	-	0.08

TRACE ELEMENTS (ppm)

Rb	150	146	163	154	150	180	135	204
Sr	212	348	365	396	347	389	294	462
Ba		670			592	817		
Nb		12			15	14		
Y		17			12	11		
Zn		-			47	47		
Zr		126			126	118		

WHOLE ROCK DATA FOR DIORITE

SAMPLE#	207	178	261.1	261.2	140
SiO2	46.97	49.86	56.29	45.90	41.17
TiO2	1.70	1.10	0.78	0.91	2.08
Al2O3	15.04	18.43	13.70	12.91	13.65
Fe2O3	14.25	10.88	8.93	12.44	13.45
MnO	0.17	0.20	0.18	0.28	0.16
MgO	7.79	5.17	8.92	15.94	16.55
CaO	9.07	7.36	5.66	7.36	9.39
Na2O	1.90	3.09	2.53	1.44	1.44
K2O	1.05	1.38	2.49	2.67	1.39
P2O5	0.93	0.68	0.14	0.15	0.22
H2O	1.13	1.86	1.10	1.50	1.20

CATION NORMS

Q	-	0.39	4.67	-	-
OR	6.45	8.41	14.78	15.58	8.17
AB	17.78	28.73	23.07	9.48	1.33
AN	30.55	33.10	18.64	20.51	26.49
OL	1.84	-	-	36.62	35.83
DI	7.93	-	6.92	11.68	14.76
HY	27.77	23.48	28.17	-	-
NE	-	-	-	2.11	7.00
MT	3.18	2.75	2.37	2.46	3.07
IL	2.46	1.58	1.09	1.25	2.88
HM	-	-	-	-	-
AP	2.02	1.47	0.29	0.31	0.46
C	-	0.09	-	-	-

TRACE ELEMENTS (ppm)

Rb	37	34	131	138	52
Sr	821	756	380	294	489
Ba		924	479	557	611
Nb		14	15	11	11
Y		23	26	31	25
Zn		133	-	-	-
Zr		111	62	51	46

WHOLE ROCK DATA FOR GARNET MUSCOVITE GRANITE

SAMPLE#	234	209.1	209.2	263	182	9	263
SiO2	73.63	76.67	78.13	76.22	75.34	75.15	75.49
TiO2	0.03	0.03	0.03	0.04	0.08	0.08	0.04
Al2O3	13.75	12.45	11.78	12.73	13.40	13.33	12.77
Fe2O3	1.00	0.88	1.04	1.08	1.09	1.39	0.91
MnO	0.17	0.10	0.03	0.02	0.03	0.04	0.07
MgO	0.36	0.21	0.07	0.09	0.27	0.26	0.37
CaO	0.17	0.75	0.79	1.09	0.92	1.11	1.03
Na2O	6.88	4.30	3.42	3.20	3.64	3.68	3.91
K2O	3.04	4.25	4.37	5.10	4.76	4.71	4.95
P2O5	0.04	0.03	0.01	0.02	0.03	0.03	0.04
H2O	0.92	0.33	0.03	0.42	0.44	0.23	0.42

CATION NORMS

Q	20.24	31.61	37.46	33.60	31.62	30.96	29.55
OR	17.83	25.33	26.29	30.65	28.48	28.14	29.53
AB	56.56	39.01	31.32	29.29	33.15	33.47	35.52
AN	-	2.10	3.93	5.31	4.26	5.25	2.67
DI	0.50	1.16	-	-	-	-	1.78
HY	1.64	-	0.20	0.25	0.76	0.73	0.14
MT	-	0.17	0.01	-	-	-	0.08
IL	0.04	0.04	0.04	0.03	0.05	0.06	0.06
HM	-	0.50	0.73	0.77	0.77	0.98	0.59
AP	0.08	0.06	0.02	0.04	0.06	0.06	0.08
C	-	-	-	0.03	0.78	0.03	-
SP	-	-	-	0.04	0.10	0.07	-
ACMITE	2.76	-	-	-	-	-	-
NAMETASIL	0.53	-	-	-	-	-	-

TRACE ELEMENTS (ppm)

Rb	312	136	136	141	221	213	141
Sr	45	181	181	201	209	185	201
Ba			684	254	401	349	
Nb			14	4	12	14	
Y			8	3	12	16	
Zn			17	18	24	36	
Zr			60	69	65	64	

WHOLE ROCK DATA FOR U-PB SAMPLES

SAMPLE#	156	95	179	246	90	300
SiO2	74.30	74.25	66.43	68.22	74.11	53.77
TiO2	0.04	0.14	0.32	0.30	0.14	0.84
Al2O3	13.89	13.19	14.97	13.83	14.33	17.00
Fe2O3	0.38	1.66	3.21	3.44	1.46	6.50
MnO	0.12	0.17	0.18	0.17	0.02	0.11
MgO	0.24	0.67	0.95	1.57	0.45	5.29
CaO	2.32	1.59	5.12	3.68	2.79	5.02
Na2O	5.92	3.77	6.28	5.08	4.61	4.74
K2O	2.41	4.14	2.18	3.21	2.06	5.03
P2O5	0.05	0.07	0.18	0.19	0.02	1.00
H2O	0.33	0.33	0.19	0.29	0.20	0.26

CATION NORMS

Q	24.83	30.38	12.17	17.32	30.82	29.36
OR	14.16	24.76	12.77	18.98	12.22	30.36
AB	52.91	34.27	55.97	45.71	41.71	9.96
AN	4.17	6.93	6.13	5.43	12.31	10.58
DI	3.44	0.48	10.26	9.28	0.84	-
HY	-	1.63	-	0.59	0.83	7.22
MT	0.20	0.16	1.88	1.88	-	2.40
IL	0.06	0.20	0.44	0.42	0.03	1.16
HM	0.13	1.05	-	-	1.02	-
AP	0.10	0.15	0.37	0.40	0.04	2.07
C	-	-	-	-	-	-

TRACE ELEMENTS (ppm)

Rb	63	151	44	125	51	141
Sr	409	350	1004	640	787	3313
Ba					1362	3492
Nb					6	90
Y					9	27
Zr					57	412

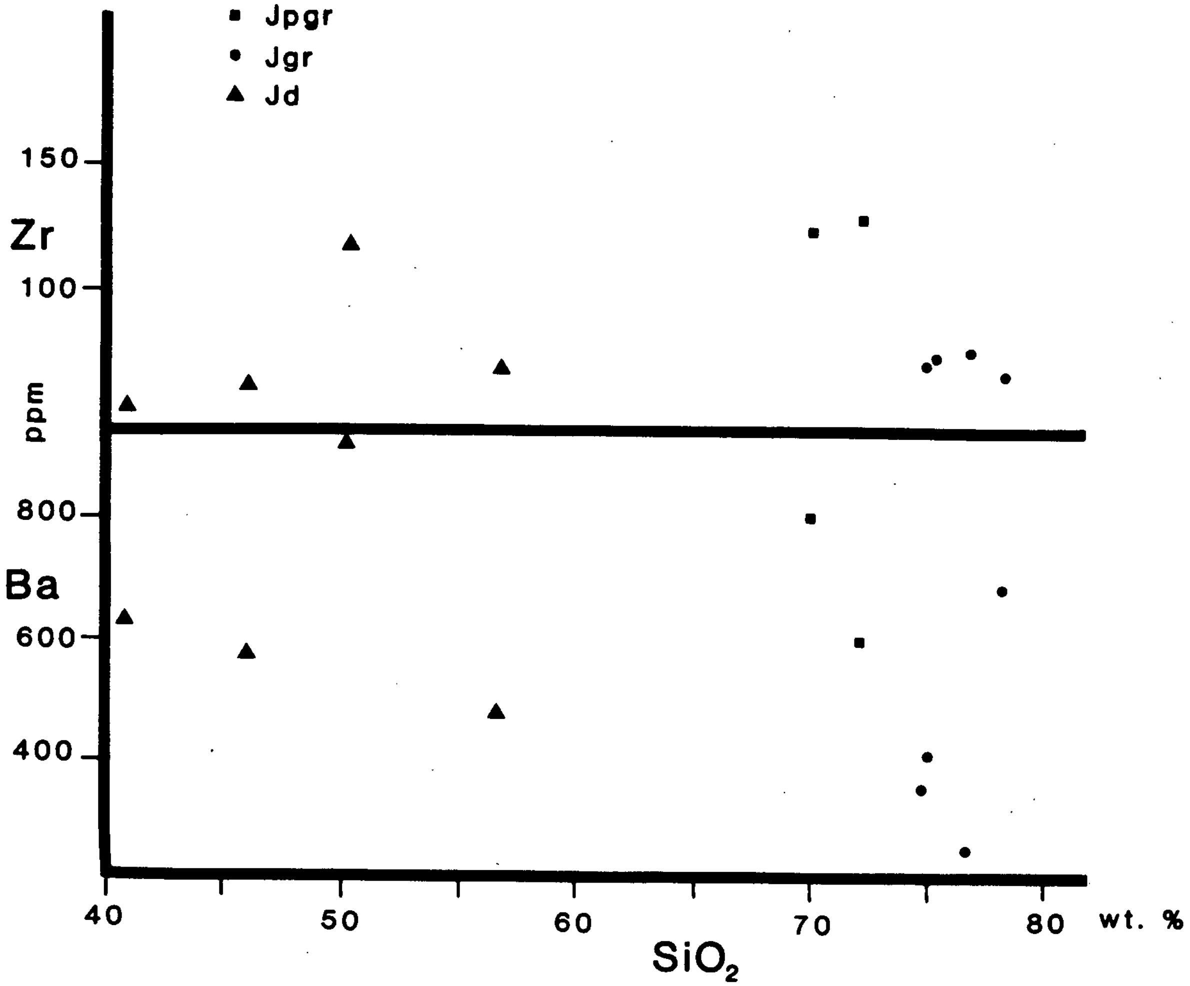

Figure 26: Zr and Ba vs SiO_2 for Jpgr and Jgr samples.

normative corundum or diopside, versus SiO_2 (Fig. 28); and B - molar $Al_2O_3/(CaO + Na_2O + K_2O)$ versus Rb/Sr ratio (Fig. 29). Rocks with normative corundum and molar $Al_2O_3/(CaO + Na_2O + K_2O) > 1.1$ are considered typical S-type granites.

Both Jpgr and Jgr units have samples which contain (<1 percent) normative corundum. Otherwise the samples are scattered mainly with low to moderate normative Di. On the molar $Al_2O_3/(CaO + Na_2O + K_2O)$ vs Rb/Sr the most striking characteristic is again the separation (in Rb/Sr values) between these two units. In terms of S and I classification the Jgr samples are all (except one) below 1.1, suggesting a highly evolved I-type magma. The Jpgr unit straddles this dividing line at 1.1, with several values up to 1.2 molar $Al_2O_3/(CaO + Na_2O + K_2O)$. Petrographically the Jpgr unit is not of S-type character. An alternate explanation for the slightly aluminous character of this unit, and very likely considering the mineralogy, is amphibole fractionation causing alumina enrichment (Cawthorn and Brown 1976, Cawthorn et al, 1976).

In summary it appears that neither of these granitic bodies is truly of S-type. The Jpgr unit has high molar $Al_2O_3/(CaO + Na_2O + K_2O)$ values due possibly to amphibole fractionation and the Jgr unit, which has S-type petrographic characteristics, does not plot neatly in S-type granite fields on either C-Di or molar $Al_2O_3/(CaO + Na_2O + K_2O)$ scales. Jgr may be a highly differentiated I-type magma or it could be the result of fusion of eugeosyclinal or lower crust rocks rather than pelitic schists and therefore does not clearly display S-type geochemistry.

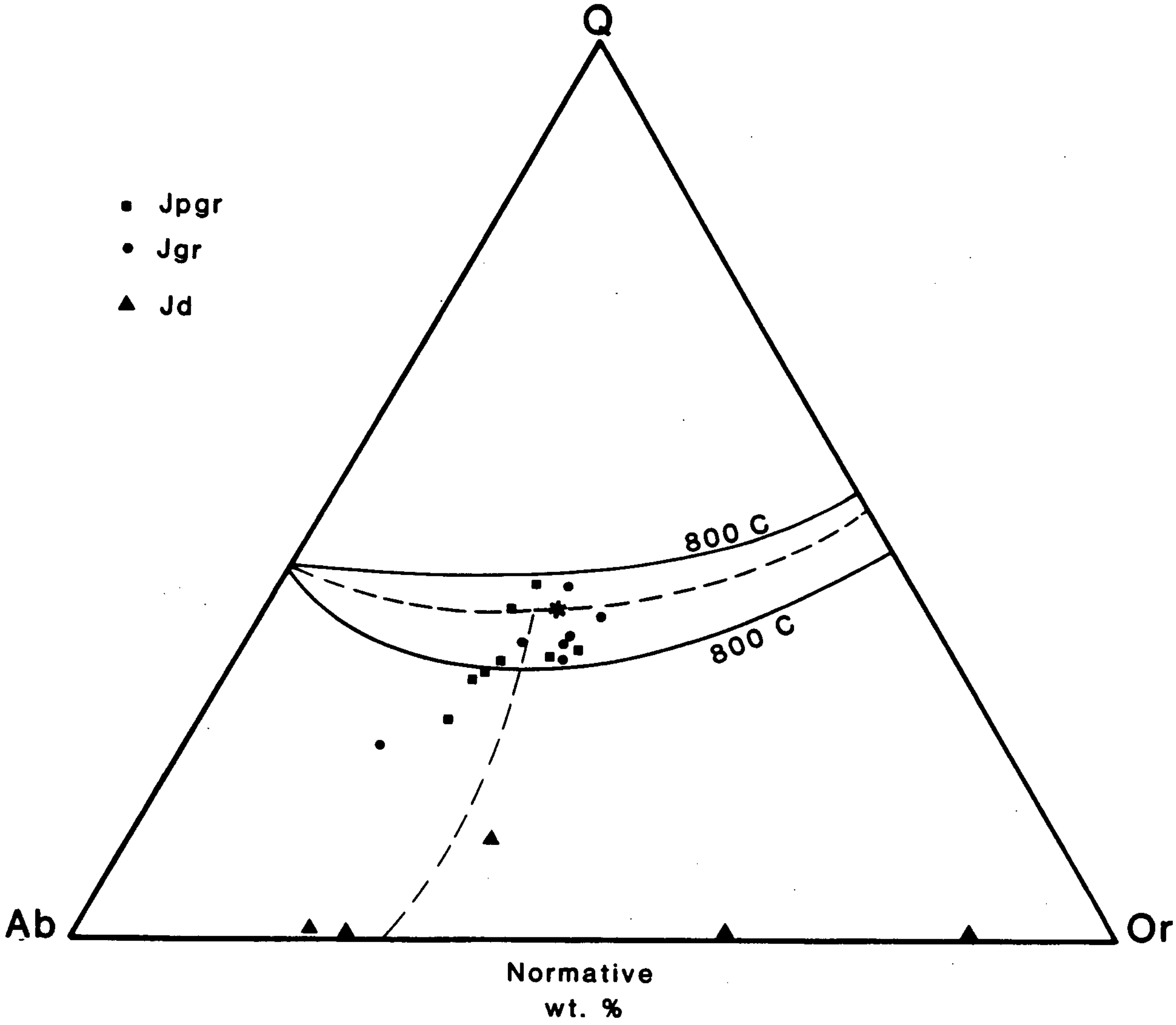

Figure 27: Q–Ab–Or for Jpgr, Jgr, and Jd samples. Boundary curves and temperature contours for water saturated liquids at P_t = 1.0 kb, from Carmichael et al. (1974).

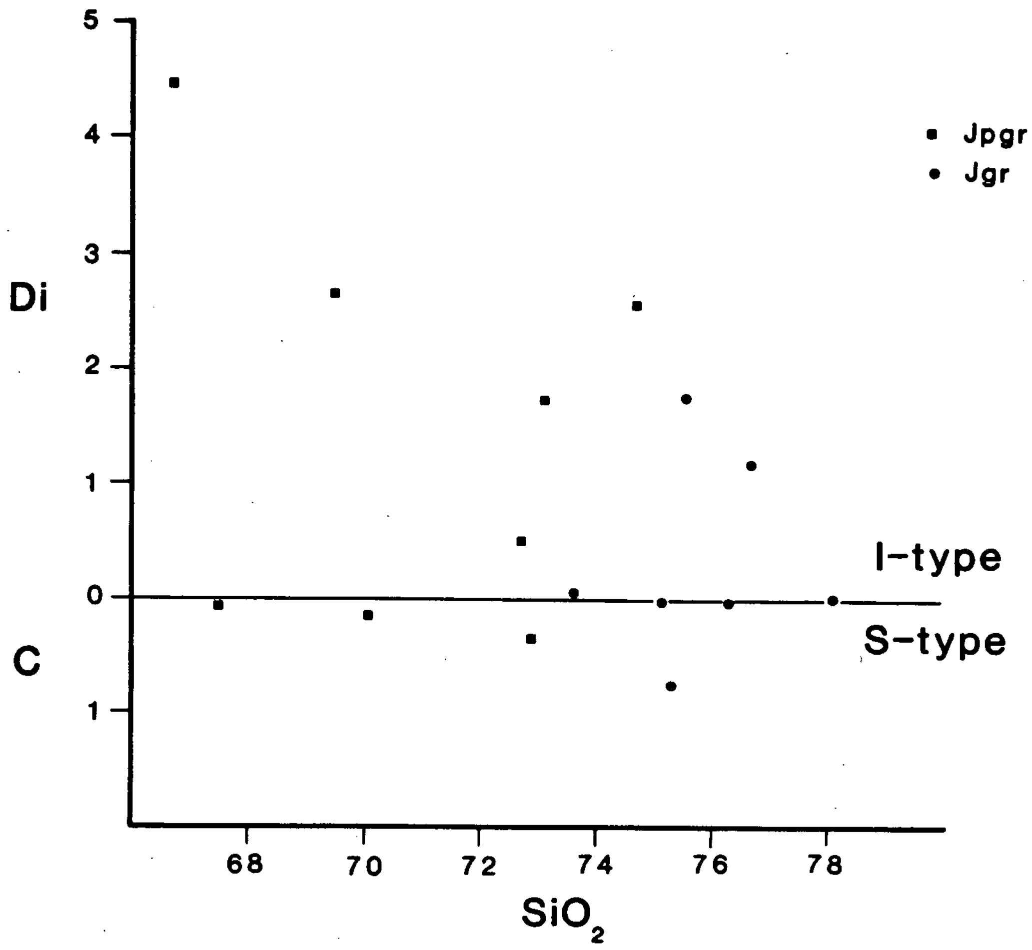

Figure 28: C and Di vs SiO_2 for Jpgr and Jgr samples.

Eocene Strata (eTv, eTs,)

Eocene volcanic rocks and coarse clastic sediments are exposed in the northwestern part of the area. They represent a small part of this study area but were examined in detail by Church (1973) and therefore the internal stratigraphy is well defined. The volcanic rocks within the study area include the Marron Formation and local occurrences of rhyodacite and pyroclastic rocks of the Marama Formation. Clastic sediments present are the Skaha Formation. In the area studied the volcanic rocks are found at lower stratigraphic, structural and topographic levels than the sediments. The contact between the volcanics and overlying sediments has been mapped (Church, 1979b, and the present study) as a fault directly north and northwest of Mahoney Lake, but elsewhere in the White Lake Basin Church has demonstrated this contact to be an angular unconformity. The contact between the volcanics and lPz–Tr to the south is also a fault, as is the contact between the Eocene rocks and the Vaseaux gneisses to the east.

The volcanic flows exposed west of Mahoney Lake are extremely altered, fractured, and faulted. They can be related to Church's detailed stratigraphy only on the basis of texture (relict "Clot Porphyry", Church, 1973). The phenocrysts, except for feldspars, are invariably altered beyond recognition. These volcanics are andesite to trachyandesite in composition; the groundmass is a mosaic of quartz and feldspar. The alteration consists of calcite, quartz, and opaques (oxidized pyrite, and fracture–filling iron oxides).

The Skaha sediments are coarse conglomerates, and form the youngest unit in White Lake Basin. Church describes them as fanglomerate, shed from highlands which lay to the southeast. The predominant clasts are chert, greenstone, and unfoliated granite. Church (1973) reports phyllite clasts which he interprets as coming from Vaseaux Formation. The Vaseaux Formation is not seen at such a low metamorphic grade, therefore the phyllite is interpreted to come from Kobau Formation to the south, or an equivalent unit of lPz–Tr age. Church reports the presence of Vaseaux clasts but this could not be confirmed in the present study. Various highly strained rocks from the lPz–Tr formations make up the greatest percentage of clasts within the Skaha.

At Green Lake this unit is faulted and fractured. The clasts, in a sand matrix, are pebble to boulder (1 m) size (Fig. 30). Bedding or stratification is not evident at this locality but from the east side of the Okanagan valley, looking west, large–scale bedding can be discerned, dipping 25° to the east.

The White Lake volcanic rocks, which include both andesitic and alkali–trachyandesitic compositions can be correlated with other Eocene volcanics in B.C., Washington, and Montana. Andesitic rocks have been well studied further north near Kamloops by Ewing (1981a) and alkaline volcanics are known from south central B.C. and north–central Washington as well as from Montana (Church, 1973).

Eocene Dikes

Tertiary dikes are the most conspicuous in the Oliver pluton. This is partly due to exposure and a marked color contrast but also because of truly greater frequency. The dikes are 1–2 m wide and can be followed for no more than 50–100 m along strike. They occur locally in swarms, particulary near Madden Lake. They invariably are fractured and commonly altered.

Mineralogically these dikes are identical to the lower volcanic units within the Marron Formation. Rhombehedral zoned anorthoclase is common, as is zoned clinopyroxene (Fig. 31). These dikes generally are altered but a few unaltered ones were observed. These show in thin section delicate pyroxene zoning and unaltered or slightly altered olivine (Fig. 32). These dikes were apparently feeders to the basal flows of the Marron Formation.

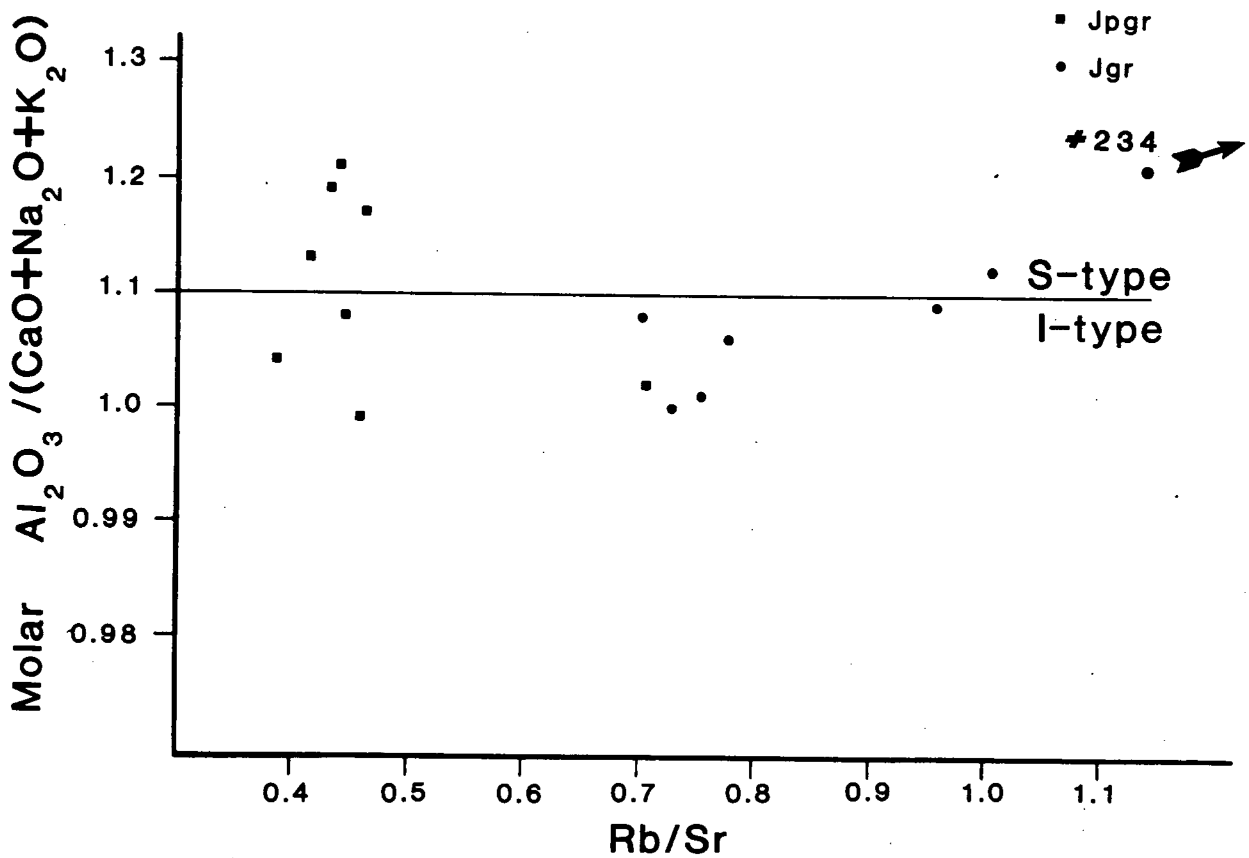

Figure 29: Molar $Al_2O_3/(CaO + Na_2O + K_2O)$ vs Rb/Sr for Jpgr and Jgr samples.

Figure 30: Photograph of fractured outcrop of Skaha Formation, west of Green Lake.

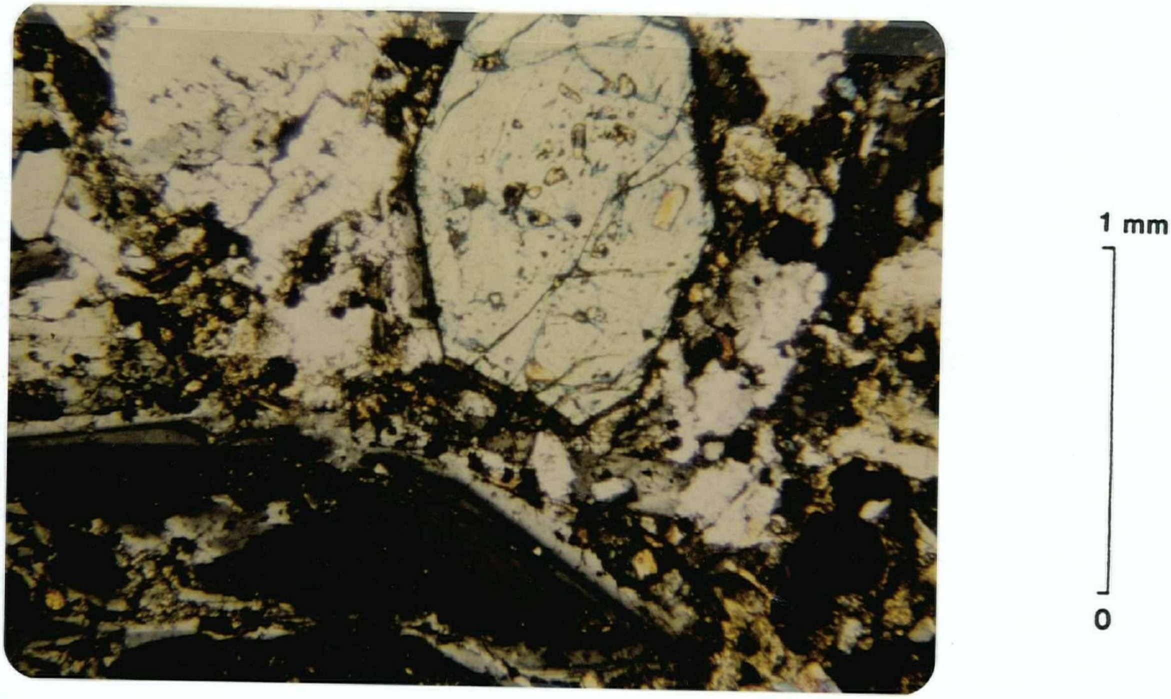

Figure 31: Photomicrographs of Eocene rhomb porphyry dike.

The number of dikes found in the pgn and lgn units is low considering their proximity to the White Lake Basin. A metamorphosed and deformed dike bearing rhomb-shaped anorthoclase phenocrysts in the pgn and lgn just north of Covert Farms (Plate 1) has for many years been suspected to be an equivalent to the basal rhomb porphyry of the Marron (Ross, 1974). This dike cuts the compositional layering and foliation in the pgn and lgn at a very low angle and is itself strongly foliated and lineated (Fig. 33). Metamorphism is expressed as garnet and biotite growth in pull-aparts of anorthoclase and clinopyroxene, as well as in the matrix (Fig. 34). Clinopyroxene appears to be reacting to form hornblende; the matrix is a recrystallized mosaic of quartz, feldspar, biotite and chlorite. A U-Pb date on zircon from this sill gives a concordant date of 51 Ma (this study). Ross (1974) has reported several other dikes/sills of similar composition and texture within the pgn and lgn units. The number of dikes or sills within the metamorphic rocks is probably not anomalously low but many have been overlooked because the metamorphism and deformation has rendered them almost indistinguishable from the pgn, except where well exposed. Only undeformed dikes are rare in the metamorphic rocks.

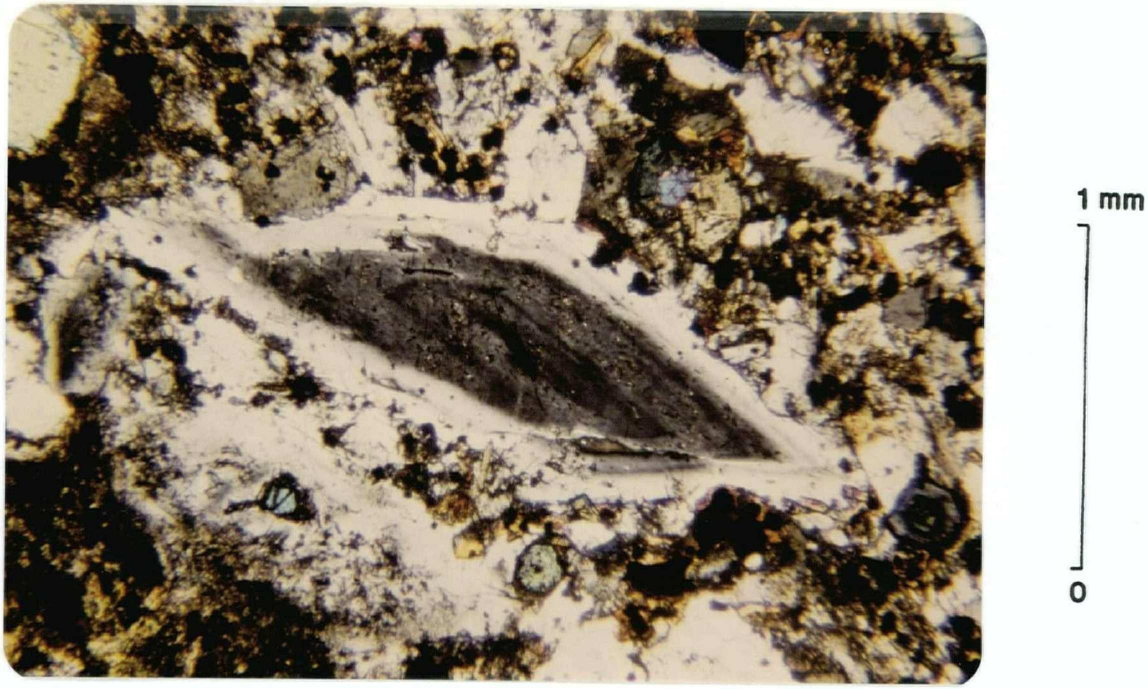

Figure 32: Photomicrograph of Eocene dike, showing pyroxene and olivine phenocrysts.

Figure 33: Photograph of foliated and lineated rhomb porphyry from within the pgn unit, north of Covert Farms area.

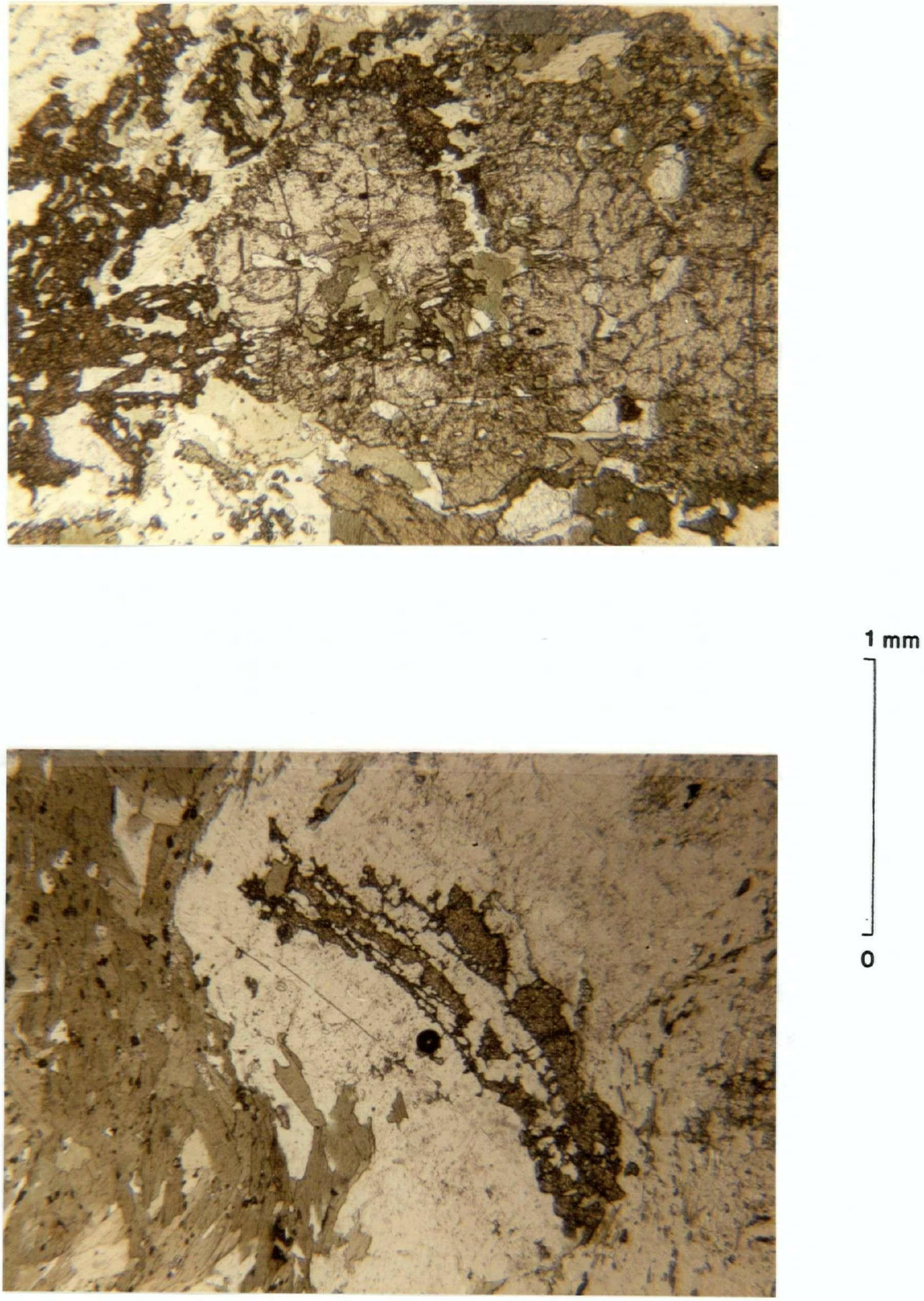

Figure 34: Photomicrographs of metamorphosed and deformed rhomb porphyry showing garnet and biotite growth in pullaparts of pyroxene (top) and feldspar (bottom).

IV. <u>GEOCHRONOMETRY</u>

In the Shuswap Metamorphic Complex of southern B.C. an extensive area of largely pre-Eocene plutonic and metamorphic rocks yields K-Ar dates of 45-55 Ma. Many authors have observed and discussed this regionally extensive pattern of reset dates (Armstrong, 1974, 1982, 1983, 1985; Ross, 1974; Medford, 1975; Miller and Engels, 1975; Fox et al., 1977; Mathews, 1981, 1983; Parrish, 1979; Okulitch, 1984; Price, 1985; Price, et al., 1981; Archibald et al., 1984). The explanations include high heat flow and tectonic unroofing. One purpose of the present study was to determine the geologic nature (abrupt or transitional) of the western boundary of this reset terrane. Another was to use the U-Pb method to obtain original ages for pre-, syn-, and post-kinematic granitic rocks to ascertain the time(s) of deformation within the metamorphic complex.

Geochronometry - Previous Work

Geochronometric studies in the Okanagan region began with reconnaisance K-Ar work on Cenozoic volcanic rocks (Mathews, 1964). Since that time both K-Ar and Rb-Sr studies have been done for a number of theses and research projects. This section summarizes the results of those studies (Fig. 35; Table 6).

The early K-Ar work done by Mathews (1964), Baadsgard et al. (1961) and White et al. (1968) established that volcanic rocks equivalent to those in White Lake Basin are Eocene, about 50 Ma old, and that intrusive rocks west of the Okanagan Valley are Mesozoic. Geochronology of the White Lake Basin was reported by Church (1970, 1973, and 1980d), and is summarized in Figure 36. Church (1975, and 1979a), Ewing (1981a, and 1981b) and Mathews (1981) have documented other Eocene volcanic

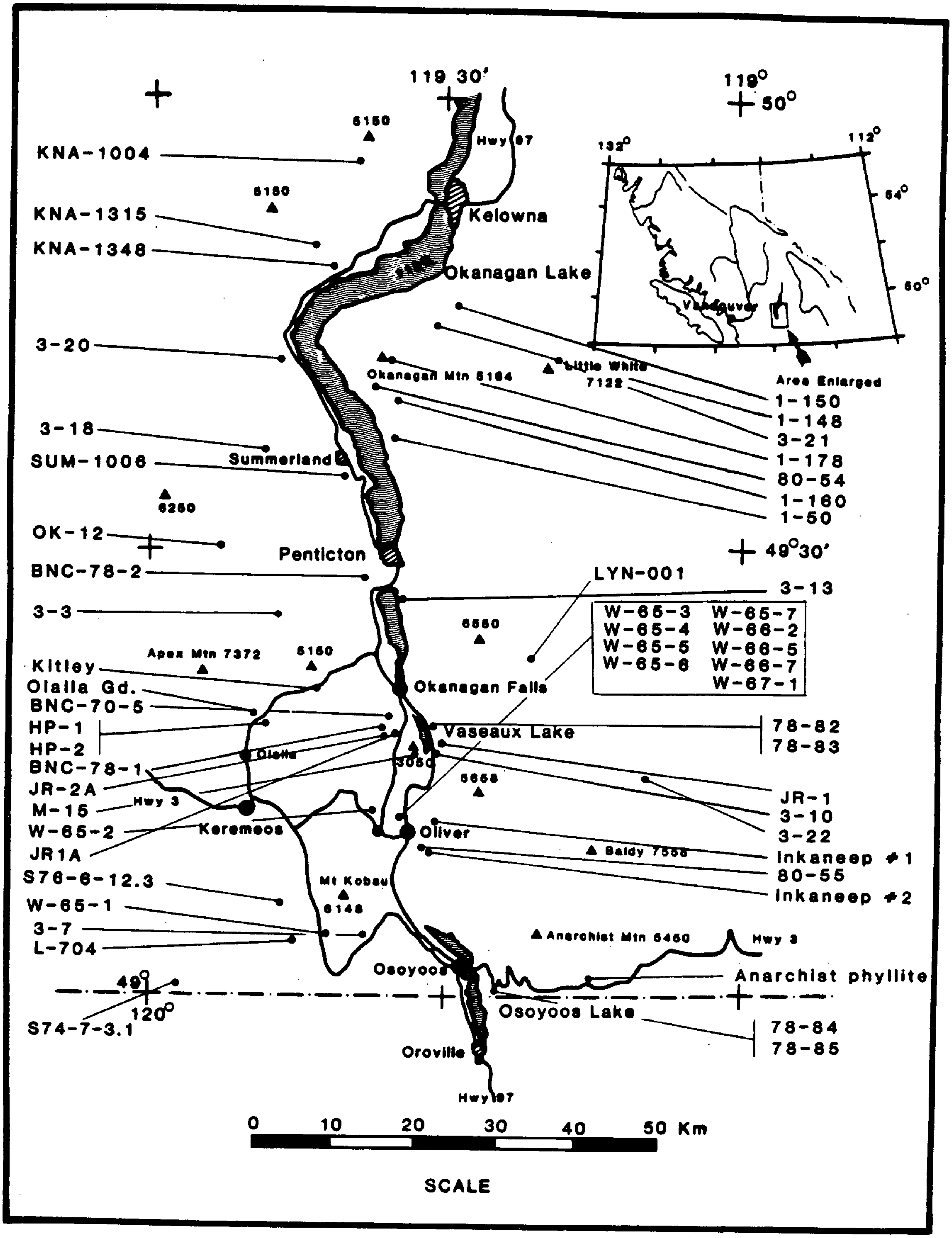

Figure 35: Location map of previous K–Ar analyses.

Table 6 - Previous K-Ar Data

Data from 49°-49°50'; 119°10'-120°

Sample #	Rock Type	Mineral	Date Ma*	Latitude	Longitude
G.S.C. analyses (Wanless et al., 1979; Stevens et al., 1982)					
76-1	gneiss	Hb	48.4	49°39'50"	119°36'10"
78-82	gneiss	Bi	47.8	49°17.5'	119°30'
78-83	gneiss	Ms	45.5	"	"
78-84	gneiss	Bi	45.6	49°00'40"	119°24'15"
78-85	gneiss	Hb	63.5	"	"
80-54	gneiss	Hb	48.8	49°39'50"	119°36'10"
80-55	gneiss	Ms	59.4	49°09'45"	119°30'15"
Analyses done for B.C.M.E.M.P.R. by U.B.C.; except * done by Geochron Labs (Church, 1970, 1979, 1980, 1982; Church et al., 1983).					
*Kitley	trachyte	Bi	52.9	49°20.6'	119°44.3'
BNC-78-1	breccia	Bi	52.5	49°18.5	119°37.5'
KNA-1004	dacite	WR	44.2	49°54.75'	119°39.5'
BNC-78-2	porphyry	Bi	52.4	49°28.52'	119°38.83'
BNC-70-5	tephrite	WR	48.4	49°18.75'	119°37'
KNA-1315	dacite(?)	Bi	52.9	49°49.65'	119°44.4'
KNA-1348	rhyolite	Mica	47.7	49°48.45'	119°43.40'
SUM-1006	dacite	WR	47.9	49°35'	119°40'
OK-12	trachyte	Bi	52.7	49°33'	119°52'
LYN-001	syenite	Bi	53.0	49°23'	119°20.4'
Analyses from Medford, 1975.					
1-50	dike	WR	48.2	49°36.7'	119°34.6'
1-148	gneiss	Hb	49.3	49°43.9'	119°31.3'
1-150	gneiss	Hb	50.7	49°44.5'	119°31.0'
1-160	dike	WR	49.8	49°39.2'	119°33.8'
1-178	gneiss	Hb	51.8	49°42.6'	119°36.0'
3-3	diorite	Bi	188	49°25.2'	119°47.2'
3-7	Kruger syenite	Hb	173	49°03.5'	119°38.5'
3-10	paragneiss	Hb	61.0	49°16.5'	119°31.2'
3-13	gneiss	Hb	53.3	49°26.6'	119°34.5'
3-18	diorite	Bi	168	49°36.6'	119°47.8'
3-20	grd.	Bi	135	49°42.5'	119°48.8'
3-21	gneiss	Bi	52.7	49°42.8'	119°16.5'
3-22	grd.	Bi	52.7	49°15'	119°10.5'

continued....

*All dates corrected to decay constants recommended by Steiger and Jager (1977).

Table 6 (con't)

Analyses from Read and Okulitch, 1977.

HP-1	dike	Hb	153	49°18'31"	119°47'39"
HP-2	dike	Hb	172	49°18'09"	119°47'48"
Olalla Gd.	grd.	Bi	155	49°18'43"	119°48'34"

Analyses from Ross, 1974.

JR-1	rhomb por.	WR	42.4	49°16.7'	119°29.0'
JR-1	rhomb por.	Bi	45.3	"	"
JR-1	rhomb por.	Hb	48.4	"	"
JR-2A	Marron Fm.	WR	42.2	49°18.0'	119°36.6'
JR-1A	Marron Fm.	WR	44.3	49°17.7'	119°35.2'
M-15	pegmatite	Ms	48.9	49°15.9'	119°32.8'

Analyses from White et al., 1968, and Sinclair et al., 1984.

W-65-1	syenite	Px-Hb	154	49°3.2'	119°41.7'
W-65-2	grd.	Bi	113	49°12'	119°38.2'
W-65-3	granite	Bi	120	49°12'	119°35.9'
W-65-4	granite	Bi	84	49°12.2'	119°35.4'
W-65-5	granite	Bi	104	49°12.1'	119°34.85'
W-65-6	granite	Ms	141	49°11.4'	119°33.3'
W-65-7	alteration	Ser	138	49°11.8'	119°33.5'
W-66-2	dike	Bi	53.8	49°11.8'	119°33.6'
W-66-5	granite	Ms	146	49°11.5'	119°35.5'
W-66-7	granite	Bi	101	49°10'	119°35'
W-67-1	alteration	Ser	115	49°13.0'	119°35.9'

Unpublished analyses from U.B.C. (1-3, collected by Mathews and Armstrong; 4 collected by Mathews; 5 and 6 collected by Soregaroli and Christopher).

Inkaneep #1	granite	Bi	87	49°10'35"	119°29'30"
Inkaneep #1	"	Ms	146	"	"
Inkaneep #2	gneiss	Bi	56.4	49°09'50"	119°29'50"
Anar. Mtn.	phyllite	WR	53.6	49°01'45"	119°21'20"
S74-6-12.3	qtz. monzo.	Hb	171	49°06'	119°48'
S74-7-3.1	grd.	Bi	112	49°01'	119°55'

K-Ar reported by:

Okulitch et al., 1977:

Olalla	syenite	Hb	184	49°16.5'	119°50'

Fox et al., 1975 and 1977:

Osoyoos #2	gneiss	Bi	50.3	49°01.4'	119°22.5'
L-704	grd.	Hb	118.6	49°3.0'	119°44.2'

south of 49°:

L-618	grd.	Hb	181	Similkameen batholith
L-618	grd.	Bi	73	"
L-301	alkalic	Hb	175	"
L-301	border	Bi	72	"

basins and erosion remnants, north and east of the southern Okanagan Valley. Engels et al. (1976) dated equivalent rocks south of 49° as Eocene as well. K-Ar studies by White et al. (1968), Roddick et al. (1972), Medford (1975), and Fox et al., (1976) dated the extensive granitic rocks west of the Okanagan Valley as Jurassic and mid-Cretaceous.

This duality of dates (Fig. 37) is in contrast to unimodal Eocene K-Ar and fission track dates for dikes, pegmatites and gneissic granites (Ross, 1974; Medford, 1975) east of Okanagan Valley, from within the Okanagan Metamorphic and Plutonic Complex. Several Geological Survey of Canada K-Ar analyses (Table 6) on gneisses from east of both Osoyoos and Vaseaux Lake, also show this pervasive Eocene event (Wanless et al., 1979; Stevens et al., 1982). These dates on metamorphosed plutonic rocks have been interpreted to be thermal reset ages, and not the intrusive age.

Published Rb-Sr data of Petö and Armstrong (1976) and Medford et al. (1983) documented Jurassic (and possible Paleozoic) intrusives to the west of Okanagan Valley with $^{87}Sr/^{86}Sr$ initial ratios below 0.705. Armstrong and Petö (1981) as well as Medford et al. (1983) demonstrated the presence of both Eocene (Shingle Creek, Trout Creek, and Siwash Creek porphyries) and Paleocene (Whiteman Creek stock) high level intrusives west of Okanagan Lake.

A wealth of unpublished Rb-Sr data (Table 7) exists for the southern Okanagan, and by far the majority of this data is on orthogneiss, paragneiss and schist from the Okanagan Metamorphic and Plutonic Complex. Much of this work was done by Ryan (Ph.D. thesis, 1973) at U.B.C. and in recent years R.L. Armstrong has supplemented this. The results from this ongoing study are varied. Armstrong (unpublished) has obtained a 157±8 Ma whole rock date on the Oliver pluton, on the west side of the Okanagan Valley. In addition three variably deformed intrusive bodies, mapped by Ryan (1973) northeast of Osoyoos from within the Okanagan Metamorphic and Plutonic Complex, yield Jurassic isochrons with large errors (Fig. 38).

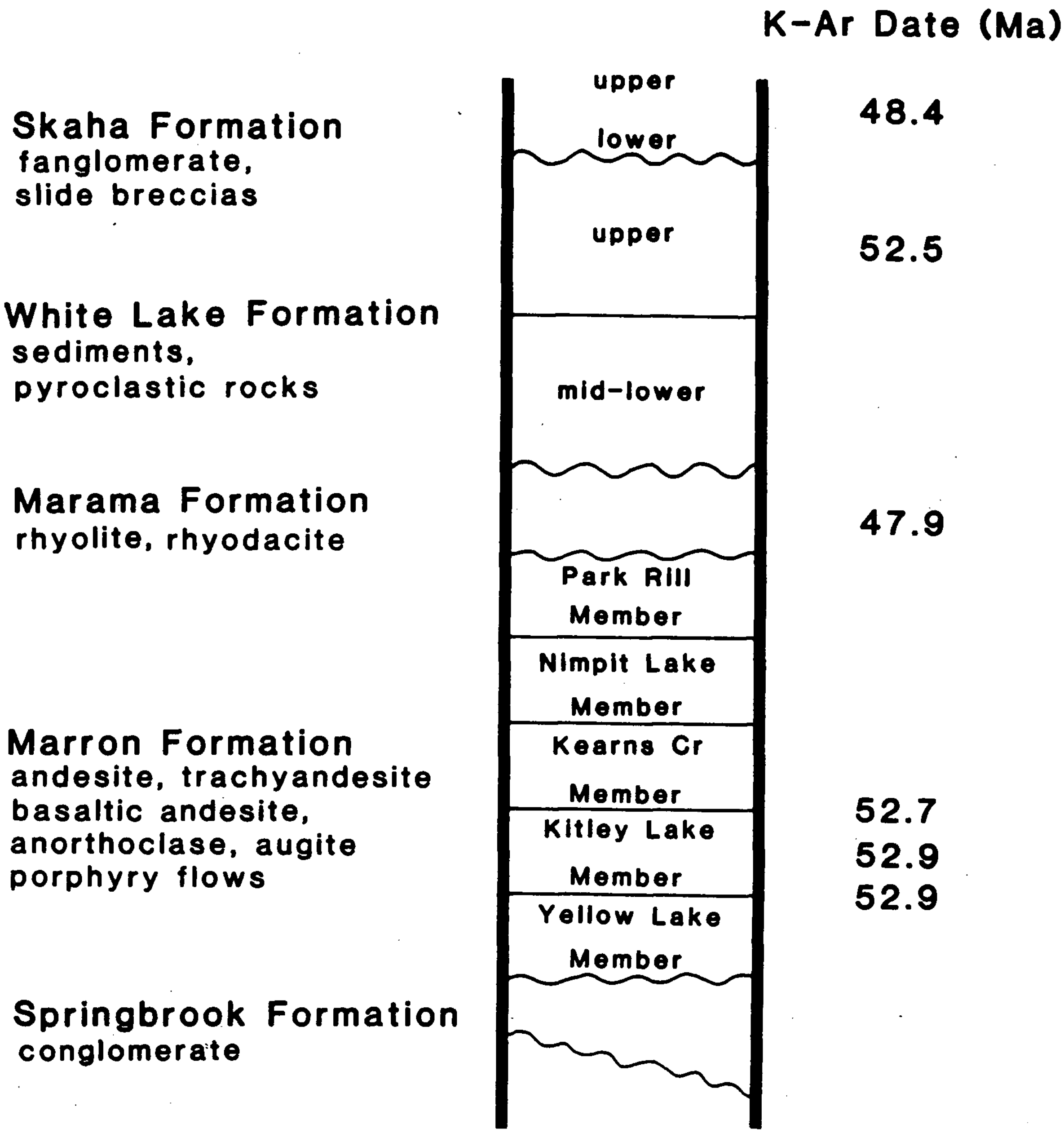

Figure 36: K-Ar chronology for White Lake Basin.

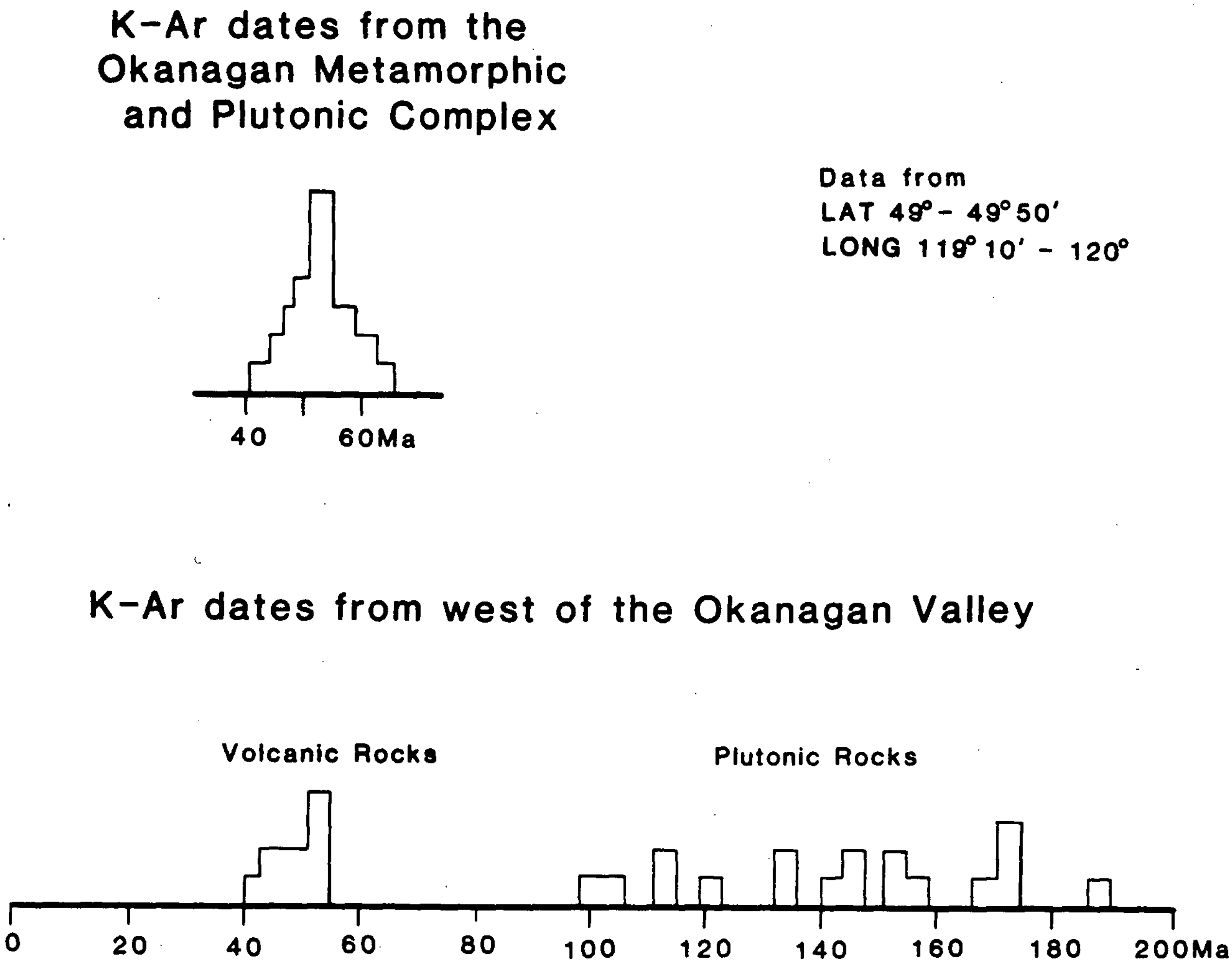

Figure 37: Histograms of K-Ar dates from plutonic rocks and volcanic rocks west of the Okanagan Valley, and metamorphic rocks east of the Okanagan Valley.

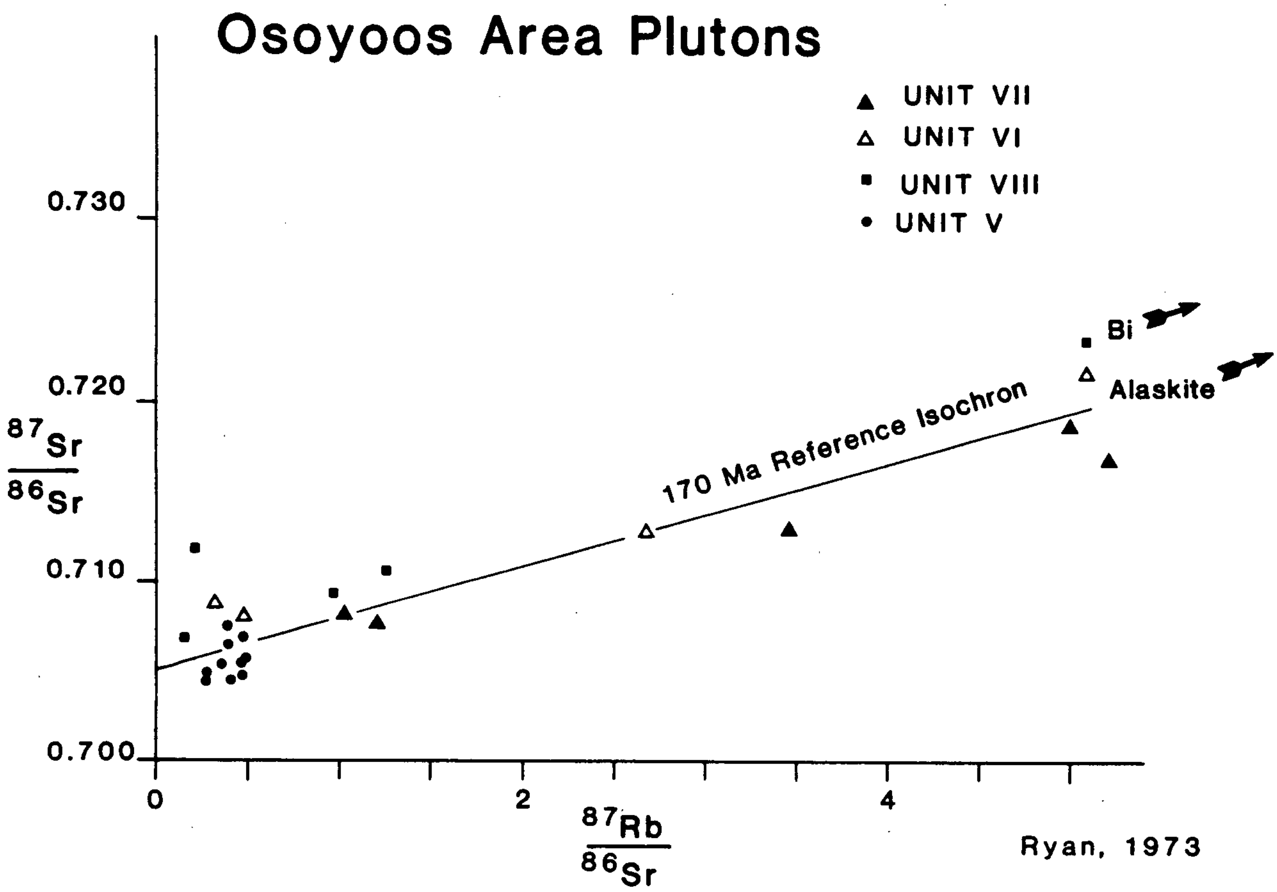

Figure 38: Rb–Sr diagram for four gneissic granitic units of Ryan (1973), east of Osoyoos.

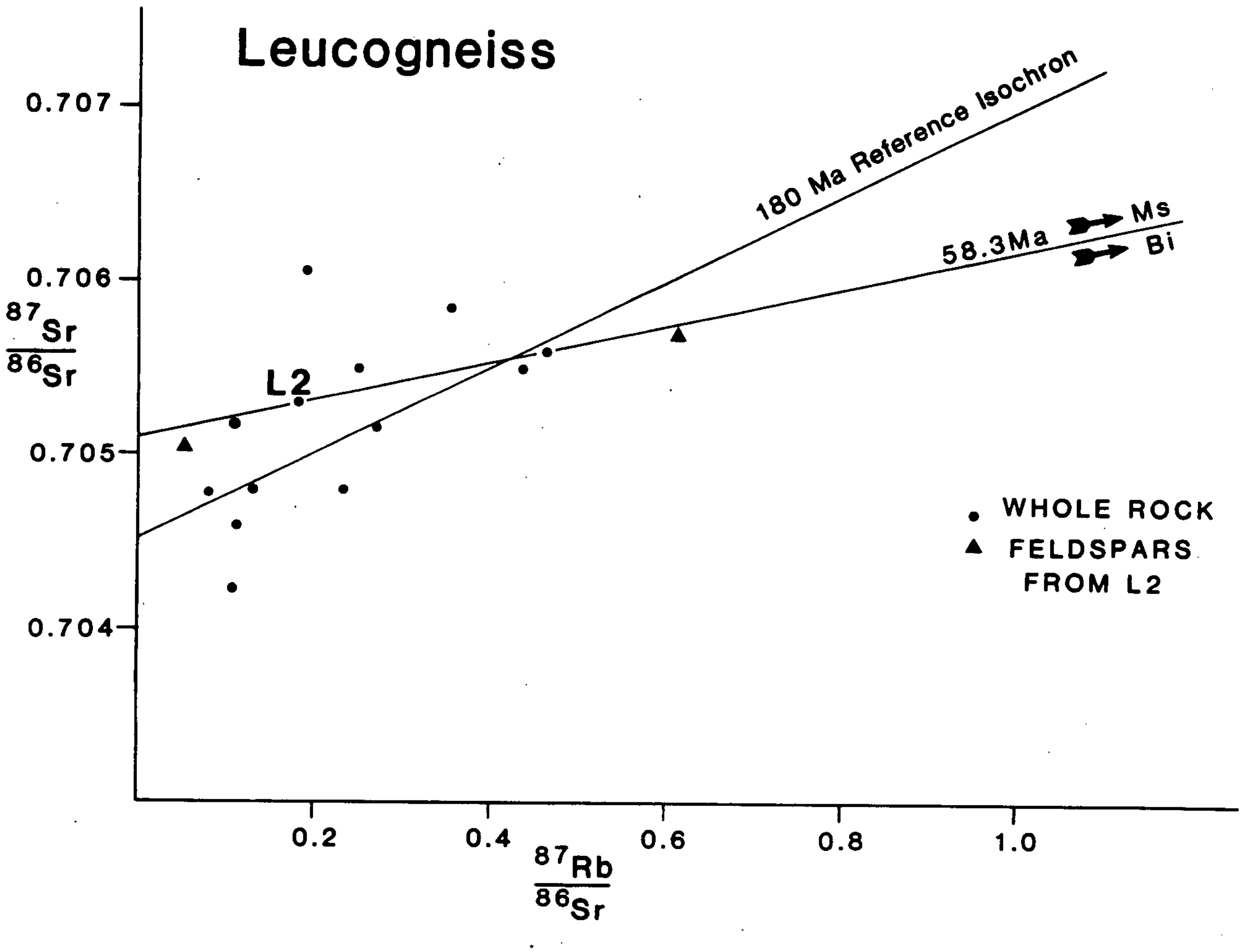

Figure 39: Rb–Sr diagram for leucogneiss.

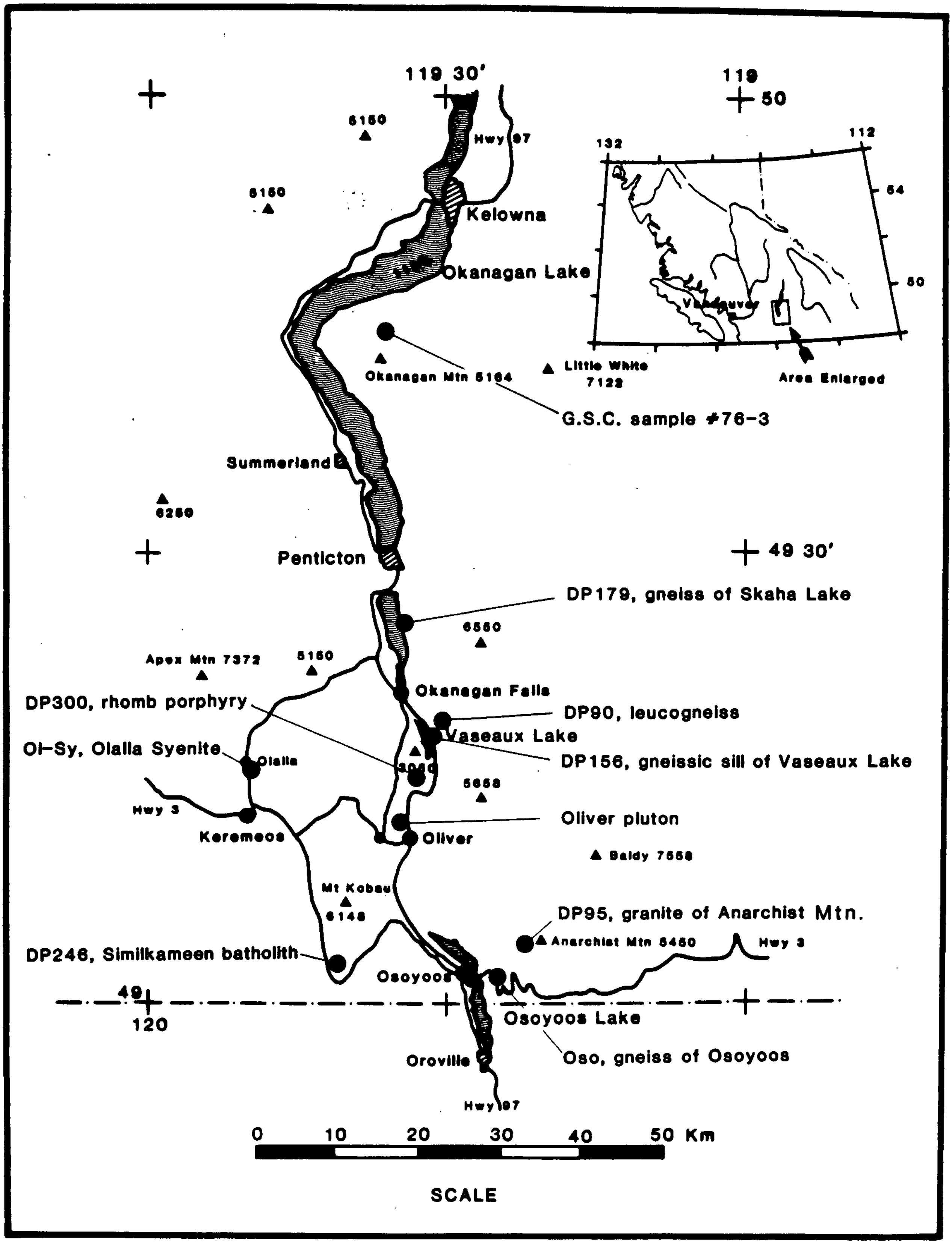

Figure 40: U–Pb sample locality map for both previous work and the present study.

One of these (granite of Anarchist Mtn.) was collected for zircons in the present study. The other orthogneiss (Unit V) from Ryan's Ph.D. area did not yield an interpretable whole rock isochron. Mineral-whole rock isochrons from these same orthogneisses yield mostly Paleocene-Eocene dates. The leucogneiss body north of Covert Farms, within the present study area (and sampled for zircons), gives a Jurassic Rb-Sr errorchron (Fig. 39; Armstrong, unpublished).

Rb-Sr data for paragneiss from the Okanagan Metamorphic and Plutonic Complex do not produce whole rock isochrons, but all the mineral-whole rock pairs yield Paleocene-Eocene dates. Some paragneiss samples have highly radiogenic strontium, supporting the interpretation that the protolith is Precambrian in age (Ryan, 1973; and Armstrong, unpublished).

Previous U-Pb work (Table 8; Fig. 40) in the Okanagan has been done on the Oliver pluton (152± 3; Armstrong and Ryan, unpublished), and on a gneissic granite from Medford's Ph.D. thesis (1973) area south of Kelowna (3 fractions concordant at 68± 2 Ma; analaysis by Geological Survey of Canada). Fox et al. (1976) reported a late Cretaceous U-Pb date from the Okanogan Dome in north-central Washington, 50 km south of the present study area.

Table 7

Previous Rb-Sr Analytical Data*

Sample #	Description	Latitude	Longitude	ppm Sr	ppm Rb	$^{87}Rb/^{86}Sr$	$^{87}Sr/^{86}Sr$
Sample Suite: Paragneiss, Covert Farms (Armstrong)							
SH L	paragneiss	49°15.13'	119°32.92'	310	150	1.400	0.7209
SH M	amphibolite	49°15.14'	119°33.16'	211	22.8	0.312	0.7066
SH R	paragneiss	49°15.0'	119°33.0'	106	84.3	3.69	0.7273
SH S	paragneiss	49°15.14'	119°33.25'	292	78.7	0.78	0.7228
SH U	hb granulite	49°15.20'	119°33.27'	704	99.4	0.409	0.7073
SH W	paragneiss	49°15.14'	119°33.16'	193	64.4	0.968	0.7185
SH K	paragneiss	49°15.11'	119°32.73'	328	51.8	0.457	0.7201
SH C	hb diorite	49°15.19'	119°32.27'	913	71.3	0.226	0.7073
SH D	hb diorite	49°15.20'	119°32.25'	763	83.2	0.315	0.7079
SH E	hb diorite	49°15.25'	119°32.22'	647	99.9	0.447	0.7083
SH A	paragneiss	49°15.08'	119°32.33'	476	108	0.659	0.7218
SH T	paragneiss	49°15.17'	119°33.25'	393	109	0.805	0.7145
Sample Suite: Paragneiss, Covert Farms (Ryan, 1973)							
S9	schist, Vaseaux Formation	49°15'10"	119°33'25"	166	116	2.039	0.7673
S10	"	"	"	117	149	3.683	0.7467
Sm10	muscovite	"	"	38.9	310	23.21	0.7640
Sample Suite: Paragneiss, Vaseaux Lake roadcut (Armstrong)							
VL 1	gneiss	49°16.7'	119°31.0'	608	43.7	0.208	0.7045
VL 2	gneiss	"	"	667	41.9	0.182	0.7051
VL 3	gneiss	"	"	1021	47.5	0.135	0.7055
VL 5	gneiss	"	"	683	57.7	0.245	0.7062
VL 6	gneiss	"	"	534	61.3	0.332	0.7065
VL 7	gneiss	"	"	793	20.0	0.073	0.7062

Previous Rb-Sr Analytical Data

Sample #	Description	Latitude	Longitude	ppm Sr	ppm Rb	$^{87}Rb/^{86}Sr$	$^{87}Sr/^{86}Sr$
Sample Suite: Plutonic Rocks; Vaseaux Lake area (Ryan, 1973)							
G1	Synkinematic Qtz-monzonite sill	49°18'0"	119°29'40"	777.3	28.9	0.1075	0.7044
Gb1	biotite	"	"	262.2	256.2	2.825	0.7058
P2	pegmatite	49°04'53"	119°27'57"	519.6	34.0	0.1892	0.7082
Pm2	muscovite	"	"	139.3	232.0	4.819	0.7106
Pm12	muscovite	49°5.5'	119°28.5'	17.98	462.2	74.7	0.7511
Sample Suite: Leucogneiss, Cover Farms (Armstrong)							
SH1	garnet leuco-gneiss	49°15.45'	119°33.35'	609	27.5	0.130	0.7048
SH3	"	49°15.43'	119°33.35'	647	55.7	0.249	0.7055
SH5	"	49°15.41'	119°33.40'	519	78.1	0.436	0.7055
SH6	"	49°15.40'	119°33.40'	521	83.3	0.463	0.7056
SHF	"	49°15.40'	119°32.28'	693	31.3	0.131	0.70515
SHG	"	49°15.40'	119°32.29'	594	47.8	0.233	0.7048
SHN	"	49°15.43'	119°33.41'	662	27.6	0.121	0.7046
SHO	"	49°15.44'	119°33.42'	657	79.8	0.351	0.70585
SHP	mylonite	49°15.60'	119°33.48'	1275	38.1	0.086	0.70475
SHQ	mylonite	49°15.60'	119°33.48'	680	66.1	0.281	0.7051
Leuco1	granod. gneiss	49°15.40'	119°32.36'	623	23.2	0.107	0.7042
Leuco2	"	49°15.42'	119°33.35'	616	39.0	0.183	0.7053
Leuco2-I	heavy feldspar	"	"	320	5.2	0.047	0.7050
Leuco2-IV	light feldspar	"	"	790	167	0.611	0.7057
Leuco2-M	muscovite	"	"	43.0	124	8.33	0.7120
Leuco2-B	biotite + chlorite	"	"	104	267	7.41	0.7098
Sample Suite: Rhomb Porphyry, Covert Farms (Armstrong)							
Rhomb P	anorthoclase augen gneiss	49°14.97'	119°33.00'	3402	151	0.129	0.7061

Previous Rb-Sr Analytical Data

Sample #	Description	Latitude	Longitude	ppm Sr	ppm Rb	$^{87}Rr/^{86}Sr$	$^{87}Sr/^{86}Sr$
Sample Suite: Anarchist Pelite (Unit III of Ryan, 1973)							
S1	pelite	49°04'59"	119°28'07"	109.4	145.6	3.354	0.7156
Sb1	biotite	"	"	8.05	568.1	207.1	0.8577
Sm1	muscovite	"	"	63.0	293.0	13.45	0.7206
S2	pelite	49°04'57"	119°28'00"	270.0	122.0	1.308	0.7139
Sb2	biotite	"	"	21.14	416.2	57.15	0.7413
S5	pelite	49°04'10"	119°25'17"	182.1	54.2	0.861	0.7115
Sb5	biotite	"	"	13.74	223.0	47.08	0.7287
S4	pelite	49°05'12"	119°25'42"	86.7	126.9	4.356	0.7250
Sb4	biotite	"	"	8.70	550.0	184.4	0.7937
Sm4	muscovite	"	"	41.38	247.0	17.31	0.7335
S6	pelite	49°02'15"	119°22'55"	273.1	142.3	1.511	0.7278
S7	pelite	49°01'45"	119°20'53"	164.3	80.4	1.416	0.7131
Sb7	biotite	"	"	66.34	233.8	10.21	0.7177
S8	pelite	49°01'40"	119°20'40"	122.4	89.1	2.107	0.7136
Sample Suite: Anarchist Amphibolite (Unit I of Ryan, 1973)							
A1	greenschist facies	49°01'00"	119°20'20"	165	4.9	0.086	0.7058
A2	amphibolite facies	49°03'15"	119°25'13"	181	7.7	0.123	0.7060
A3	"	49°05'17"	119°28'26"	309	41.0	0.384	0.7088
A4	"	49°06'35"	119°30'58"	166	22.0	0.384	0.7071

Previous Rb-Sr Analytical Data

Sample #	Description	Latitude	Longitude	ppm Sr	ppm Rb	$^{87}Rb/^{86}Sr$	$^{87}Sr/^{86}Sr$
Sample Suite: gneiss of Osoyoos (Unit V of Ryan, 1973; *analysed by Armstrong)							
F1	bi granod gneiss	49°00'40"	119°20'43"	487.3	63.2	0.376	0.7074
F2	"	49°01'53"	119°23'00"	459.8	74.4	0.468	0.7054
F3	"	49°01'33"	119°24'50"	549.3	56.3	0.296	0.7050
F4	"	49°04'37"	119°25'15"	536.2	69.1	0.373	0.7066
F5	"	49°04'34"	119°27'20"	458.9	63.7	0.401	0.7045
F6	"	49°04'50"	119°29'20"	442.8	71.1	0.487	0.7054
F7	"	49°05'45"	119°31'04"	455.3	74.6	0.474	0.7048
F8	separate body	49°08'40"	119°26'50"	459.7	76.9	0.484	0.7070
F9	"	49°09'20"	119°26'55"	616.5	54.7	0.257	0.7045
*BDRgn	gneiss	49°0.65'	119°24.0'	515	68.4	0.384	0.7045
*BDRap	def. aplite	49°0.65'	119°24.0'	119	239.0	5.82	0.7158
Sample Suite: quartz monzonite (Unit VI of Ryan, 1973)							
E1	qtz. monzonite	49°08'15"	119°30'40"	637.8	103.8	0.471	0.7081
E2	"	49°02'44"	119°23'53"	310.1	281.5	2.63	0.7128
Eb2	biotite	"	"	192.0	840.0	12.69	0.7220
Em2	muscovite	"	"	223.0	658.3	8.55	0.7182
E3	separate body	49°04'55"	119°28'40"	740.2	79.0	0.309	0.7088
E4	alaskite	49°02'48"	119°20'38"	5.72	344.1	181.8	1.166
Sample Suite: quartz monzonite (Unit VII of Ryan, 1973)							
D1	qtz. monzonite	49°08'20"	119°26'35"	101.0	175.1	5.022	0.7186
Dm1	muscovite	"	"	36.38	615.8	49.23	0.7622
D2	qtz. monzonite	49°08'15"	119°26'25"	99.77	180.5	5.238	0.7168
Dm2	muscovite	"	"	42.09	596.6	41.2	0.7562
D3	qtz. monzonite	49°08'10"	119°26'17"	133.8	160.6	3.474	0.7134
D4	"	49°07'50"	119°21'35"	257.7	92.72	1.041	0.7083
D5	"	49°07'40"	119°21'30"	243.5	100.0	1.188	0.7079

Previous Rb-Sr Analytical Data

Sample #	Description	Latitude	Longitude	ppm Sr	ppm Rb	$^{87}Rb/^{86}Sr$	$^{87}Sr/^{86}Sr$
Sample Suite: late quartz monzonite (Unit VIII of Ryan, 1973)							
C1	qtz. monzonite	49°11'35"	119°28'00"	1941.0	51.1	0.142	0.7070
Cb1	biotite	"	"	449.4	804.0	5.181	0.7169
C2	altered, saussuritized, fractured	49°11'02"	119°27'30"	456.0	151.7	0.963	0.7092
C3	qtz. monzonite	49°12'10"	119°26'30"	1003.0	66.4	0.192	0.7119
Sample Suite: Oliver pluton (Armstrong)							
O1	granite	49°11'29"	119°33'07"	10.6	314	87.56	0.9014
O1-m	muscovite	"	"	4.1	1199	1057.0	3.253
W-65-7	muscovite from Gypo mine	49°11'45"	119°33'31"	12.9	1813	448.0	1.744
Sample Suite: Olalla area plutons (Armstrong)							
HP2	hb andesite	49°18'09"	119°47'48"	555	29.3	0.158	0.7071
HP1	porph hb andesite	49°18'31"	119°47'39"	510	29.5	0.167	0.7058
Gd-Olalla	granodiorite	49°18'43"	119°48'34"	533	125	0.679	0.7059
Horn Silver	hb monzonite	49°03.4'	119°41.5'	1638	142	0.251	0.7045

Rb-Sr Analytical Data
from this study

Sample #	Description	Latitude	Longitude	ppm Sr	ppm Rb	$^{87}Rb/^{86}Sr$	$^{87}Sr/^{86}Sr$
Sample Suite: Oliver pluton (Jpgr)							
DP275.1	hb-bi granod.	49°12.1'	119°31.2	395	154	1.127	0.7094
DP275.2	"	"	"	365	163	1.293	0.7098
DP245.2	"	49°11.6'	119°34.0'	462	204	1.276	0.7091
Sample Suite: U-Pb samples							
DP156	plag. gneiss	49°18.0'	119°31.5'	409	63	0.446	0.70466
gneissic sill of Vaseaux Lake							
DP95	gar-bi granite	49°03.5'	119°21.1'	350	151	1.246	0.7106
granite of Anarchist Mtn.							
DP179	hb granod. gneiss	49°24.5'	119°34.0'	1004	44	0.129	0.7095
gneiss of Skaha Lake							
DP246	hb granodiorite	49°02.0'	119°41.5'	640	125	0.564	0.7056
Similkameen batholith							
DP90	bi gneiss	49°18.5'	119°30.2'	772	51	0.190	0.7061
leucogneiss							

*(See Appendix C for procedures and error estimates).

Geochronometry - This Study

Detailed mapping done west of the Okanagan Valley by Bostock (1940, 1941a, 1941b) and east of the Okanagan Valley by Ryan (1973), and Christie (1973), along with the regional map of Little (1961) provided a basis for the U-Pb study undertaken (Fig. 40).

Two samples from west of the Okanagan Valley fault and six samples from the Okanagan Metamorphic and Plutonic Complex east of the fault were dated using analytical procedures given in Appendix B. A summary of analytical data and dates is given in Table 9, with complete analytical data and rock descriptions in Appendix B. All U-Pb errors stated are at a 2 σ level (95% confidence limit).

West of the Okanagan Valley

Similkameen batholith (DP246)

The Similkameen batholith is a mesozonal hornblende granodiorite (Fig. 2). It crosscuts structures in the lPz-Tr unit and is itself undeformed (Bostock, 1941a; Fox et al., 1977). Fox et al. (1977) published K-Ar dates of 171 and 177 Ma for hornblendes of the Similkameen batholith. To confirm this a sample for U-Pb analysis was collected from the northern border of this batholith, southeast of Keremeos (Fig. 40). Two zircon fractions (Table 9) were analysed (Fig. 41). The coarse nonmagnetic fraction is concordant at 170$\pm$2 Ma, and the fine magnetic fraction is slightly discordant at 169$\pm$2 Ma. The zircons appear to be magmatic, and are colorless to slightly pink, euhedral with occasional opaque inclusions. The discordance, which can be attributed to minor low temperature lead loss, is not considered significant because at the 95% confidence level the ages for the two fractions overlap. The U-Pb date of 170$\pm$2 Ma confirms the K-Ar date and represents the crystallization age of the

Table 8

Previous U-Pb Geochronometry

Sample #	Fraction	Dates Ma $^{206}Pb/^{238}U$ $^{207}Pb/^{235}U$ $^{207}Pb/^{206}Pb$	Source
CAa76-3 foliated hb granod.	very coarse	68.3 68.5 73.4	G.S.C. Wanless and Loveridge (unpublished; Okulitch, pers. comm.)
	coarse nonmag.	67.8 68.0 72.0	
	fine magnetic	67.2 67.1 64.4	
O-176E	?	87.3 100.0 ---	Fox et al.,1976
Oliver pluton	?	151.9 +/- 2 152.1 +/- 3 156.2 +/- 15	Ryan and Armstrong, unpublished.

Table 9

U-Pb isotopic data

size (μ)		weight (mg)	U (ppm)	rad. Pb (ppm)	Isotopic abundance[1] Pb 206 = 100: 207	208	204	Measured $^{206}Pb/^{204}Pb$	Dates (Ma) +/- 2σ error[2,3]: $^{206}Pb/^{238}U$	$^{207}Pb/^{235}U$	$^{207}Pb/^{206}Pb$
DP156; gneissic sill of Vaseaux Lake											
45-75	M	37.4	1474	20.5	4.8808	3.0853	0.0002	38,426	95.7±1.0	97.3±1.0	137.3±8.2
45-75	NM	0.3	3594	49.4	4.8454	1.7174	0.0085	2,005	95.8±1.2	94.4±1.8	59.7±38
75-150	NM	38.5	1272	17.4	4.8855	1.7445	0.0006	20,105	95.6±1.0	97.3±1.0	136.9±5.8
>150	NM	3.9	1620	22.6	4.9296	1.8944	0.0028	17,459	97.2±1.0	99.0±1.2	142.3±12.8
Oso; gneiss of Osoyoos											
45-75	M	37.6	464	14.2	5.0794	7.6381	0.0016	19,421	200.2±2.2	201.8±2.0	220.7±8.4
45-75	NM	0.6	891	27.8	5.2043	8.6363	0.0105	5,384	201.7±2.2	203.0±2.8	218.2±22.6
75-150	NM	27.5	476	14.5	5.0651	7.1205	0.0005	19,468	200.5±2.2	202.2±2.0	221.9±6.0
DP95; granite of Anarchist Mtn.											
45-75	M	31.9	7852	185	4.9749	4.2912	0.0015	36,116	159.7±1.8	160.6±1.6	172.9±5.8
75-150	NM	39.0	3983	94.6	4.9660	4.2654	0.0003	34,856	160.9±1.8	162.0±1.6	176.9±4.8
DP246; Similkameen batholith											
45-75	M	36.4	633	17.3	5.4754	13.7505	0.0338	2,555	168.6±1.8	169.7±1.8	185.3±13.6
75-150	NM	35.2	488	13.6	5.9722	13.4675	0.0700	1,000	169.9±1.8	169.8±2.0	168.6±17.0
DP90; leucogneiss											
45-75	M	31.6	1111	18.5	5.3178	4.4765	0.0032	11,877	112.9±1.2	122.6±1.2	316.3±6.4
45-75	M	14.9	1132	18.8	5.4198	4.3973	0.0017	21,819	112.6±1.2	125.1±1.2	368.6±6.0
45-75	NM	16.4	1080	18.33	5.3411	4.5535	0.0032	12,864	114.7±1.2	125.1±1.2	326.1±5.8
75-150	NM	16.4	954	17.4	5.5007	5.0930	0.0032	11,107	122.2±1.4	136.5±1.4	393.1±5.6
>150	NM	9.5	845	15.5	5.1965	7.6540	0.0091	6,774	120.7±1.4	125.8±1.2	223.8±7.0

U-Pb isotopic data

size (μ)		weight (mg)	U (ppm)	rad. Pb (ppm)	Isotopic abundance[1] Pb 206 = 100: 207	208	204	Measured $^{206}Pb/^{204}Pb$	Dates (Ma) +/- 2σ error[2,3]: $^{206}Pb/^{238}U$	$^{207}Pb/^{235}U$	$^{207}Pb/^{206}Pb$
DP179; gneiss of Skaha Lake											
45-75	M	34.2	308	4.7	4.9393	10.0325	0.0064	5,885	98.7±1.0	99.7±1.2	121.6±13.2
75-150	NM	33.0	381	6.1	4.9574	9.4778	0.0064	4,233	104.3±1.2	105.4±1.2	130.1±16.0
DP300; rhomb porhyry											
45-75		1.6	1100	9.5	5.8566	18.0336	0.0658	799	51.5±0.6	53.4±0.8	142.2±25
75-150	NM	1.4	1923	16.1	5.6498	15.7190	0.0661	617	50.9±0.6	50.6±1.8	36.7±40
Olalla Syenite											
45-75	NM	6.7	1341	51.2	5.1738	46.3786	0.0060	9,279	185.6±2.0	189.2±1.8	234.6±6.2

[1] Corrected for blank with composition = $^{208}Pb/^{204}Pb$: 37.00; $^{207}Pb/^{204}Pb$: 15.54; $^{206}Pb/^{204}Pb$: 17.75.

[2] Isotopic composition of common Pb is based on $^{207}Pb/^{206}Pb$ age and is derived from the growth curve of Stacey and Kramers (1975).

[3] $\lambda_{238} = 0.155125 \times 10^{-9}/yr$; $\lambda_{235} = 0.98485 \times 10^{-9}/yr$; $^{238}U/^{235}U = 137.88$.

M = Magnetic fraction (magnetic at 1.5A and 0.5° side tilt on Franz); NM = Nonmagnetic.

intrusive.

Olalla Syenite (Ol-Sy)

A sample of the Olalla Syenite Complex (Sturdevant, 1963) was collected by R.L. Armstrong, and dated in this study (Fig. 41). More work is required, but one fraction (fine) from this rock is slightly discordant at 185-189 Ma. This supports a K-Ar hornblende date on this body of 184 Ma from Queens University reported by Okulitch et al. (1977).

Samples from the Okanagan Metamorphic and Plutonic Complex

Two samples were collected from B. Ryan's Ph.D. thesis area (his Units V and VIII). One (the gneiss of Osoyoos, unit V) is exposed at the lookout above Osoyoos on Highway 3. Ryan interpreted it to be possibly syn-F_1, but definitely pre-F_2, and the oldest granitic unit in the succession.

gneiss of Osoyoos (Oso)

Three zircon fractions (Table 9) were analysed. All three are very slightly discordant at 201.5 Ma (Table 9 and Fig. 41,) the $^{207}Pb/^{206}Pb$ dates are 219±20Ma. The zircons appear to be magmatic, and are transparent, pink, generally euhedral with common cloudy cores. The intrusive age is interpreted to be 201.5±2.2 Ma (Early Jurassic). The discordance, though slight, may be ascribed to inheritance, or to slight lead loss from a latest Triassic pluton. A geologic maximum age limit for this pluton is mid-Permian to early Triassic, the age of the Anarchist Group which is intruded by the body. A minimum age is 150 Ma, provided by a Rb-Sr whole rock date on an aplite from the Osoyoos lookout (Table 7; Armstrong, unpublished). Both K-Ar and Rb-Sr mineral dates from this gneiss are Eocene.

granite of Anarchist Mtn. (DP95)

The other unit from Ryan's thesis area is a slightly foliated garnet-biotite granite (Unit VIII of Ryan, 1973). This unit is interpreted by Ryan to have been emplaced late in the deformation (post F_2 and pre- or syn-F_3). Two fractions of zircon (Table 9) were analysed and plot very near (within two sigma error) concordia at 160.2±1.8 Ma and 161.4±1.8 Ma. The $^{207}Pb/^{206}Pb$ ages are 173 Ma and 177 Ma, and probably represent an upper age limit (Fig. 41). The zircons, interpreted to be magmatic, are generally euhedral but highly fractured, and cloudy. The discordance, though very slight, is probably attributable to inheritance, particularly with the hint of S-type character of the intrusive. The interpretation is that 160.5±2 Ma represents a minimum crystallization age.

Three samples were collected from Christie's thesis area at Vaseaux Lake: 1) A crosscutting, but foliated, intrusive sill (gneissic sill of Vaseaux Lake); 2) The leucogneiss body north of Covert Farms; 3) the rhomb porphyry sill at Covert Farms. The latter two are also within the area mapped for this study.

1) gneissic sill of Vaseaux Lake (DP156)

This gneissic sill (Fig. 42) was collected 0.5 km east of Vaseaux Lake where it crosscuts the paragneiss but is itself foliated and lineated. Four zircon fractions (Table 9) from this rock plot between 95.5 and 97.2±1.2 ($^{206}Pb/^{238}U$ ages). The $^{207}Pb/^{206}Pb$ dates for the fine magnetic, coarse nonmagnetic, and very coarse fractions are all approximately 140±10 Ma. The fine nonmagnetic handpicked fraction (0.3 mg) is essentially concordant, although slightly above concordia, at 95.8±1.2 Ma ($^{206}Pb/^{238}U$ age; Fig. 43). The zircons are transparent, slightly pink, euhedral, with no visible cores; they are interpreted to be magmatic. The minimal spread of these analyses, with large variation in uranium and lead content, suggests that lead loss is probably not significant (not > 5 percent) and that the intrusive age for this gneissic sill is

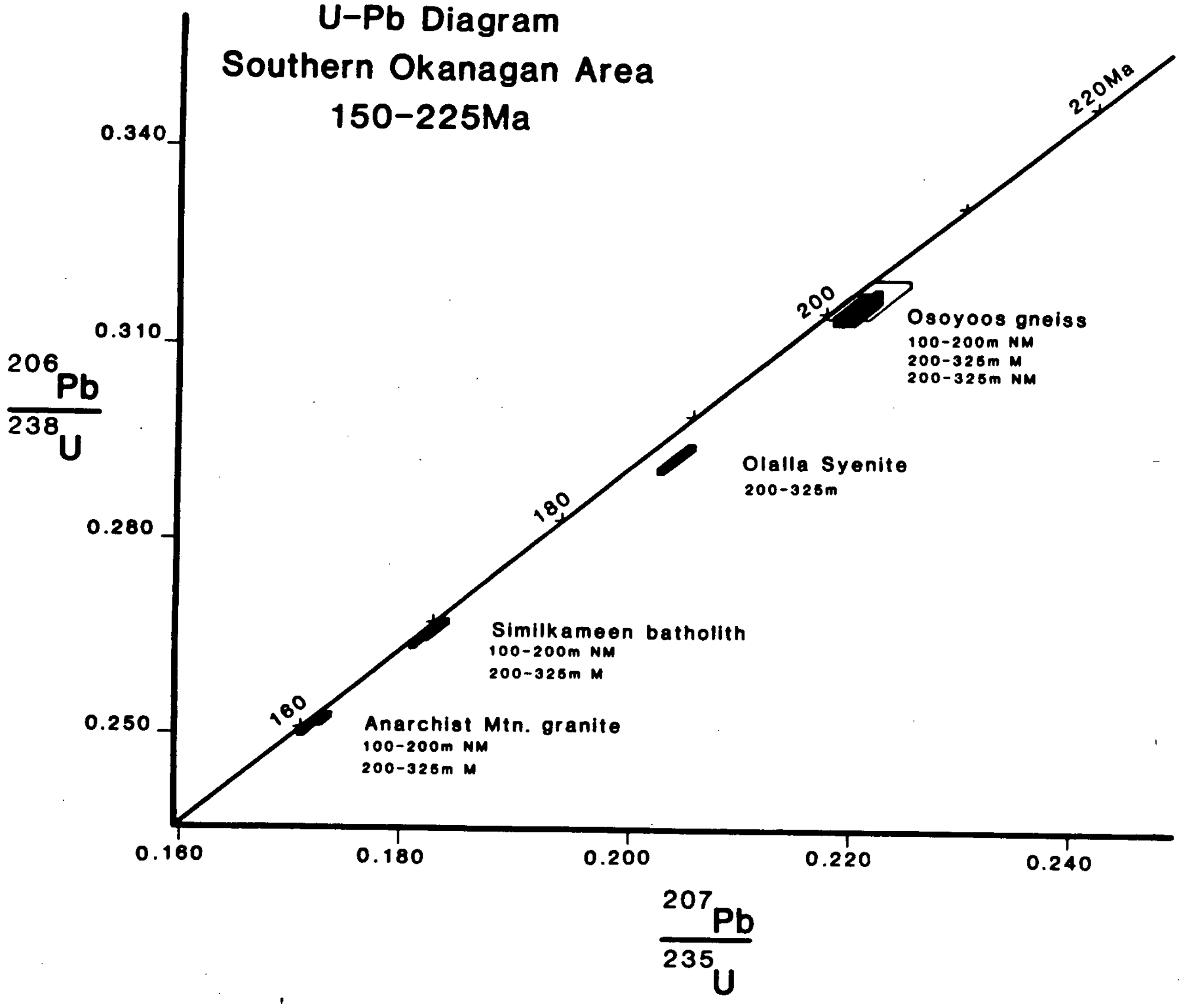

Figure 41: Enlargement of 150–225 Ma section of U–Pb concordia diagram.

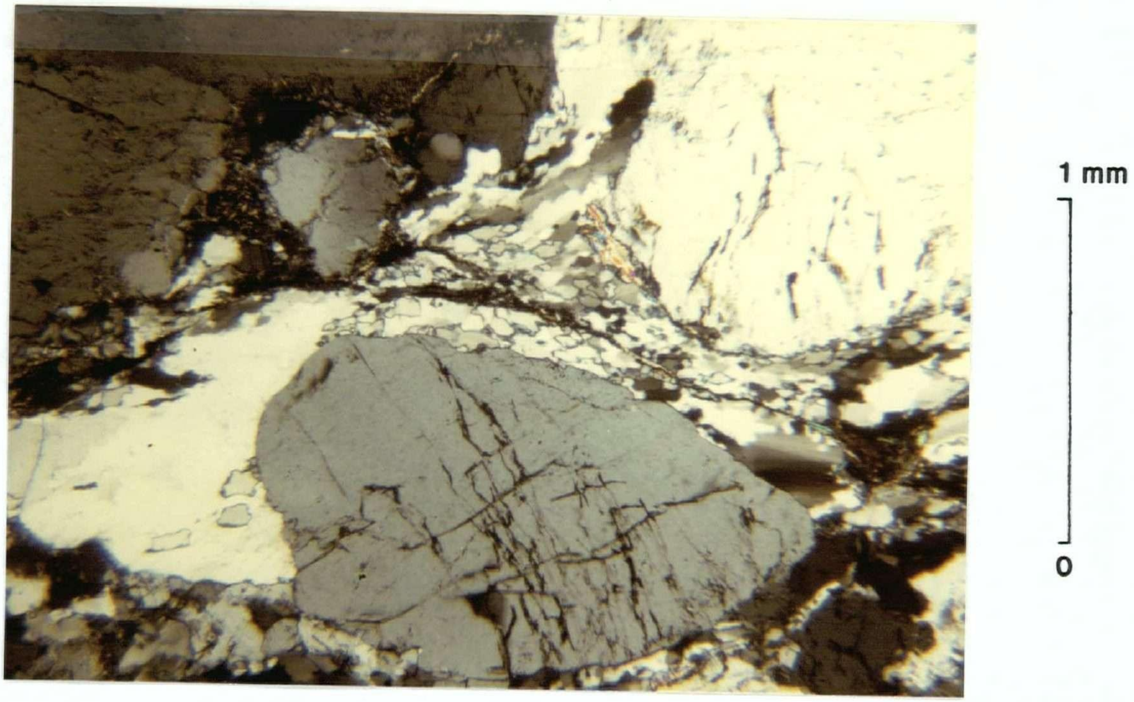

Figure 42: Photomicrograph showing deformation in gneissic sill of Vaseaux Lake.

Figure 44: U-Pb sample locality for gneiss of Skaha Lake, note deformed mafic dikes(?).

probably on the Early–Late Cretaceous boundary.

2) leucogneiss (DP90)

The leucogneiss north of Covert Farms has not yielded an interpretable zircon array after analysing five fractions. The zircons are clear, euhedral, with common cloudy cores and apparent overgrowths. The points are all discordant and scatter between 112 Ma and 135 Ma (Fig. 43). Unlike most discordant zircons, these do not lie along a single line but instead plot in a cluster. A probable interpretation (there are an infinite number of interpretations) is that the leucogneiss body was intruded in the Jurassic, based on the Rb–Sr errochron (Fig. 39; Armstrong, unpublished), and was subjected to later metamorphism. This would have to have occured in post–Aptian time based on the discordance pattern of the zircons. The problem is compounded by a small inherited component and possible later low temperature lead loss.

3) rhomb porphyry (DP300)

The rhomb porphyry body (as described in Chapter 3) was collected from the north edge of Covert Farms (Plate 1). At this locality the rhomb porphyry can be followed for 1 km as it cuts through the paragneiss and leucogneiss. It is deformed and metamorphosed. Two zircon fractions (both very small amounts) were analysed. The zircons are slightly to deeply pink colored, equant, and barrel shaped. They are interpreted to be magmatic. The fine zircon fraction from this rock plots very nearly concordant at 52±1 Ma, a second (coarser) fraction is concordant at 51±1 Ma (Fig. 43). The slightly discordant point probably indicates traces of xenocrystic zircon, and the concordant date of 51±1 Ma is interpreted to be the crystallization age. The deformed rhomb porphyry is therefore equivalent in age to the basal rhomb porphyry flows of the Marron Formation, as has long been inferred but never proven, and in accord with U–Pb ages of Coryell syenites dated by Parrish (pers. comm., 1985).

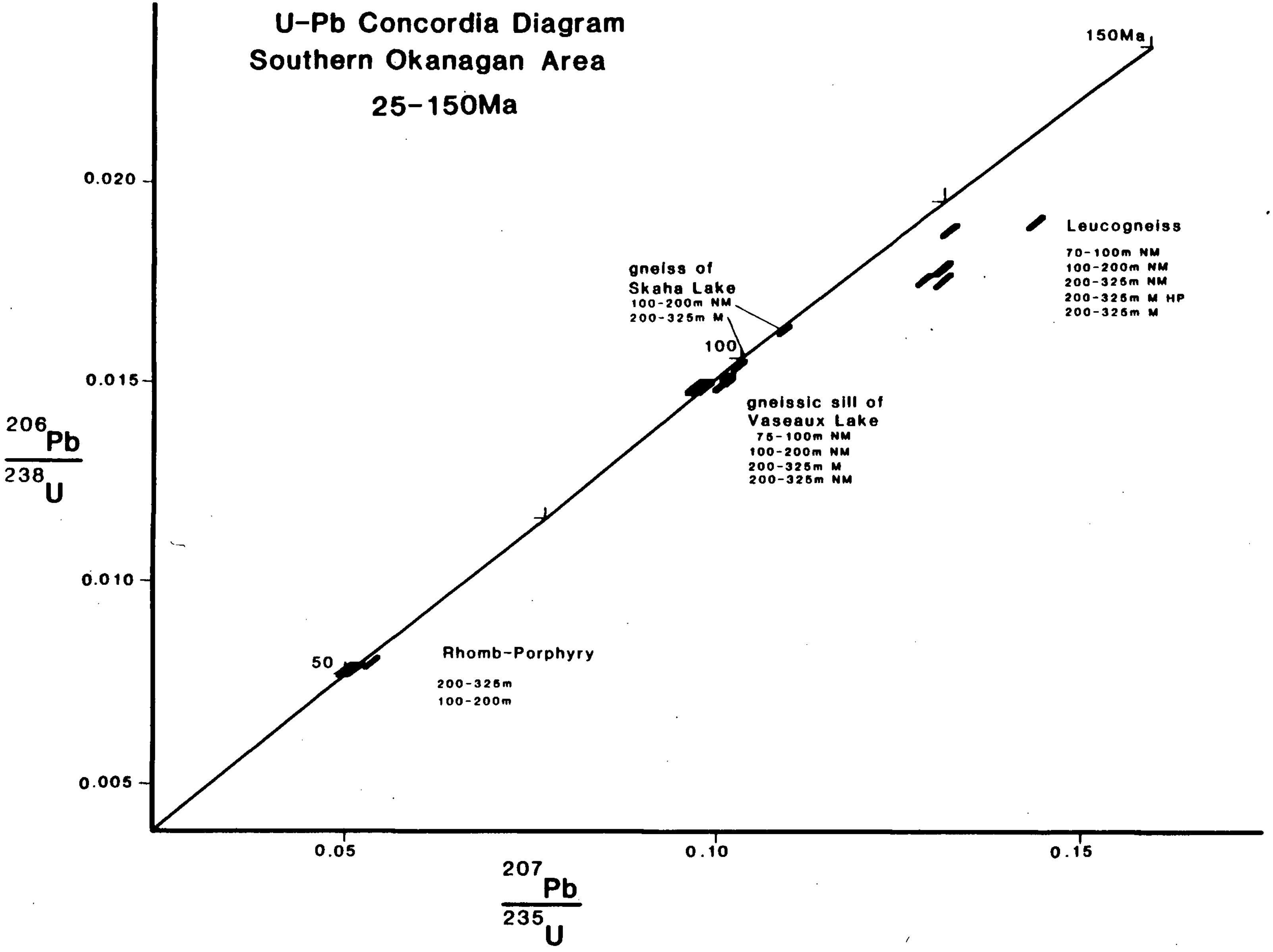

Figure 43: Enlargement of 25–150 Ma section of U–Pb concordia diagram.

gneiss of Skaha Lake (DP179)

The other unit sampled east of the Okanagan Valley, but not in Ryan or Christie's thesis areas, is a large gneissic granodiorite mapped by Little (1961) as crosscutting the paragneiss but itself foliated and lineated. The outcrop sampled (Fig. 44) is on Skaha Lake, 5.5 km south of Penticton.

Two zircon fractions were analysed, both are slightly discordant: the fine magnetic fraction discordant at 99.5±1.2 Ma ($^{207}Pb/^{206}Pb$ age = 122±12 Ma), the coarse nonmagnetic discordant at 104.5±1.2 Ma ($^{207}Pb/^{206}Pb$ age = 130±16 Ma) (Fig. 43). There are no cores visible in the zircons, which are clear, and generally euhedral. This is interpreted as a Cretaceous intrusive that was subsequently metamorphosed. The discordance could be due to lead loss, in which case the Cretaceous dates represent a minimum age for the intrusive. If lead loss was significant then this intrusive could be as old as Jurassic.

The discordance of zircons from the leucogneiss north of Covert Farms (in addition to an inherited component), the gneissic sill of Vaseaux Lake, and the gneiss of Skaha Lake, is inferred to be due to metamorphism and deformation. During the metamorphic event the zircons either lost lead or overgrowths of new zircon developed (or both). The latter interpretation is favoured based on the nonmetamict character of the zircons and work done by Mattinson (1972, and 1978) and Williams et al. (1984). Either interpretation is viable however, given the present data. The lead loss or zircon growth episode would have to be in post-middle Cenomanian time.

Summary of Geochronometry

The K–Ar work in the southern Okanagan demonstrates that the volcanic rocks of White Lake Basin, and equivalents, are Eocene and that the intrusive age for plutonic rocks west of the Okanagan Valley is generally Jurassic. The gneisses of the Okanagan Metamorphic and Plutonic Complex have had an Eocene thermal overprint however, and therefore their original ages are not obtainable by K–Ar techniques.

The Rb–Sr work done in the Okanagan has documented Jurassic and Paleocene–Eocene intrusives to the west of the valley. In addition unpublished data of Armstrong and Ryan indicate Jurassic intrusives both east and west of the Southern Okanagan Valley. This data also shows that, like K–Ar, the Rb–Sr mineral dates on the Okanagan Metamorphic and Plutonic Complex are Paleocene and Eocene.

The results of the U–Pb geochronometry reveal:

–Early Jurassic or Late Triassic intrusive within the Okanagan Metamorphic and Plutonic Complex (gneiss of Osoyoos).

–Middle to Late Jurassic intrusives both east (granite of Anarchist Mtn., deformed) and west (Oliver pluton, Similkameen batholith, and Olalla Syenite, all undeformed) of the Okanagan Valley.

–Jurassic or Cretaceous intrusives (leucogneiss north of Covert Farms, gneiss of Skaha Lake, gneissic sill of Vaseaux Lake, all deformed) within the Okanagan Metamorphic and Plutonic Complex.

–Eocene intrusive (rhomb porphyry, deformed) within the Okanagan Metamorphic and Plutonic Complex.

Discussion

A plot of closure temperature versus age (cooling curve) has been constructed for the gneisses east of the Okanagan Valley using K–Ar, fission track, and Rb–Sr muscovite data (Medford, 1975; Armstrong, unpublished) (Fig. 45). Also plotted are zircon ages and closure temperatures from the rhomb porphyry, gneissic sill of Vaseaux Lake, and gneiss of Skaha Lake. Closure temperatures for K–Ar and fission track dates are from Harrison (1981) and Harrison and McDougall (1980, and 1982). (For an alternate assessment of the K–Ar closure temperature concept in amphiboles, see Deutsch and Steiger, 1985). For zircons, estimates of closure temperatures are from Parrish and Roddick (1985), and Mattinson (1978). Rb–Sr muscovite–whole rock closure temperatures are estimated at $550^{\circ} \pm 50^{\circ}C$ (Wagner et al., 1977).

A Rb–Sr muscovite–whole rock date of 58 Ma from the leucogneiss north of Covert Farms indicates that the gneisses were below approximately $600^{\circ}C$ by this time. The K–Ar hornblende dates (with closure temperature of approximately 530° C) cluster with minimal spread around 51 Ma. Both the K–Ar biotite and fission track sphene dates have considerable spread, both in age and error; the fission track apatite is well constrained (closure temperature = $105^{\circ}C$) between 44 and 48 Ma. This data alone dictates that the gneisses of the Okanagan Metamorphic and Plutonic Complex cooled through $400^{\circ}C$ in 3–10 Ma.

Assuming a geothermal gradient it is possible to calculate the depth of the gneisses at 51 Ma, and at 45–48 Ma (Fig. 46), and thereby estimate uplift rates during that time interval. Using $50^{\circ}C$/km, the gneisses would have been uplifted from 11 km (at 51 Ma) to 2 km (at 45–48 Ma); this implies a 2–4 mm/yr uplift and erosion rate. Using $30^{\circ}C$/km, a more reasonable estimate (being the present-day Basin and Range geothermal gradient according to Eaton, 1982), the gneisses would have been uplifted from 18 km (at 51 Ma) to 3 km (at 45–48 Ma); this implies a 3–5

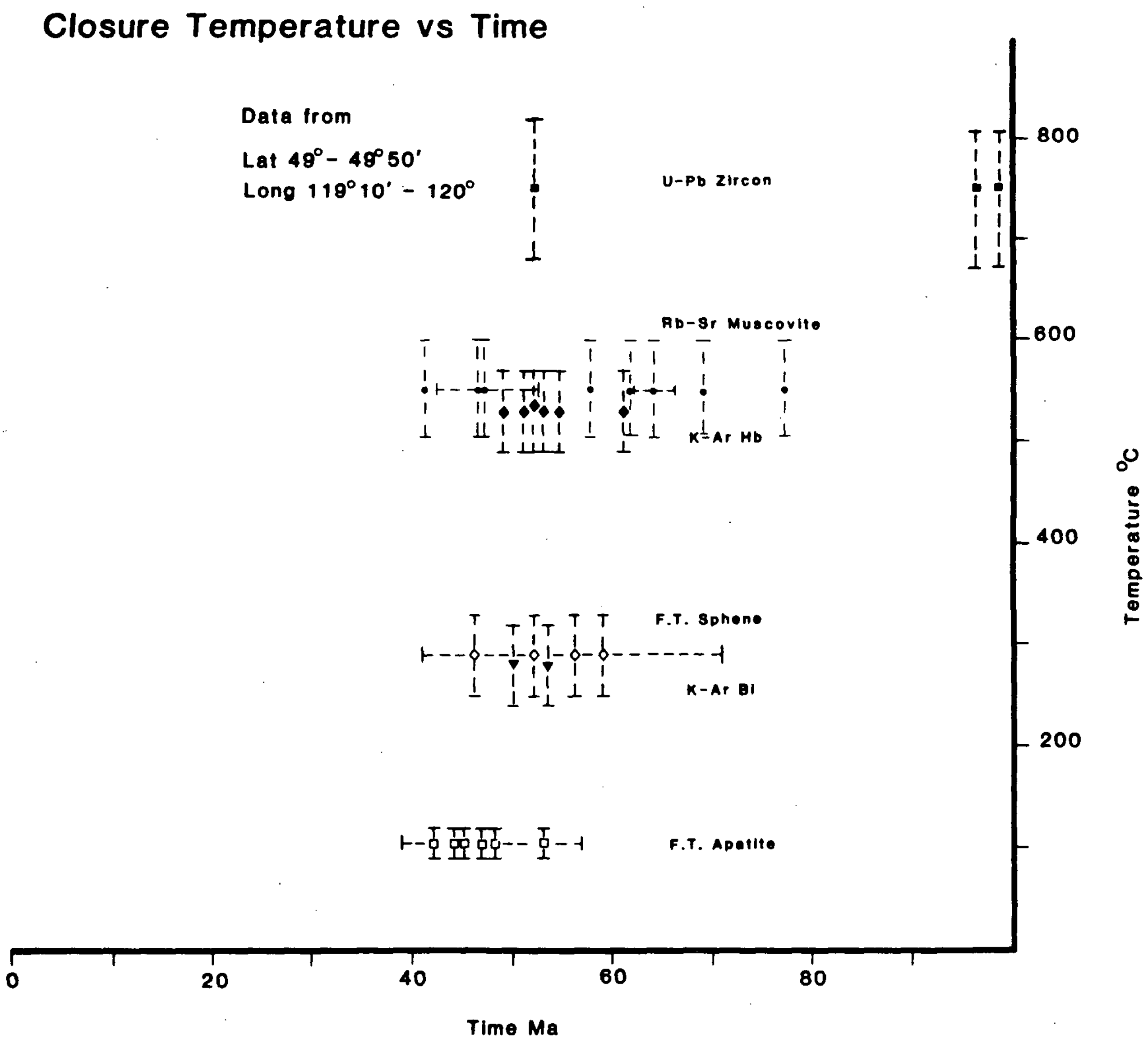

Figure 45: K–Ar, fission track, and muscovite Rb–Sr mineral dates versus their respective blocking temperature for gneisses of the Okanagan Metamorphic and Plutonic Complex; sources: Ryan (1973), Medford (1975), and Armstrong (unpublished).

Approximate Uplift Rates

Geothermal Gradient	Depth of Gneisses at 51Ma	Uplift Rate a)for 3Ma interval b)for 5Ma interval c)for 10Ma interval
50 C/km	11 km	a) 3 mm/yr b) 1.8 mm/yr c)0.9 mm/yr
30 C/km	18 km	a) 5 mm/yr b) 3 mm/yr c) 1.5 mm/yr

Figure 46: Uplift rates for the gneisses of the Okanagan Metamorphic and Plutonic Complex using assumed geothermal gradients.

mm/yr uplift and erosion rate. In contrast the granitic rocks west of the Okanagan Valley were well below the blocking temperature for hornblende and biotite by 100 Ma, indicating a depth of only 2 to 3 km.

Recent work on uplift of the Himalaya reports rates not much higher than 1 mm/yr and generally much less (Zeitler, 1985). Bradbury and Nolen-Hoeksema, (1985) calculate uplift rates for the Lepontine Alps of between 1 and 2 mm/yr. Taken at face value the Okanagan data require either exceptional erosion rates (filling unknown basins), exceedingly high geothermal gradients, or a tectonic explanation.

V. STRUCTURE

The most important structural feature within the study area is a low-angle (10-20°) west-dipping fault (named the Okanagan Valley fault by D.J. Templeman-Kluit, 1984). In the upper plate of this fault the rocks were deformed in a brittle fashion whereas in the lower plate the rocks were deformed ductily, and show a complex overprint of metamorphic fabrics. This chapter will be divided into four parts 1) upper plate structure; 2) Okanagan Valley fault and related fault rocks; 3) lower plate structure; and 4) timing of deformation.

Upper Plate

The late Paleozoic to Triassic formations were isoclinally folded (Fig. 8) prior to the deposition of the Upper Triassic Nicola Group (Read and Okulitch, 1977). Within the study area this deformation predates the Oliver pluton which is itself unfoliated. Other than the results of this Triassic deformation the predominant structure seen in the upper plate rocks is brittle fracturing. Within the study area, this is best observed in the Oliver pluton, and to the north in the Eocene volcanic and sedimentary rocks of White Lake Basin. Fractures are pervasively developed within the Oliver pluton (Fig. 47). In addition there are distinctive topographic lineaments which contain fault gouge but, in the absence of identifiable markers, any sense and amount of offset is uncertain. Tertiary dikes within the Oliver pluton commonly intrude a fracture system (trend N40E, dip 60-90NW; Fig. 48) and are themselves fractured. Fracturing and faulting in the Oliver pluton is more intense approaching the Okanagan Valley fault; in addition, fractures become predominantly low angle (Fig. 49). Ultimately this intense fracturing produces a monolithologic breccia (Fig. 47). A highly fractured

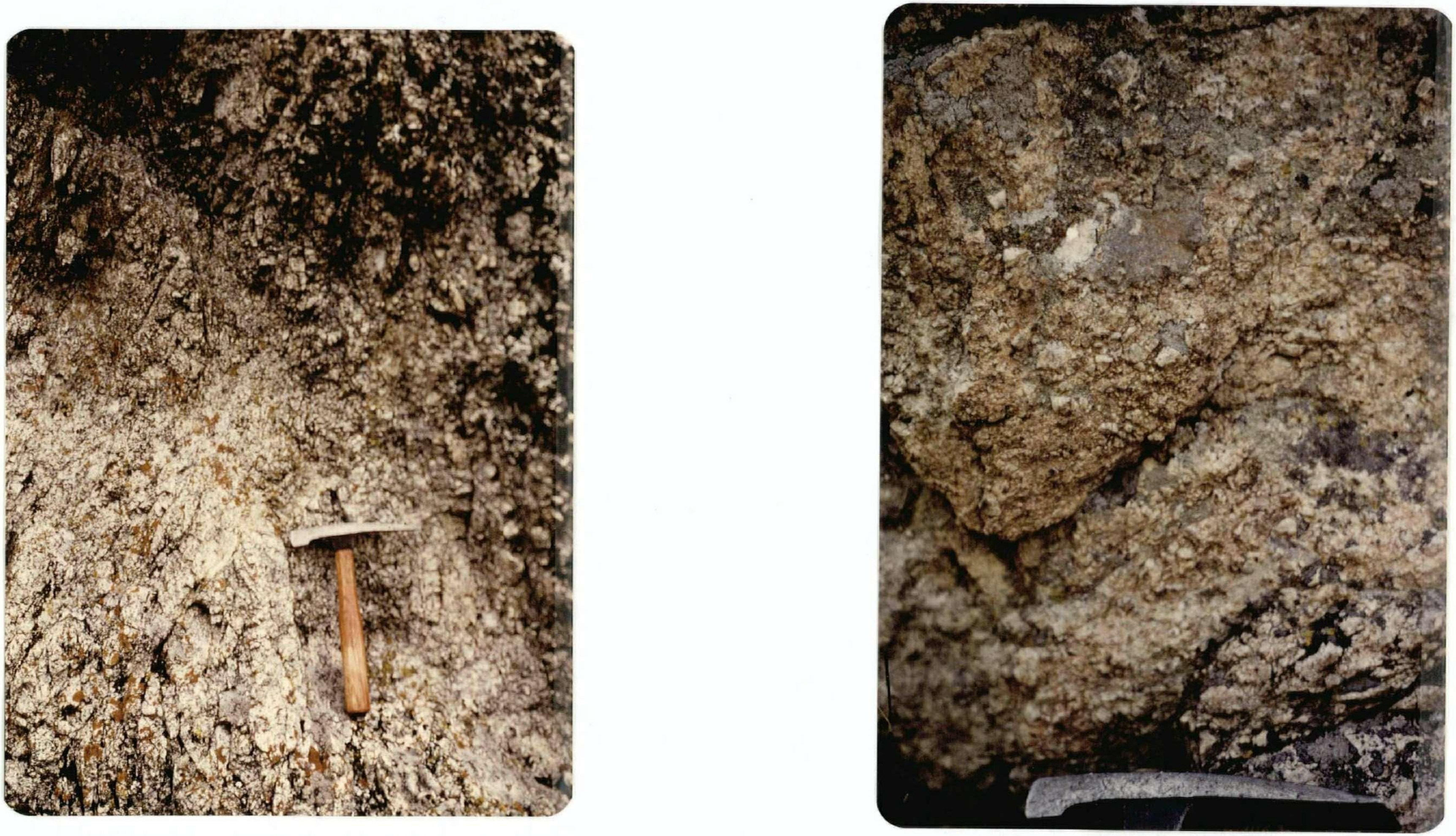

Figure 47: Photographs of fractured and brecciated Oliver pluton.

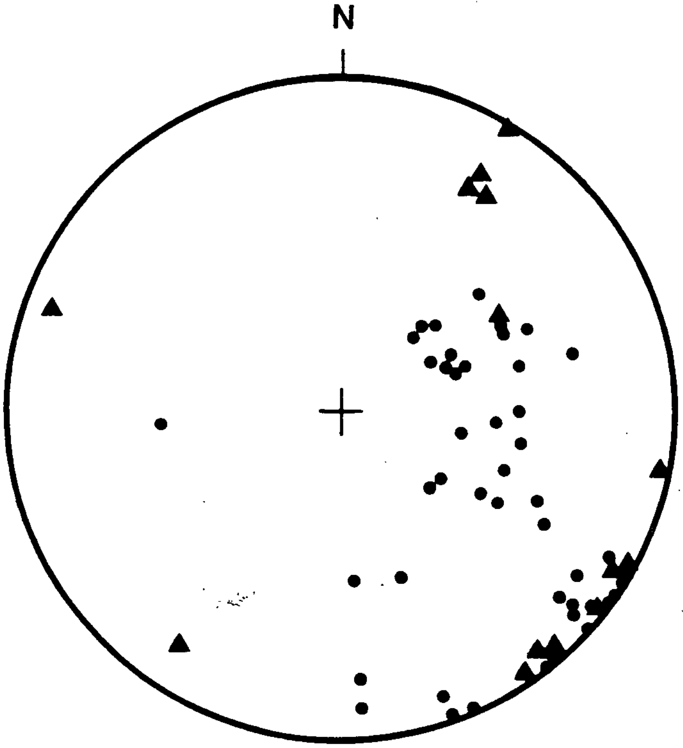

Figure 48: Stereonet of poles to fractures and Eocene dikes in upper plate of Okanagan Valley Fault. Triangles=dikes; dots=fractures.

Figure 49: Photographs of low angle faults and fractures in Oliver pluton.

and faulted section has been documented by Church (1973) in the southeastern White Lake Basin.

In addition to the pervasive northeast-trending northwest-dipping fracture and fault set there are less abundant but possibly large westnorthwest-trending, north-dipping faults in the upper plate. The largest one in the map area is in Orofino Creek and can be followed for several kilometers to the westnorthwest. It separates the Oliver pluton from lPz-Tr rocks. Another north-dipping fault, just north of the map area, separates lPz-Tr from White Lake Basin volcanic rocks. These faults are not well understood, but are restricted to the upper plate. They have normal displacement, and may be partly responsible for the large megabreccias/landslide blocks of lPz-Tr and Oliver pluton in the Skaha Formation.

Okanagan Valley Fault and Related Fault Rocks

The Okanagan Valley fault can be traced from Green Lake where it enters the map area from the north, to southeast of Oliver, where it leaves the map area. It is exposed only locally east of Oliver and at Mahoney Lake, (Fig. 50) where the map pattern shows it to be low angle ($10^\circ-20^\circ$), and west dipping. The fault is, in these exposures, marked by underlying mylonitic pgn, orthogneiss, or ultramylonite (Fig. 51), which grades upward into microfaulted mylonite, brecciated mylonite and ultimately brecciated, chloritized, and silicified upper plate rocks (Fig. 52). This fault everywhere juxtaposes intensely fractured rocks against ductiley deformed rocks. The fault itself was presumably ductile at depth (represented by mylonitic pgn) and brittle at shallow levels (represented by abrupt truncation of the brecciated upper plate). The overprinting of contrasting strain types is seen in brecciated mylonite. In this interpretation the fault embraces a brittle-ductile transition, and now juxtaposes rocks from contrasting strain environments.

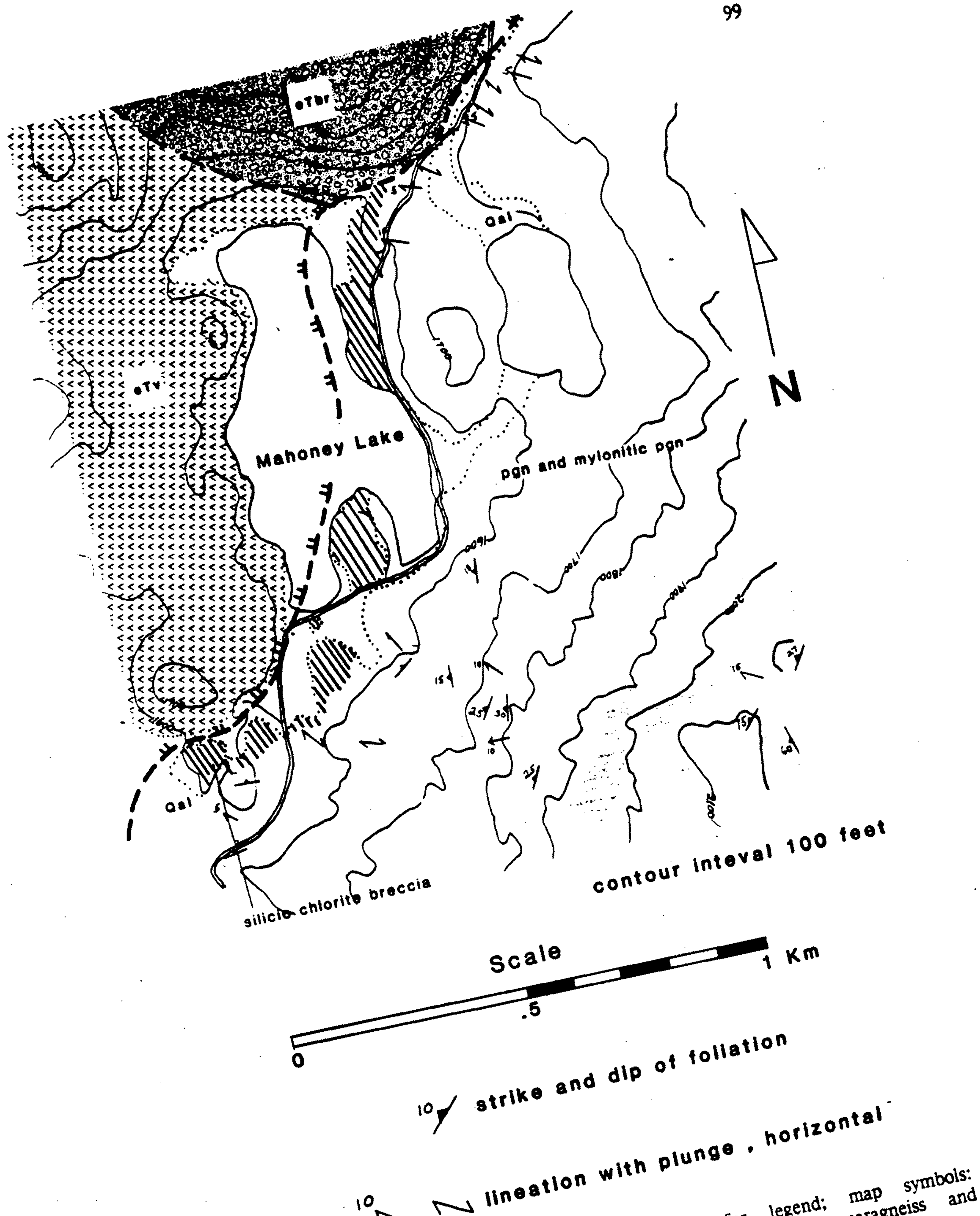

Figure 50: Map of Mahoney Lake; see figure 2 for legend; map symbols: eTv = Eocene volcanic rocks; eTbr = Eocene Skaha Formation; pgn = paragneiss and mylonitic paragneiss.

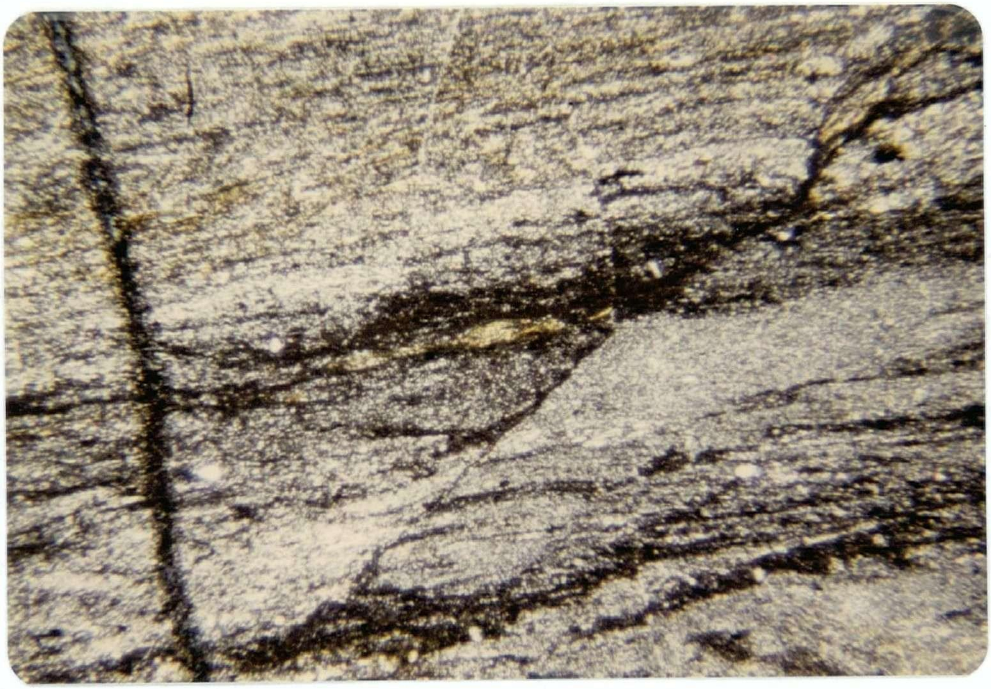

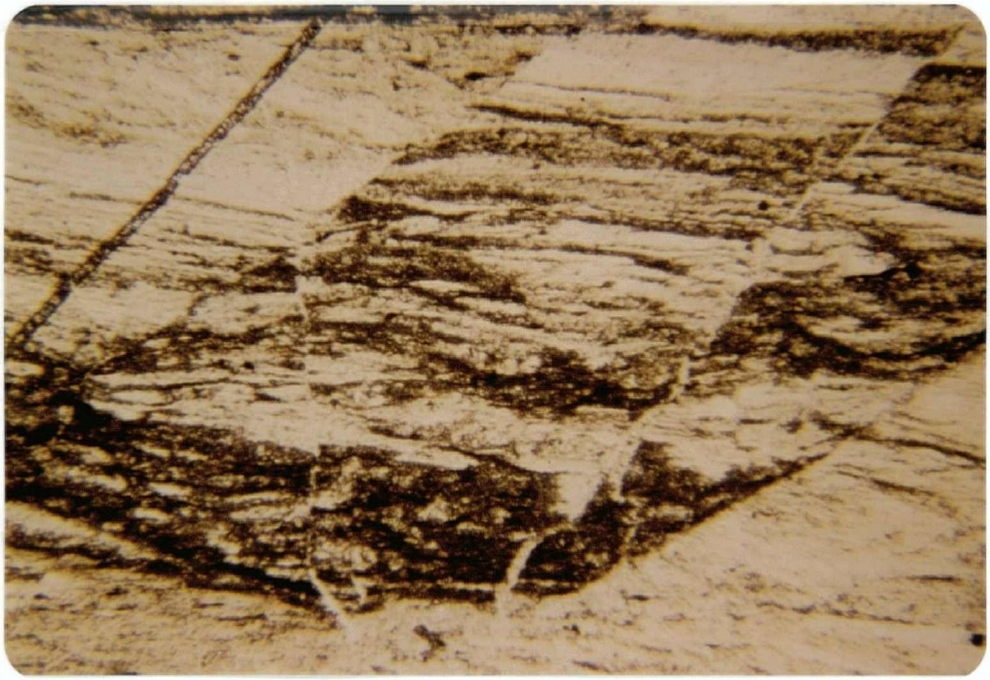

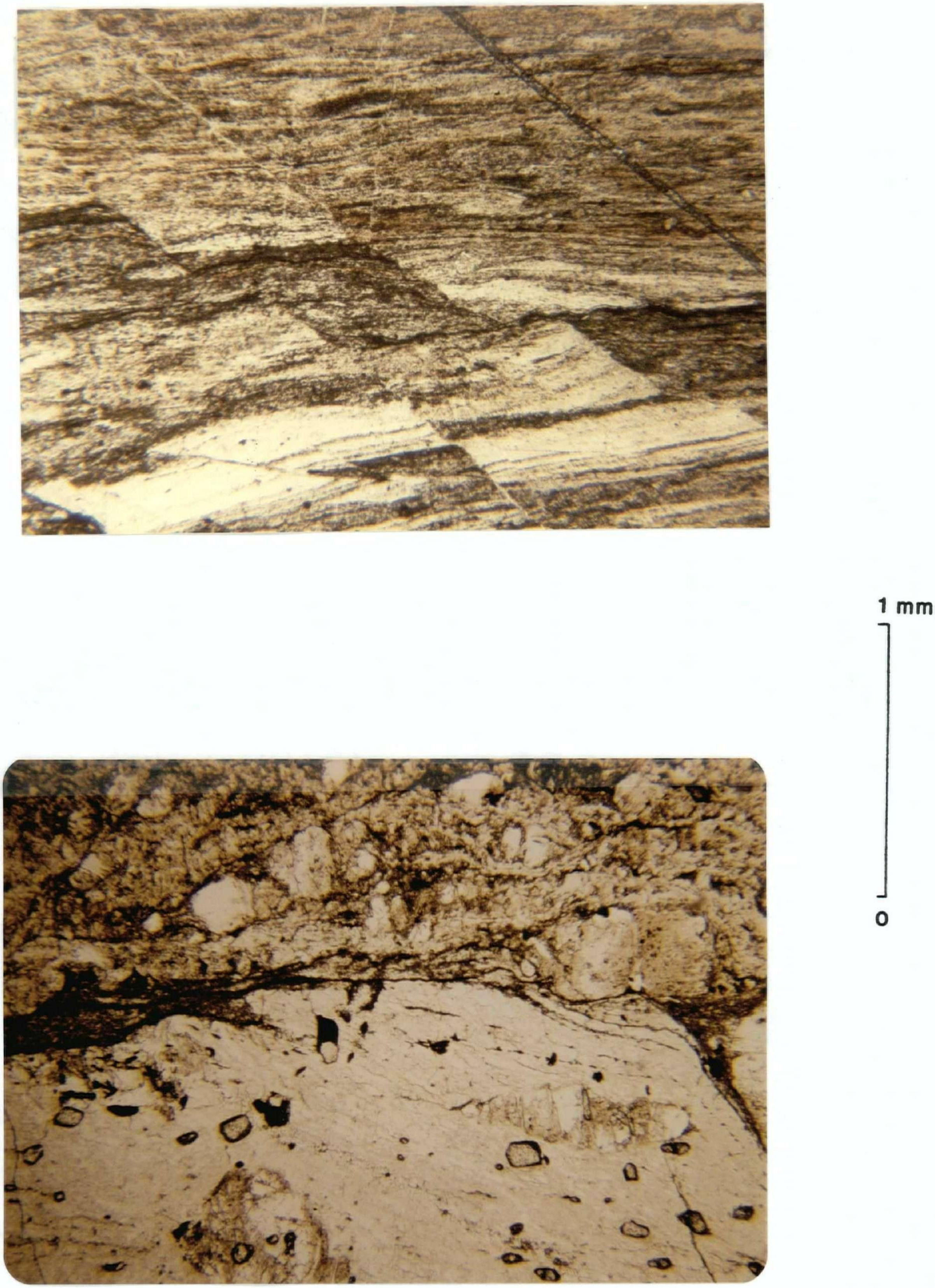

Figure 51: Photomicrographs of mylonitic pgn at Mahoney Lake.

Sense of shear indicators (Simpson and Schmid, 1983) (Fig. 53) from mylonitic rocks at Mahoney Lake are not everywhere unambiguous (Ross, 1973, and 1981) but are interpreted to be consistent with westward movement of the upper plate. This same sense of shear can be seen in asymmetric fabrics (Bell and Etheridge, 1973; Berthe et al., 1980; White et al., 1980; Lister and Snoke, 1984) parallel to the stretching lineation in rhomb porphyry 1 km east of Willowbrook (Fig. 54) and in gneiss east of the Okanagan Valley (Bardoux, 1985; Parrish et al., 1985).

Lower Plate

Rocks structurally beneath the Okanagan Valley fault have been deformed at temperatures of at least $400° - 500°$C. The structural geometry of these gneisses has been well documented (Christie, 1973; and Ross and Christie, 1979), and is summarized in Table 10. The predominant fabric within the gneisses is the foliation (Fig. 55) (F_2 of Christie) which consistently dips gently westward. The leucogneiss body (lgn) has been demonstrated to crosscut the earliest fabric (F_1) but contains the F_2 foliation. This foliation is generally defined by compositional layering and is commonly mylonitic. This mylonitic foliation becomes more common, and more strongly developed structurally upward and towards the west. Within the mylonites there is a consistent stretching lineation, outlined by elongated quartz and pulled apart feldspars (Fig. 56), which trends N65W, 10SW (Fig. 57). F_2 fold axes parallel this stretching lineation (Christie, 1973), and are interpreted to be rotated into parallelism by progressive simple shear (Bell, 1978; Bell and Hammond, 1984). The rhomb porphyry (dated at 51 Ma) can be shown to locally crosscut this mylonitic fabric but is also foliated and lineated parallel to F_2. The post-51 Ma deformation must have been at temperatures higher than $450° - 500°$C (Harrison, 1981), because of garnet and biotite growth in pullaparts of feldspar and pyroxene in the rhomb porphyry, and 51 Ma hornblende dates on the

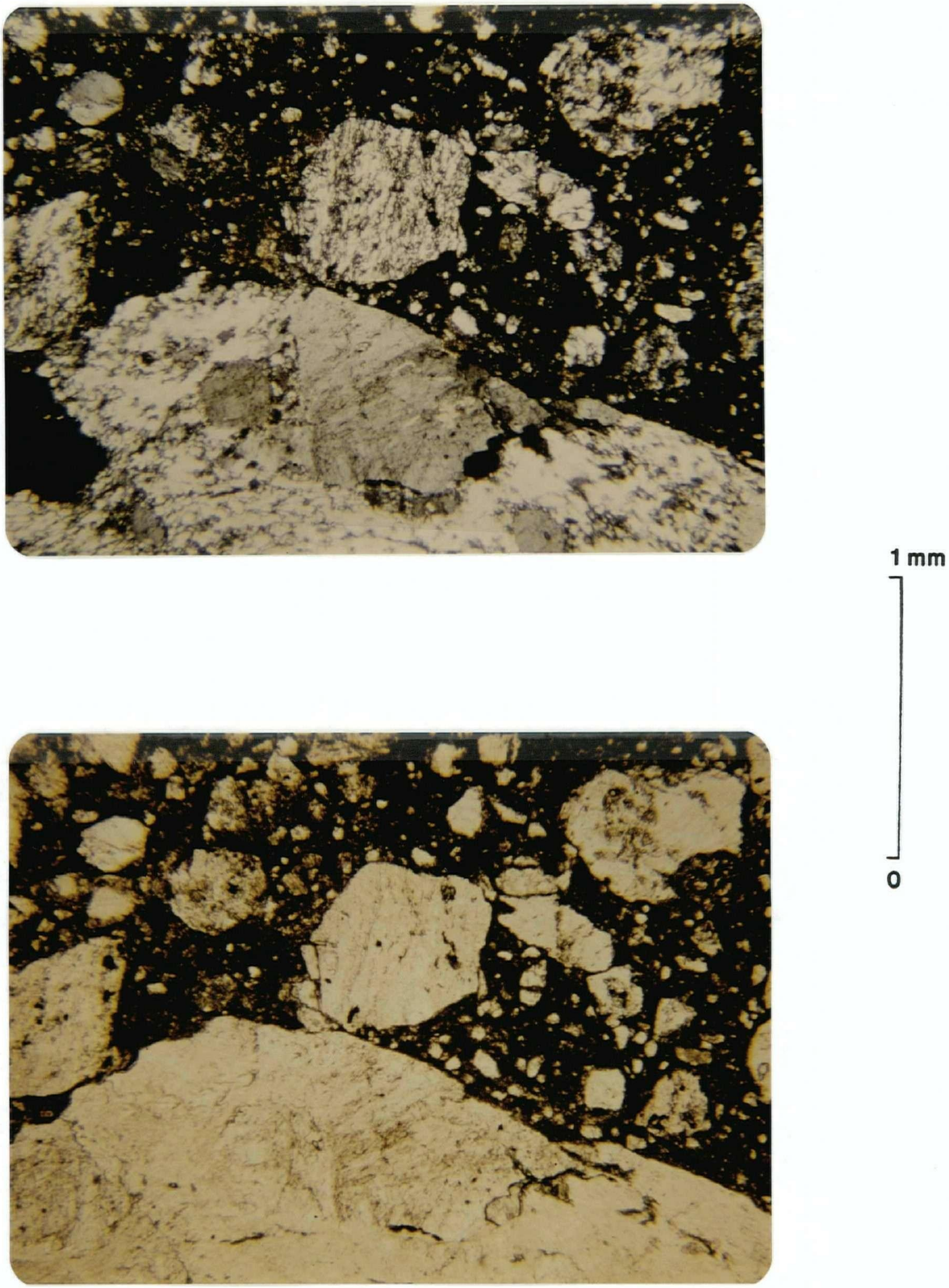

Figure 52: Photomicrographs of brecciated mylonite from Mahoney Lake.

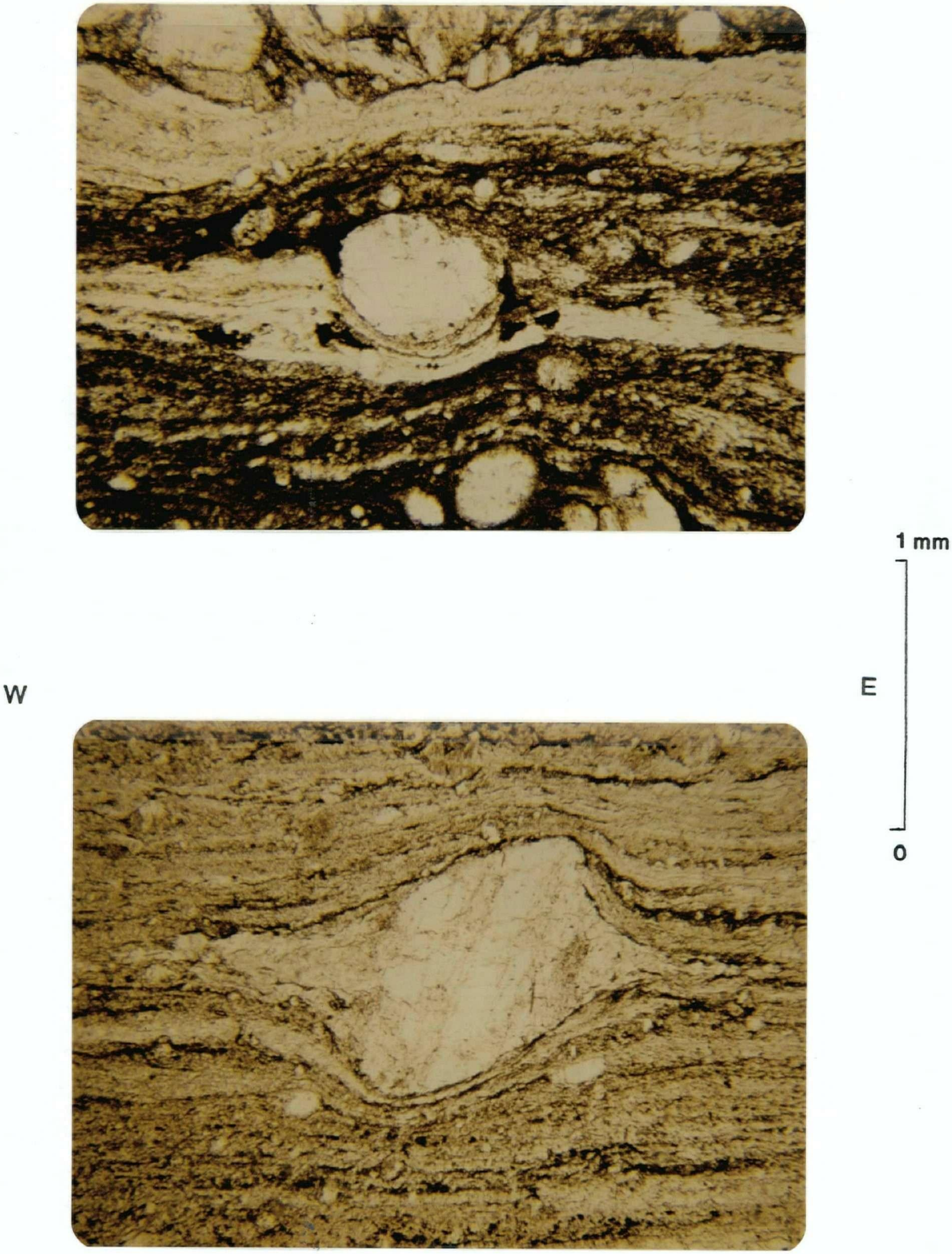

Figure 53: Photomicrographs of mylonites showing sense of shear of top to the west. Looking north.

E

W

Figure 54: Asymmetric fabric (C–S) developed in rhomb porphyry showing sense of shear of top to the west. Looking south.

Table 10

Summary of the Structural Elements
In the Vaseaux Formation
(Christie, 1973)

F_1 - isoclinal rootless folds; fold axes and penetrative lineations plunging variably N and S.

F_2 - tight often rootless folds; fold axes and penetrative lineations gently plunging NW and SE.

F_3 - open to tight folds; SSW and NNE gently inclined axial surfaces; fold axes and penetrative lineations plunging gently WNW and ESE.

F_4 - open folds; steeply dipping NE fractures; rare fold axes gently plunging N and S.

F_5 - open folds; steeply dipping W to NNW fractures; minor fold axes gently plunging NW and SE.

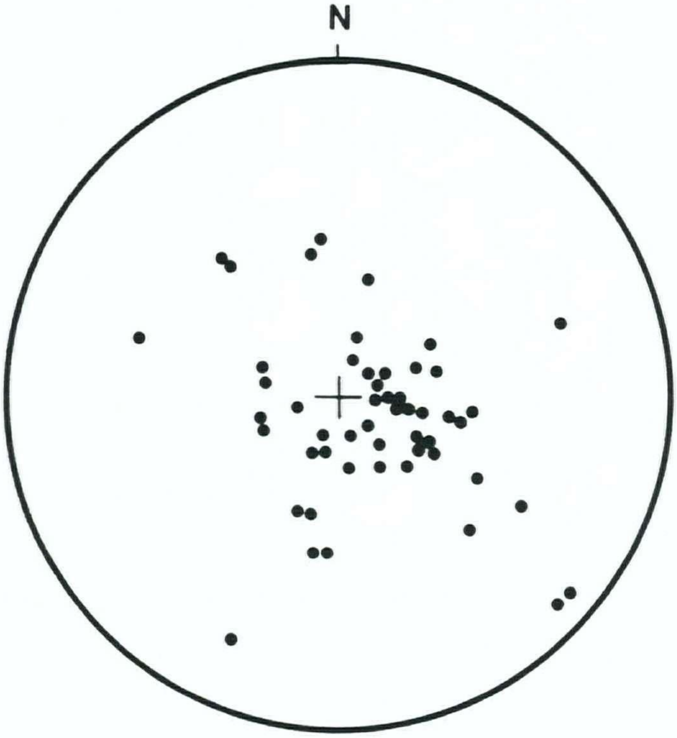

Figure 55: Stereonet of poles to foliations in pgn and lgn units.

Figure 56: Photograph of lineations in lgn unit.

gneisses. Temperatures could not have exceeded 500°–600° C (Wagner et al., 1977), because of only partially reset 58 Ma Rb–Sr date on muscovite from the leucogneiss. This ductile fabric is overprinted by several sets of minor warps (F_3, F_4, F_5, of Christie, 1973) which interfere to produce a foliation dome evident in the topography.

Possible interpretations for the rhomb porphyry both cutting and containing an apparent F_2 fabric, are: 1) That it was intruded late in a single protracted mylonitic event, and crosscut some mylonitic zones but was caught up in continuing deformation; 2) that the rhomb porphyry crosscuts an earlier fabric (syn–, or post–intrusion of lgn) which was reactivated after 51 Ma. In either case, the deformation responsible for the fabric in the rhomb porphyry is also responsible for bringing the gneisses to the surface.

In summary, the lower plate shows ductile strain. The overwhelming fabric is a gently west dipping foliation (F_2). This fabric affects all rocks within the lower plate, except the rhomb porphyry which apparently both contains and crosscuts it. This deformation was either one protracted event or was reactivated after the intrusion of the rhomb porphyry. The interpretation is that the deformation seen in the rhomb porphyry is responsible for much of the mylonite which becomes increasingly pervasive structurally upwards (towards the west). This mylonitization represents mid–crustal movement related to the Okanagan Valley fault. These mylonitic rocks were then overprinted by the chlorite breccia as they approached the surface.

Timing of Brittle and Ductile Deformation

The brittle deformation in the upper plate is known to be as young as Eocene because it affects White Lake Basin rocks. There are several angular unconformities in the upper parts of White Lake Basin, with associated conglomerates and megabreccias, deposited in active–fault bounded basins. The lower half of White Lake Basin shows little evidence of syn-depositional faulting. Extensive tectonism appears to have affected White Lake Basin only after deposition of the Marron Formation at approximately 50 Ma.

The age of structures in the lower plate is not well constrained. In a relative order there is a fabric (foliation, early isoclinal folds) within the paragneiss which is older than the intrusion of the leucogneiss body. The second, predominant fabric overprints the lgn body. Apparently this fabric also affects the rhomb porphyry. The best absolute age relationship is that the fabric in the rhomb porphyry is younger than 51 Ma. The earliest fabric (pre-lgn) is pre-Jurassic, and may be as old as Precambrian. The main F_2 event is post-Early Jurassic to possibly post-Aptian.

A strong argument that the mylonites in the lower plate are Eocene is that they are not annealed even though, from geochronometric evidence, the gneisses must have been at relatively high temperatures at this time. The deformation of the rhomb porphyry, and presumably formation of the mylonites, is coincident in time with the Eocene extensional deformation in the upper plate.

Discussion and Regional Implications

In recent years the literature on crustal extension has blossomed (McKenzie, 1978; Frost and Martin, 1982; Wernicke, 1981, 1985; Wernicke and Burchfiel, 1982; Wernicke et al., 1982; Wernicke et al., 1985; Allmendinger et al., 1983; Miller, 1983; Miller et al., 1983). Quantitative evaluation of the amount of extension and diplacement on known faults has been the focus of much of this work. Because no units or structures can be matched across the Okanagan Valley fault, reconstruction to a pre-extension configuration is not possible. However, an estimate for structural omission across the Okanagan Valley fault can be derived using geochronometric data presented in the previous chapter.

Granitic rocks west of the fault give Jurassic and Cretaceous K-Ar hornblende and biotite dates. Gneisses immediately in the footwall of the Okanagan Valley fault give K-Ar hornblende dates averaging 51 Ma. Using assumed geothermal gradients of 50° C/km and 30° C/km implies between 9 and 15 km structural omission across this fault. Combining this with a simplified fault geometry implies displacements between 10 and 60 kilometers. These estimates are meant to show: a) the extremes in possible displacement due to fault geometry (listric versus planar; Wernicke and Burchfiel, 1982), and b) that displacement must be on the order of 10's of kilometers.

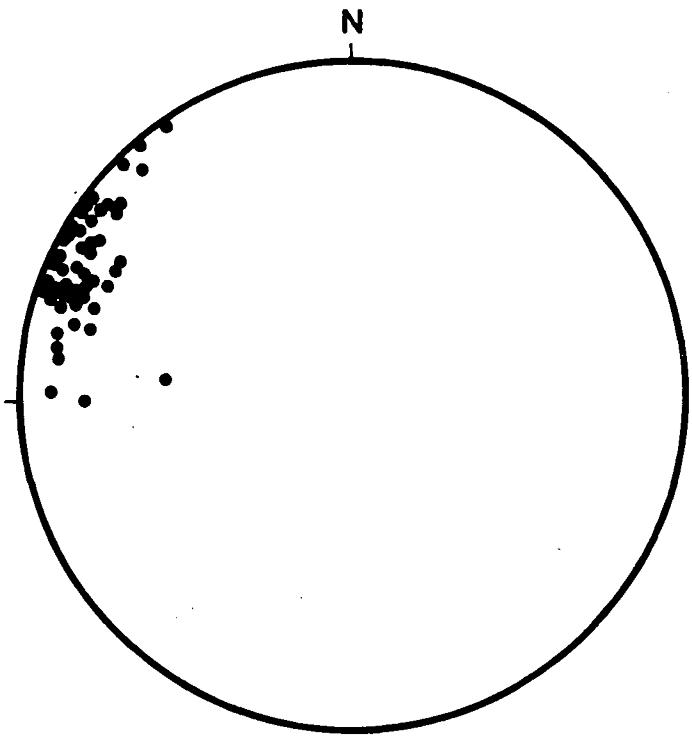

Figure 57: Stereonet of mylonitic lineations.

Conclusions

Although there is evidence for early structures (pre-Late Triassic) in both the upper and lower plates, the latest, and locally pervasive structures are interpreted to be Eocene. This includes both the brittle deformation of the upper plate and some ductile deformation and mylonitization in the lower plate. The explanation for these late structures is a low angle normal fault regime (Fig. 58) as described by many workers in the Basin and Range area of the western U.S. (Armstrong 1972, 1982; Crittenden et al., 1980; Coney, 1980; Coney and Harms, 1984; Davis, 1983; Davis and Coney, 1979; Wernicke, 1981; Wernicke, et al., 1985). The resulting interpretation is that the Okanagan Valley fault is responsible for the tectonic unroofing and rapid cooling of the Okanagan Metamorphic and Plutonic Complex. This idea is compatible with both structural and geochronometric evidence, and implies 10's of kilometers displacement on the Okanagan Valley fault.

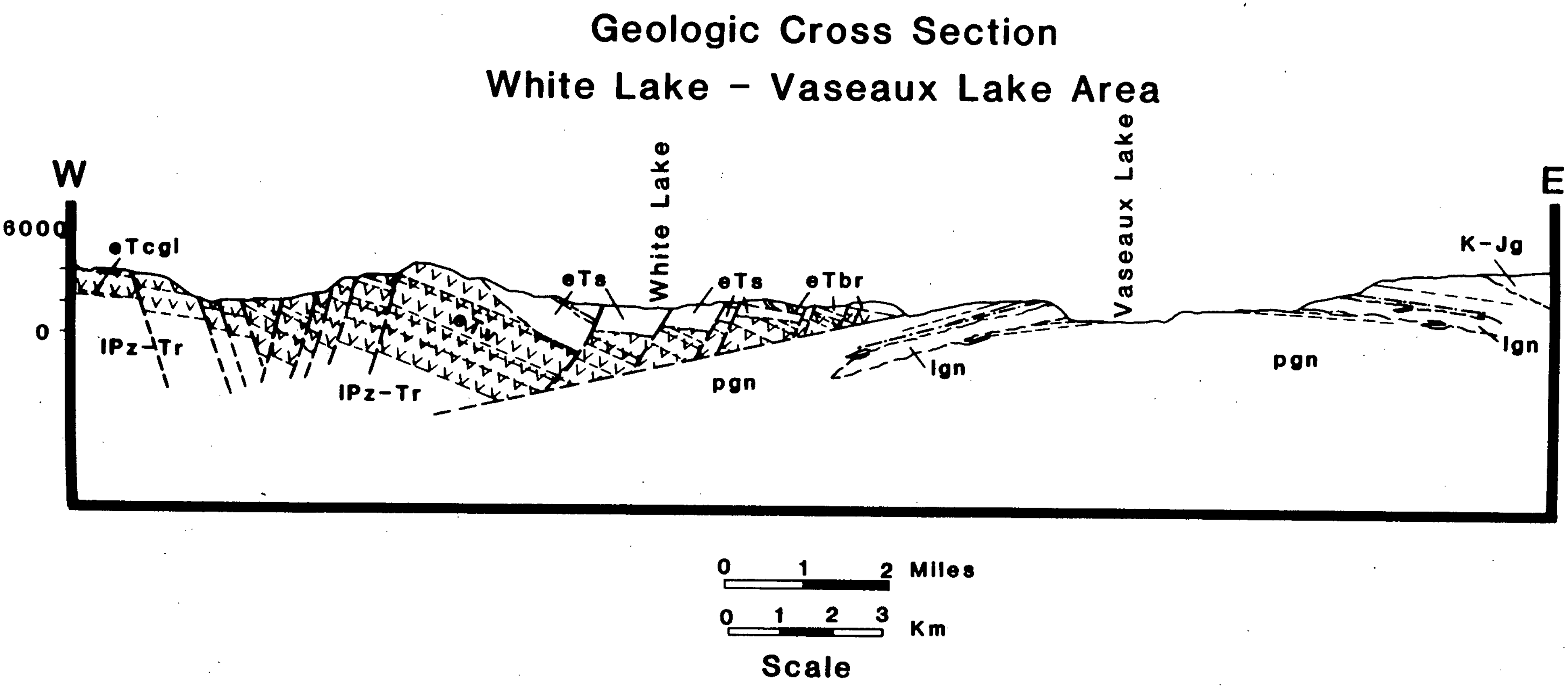

Figure 58: Cross-section through White Lake and Vaseaux Lake area (see Figure 2 for location and legend); unit symbols: eTv=Eocene volcanic rocks; eTs=Eocene sedimentary rocks; lPz-Tr=late Paleozoic to Triassic eugeosynclinal formations; lgn=leucogneiss; pgn=paragneiss of Vaseaux Formation; K-Jg=Cretaceous or Jurassic gneissic granitic intrusives. Elevations in feet. Modified from Christie (1973), and Church (1973).

VI. GEOLOGIC HISTORY OF THE SOUTHERN OKANAGAN REGION

The pre-late Paleozoic history of the southern Okanagan region can be, at present, only inferred. The age of the Vaseaux Formation protoliths is unknown. Highly radiogenic Sr from these gneisses suggests that they could be Precambrian in age. This Precambrian component is not evident in the U-Pb work. (Except possibly the leucogneiss discordance).

Deposition of the eugeosynclinal formations (Apex Mountain, Kobau, Anarchist; Milford, 1984; Okulitch, 1973; Read and Okulitch, 1977; Monger, 1977) began in the mid-Carboniferous and continued through the early Triassic. This sequence (ultramafic, greenstone, chert, limestone, argillite) represents an ocean floor, interarc, or back arc basin. By late Triassic time these eugeosynclinal formations had been intensely folded and deeply eroded (Read and Okulitch, 1977). This pre-Late Triassic deformation probably represents telescoping of this basin before the beginning of the Nicola-Rossland volcanic arc environment (Monger and Price, 1979).

Following this deformation the Late Triassic Nicola Group equivalents at Olaila Creek were deposited (Read and Okulitch, 1977). The Nicola Group represents a Late Triassic to Early Jurassic island arc sequence. The gneiss of Osoyoos is time correlative with the Guichon Batholith and other early Jurassic intrusives associated with Nicola Group. An important observation in the history of the rocks west of the Okanagan Valley is that the Late Triassic rocks are only mildly deformed (tilted and faulted) and unmetamorphosed except near Jurassic or younger plutons.

Jurassic time in the southern Okanagan was marked by abundant plutonism. This began with the intrusion of the granodioritic gneiss of Osoyoos (eJ) into deformed Anarchist Formation, followed by the Olalla Syenite and Similkameen granodioritic batholith (mJ) intruding deformed Apex Mountain, and Kobau strata. The

Late Jurassic was marked by more felsic intrusions (Miller and Bradfish, 1980) of the Oliver pluton (garnet-muscovite phase) and the granite of Anarchist Mountain (garnet-biotite). This Jurassic intrusive event has correlatives farther east with Kuskanax (Miller, 1978; Parrish and Wheeler, 1983; Olalla, Similkameen), Nelson (granite of Anarchist Mountain), and Galena Bay Stock (Oliver Granite), both in time and sequence of composition (Gabrielse and Reesor, 1974).

Within the Okanagan Metamorphic and Plutonic Complex several plutons were emplaced in either Jurassic or Cretaceous time which have since been highly deformed and metamorphosed (leucogneiss, gneiss of Skaha Lake, and gneissic sill of Vaseaux Lake). The Kettle (Cheney, 1980; Rhodes and Cheney, 1981), Okanogan (Fox et al., 1976; Goodge and Hansen, 1983) and Valhalla (Parrish, 1984; Parrish et al., 1985; Carr, 1985) gneissic culminations all contain deformed Cretaceous and Cretaceous(?) intrusives. This observation may be the key to explaining the later evolution of these domes. Cretaceous time in southeastern B.C. is marked by crustal melts indicating large amounts of crustal thickening (Monger et al., 1982; Armstrong, 1983). A scenario of crustal thickening prior to and spatially related to later crustal extension fits the model of Coney and Harms (1984) for the development of metamorphic core complexes.

The Paleocene was a time of relative quiescence with only a few known intrusives of this age (Medford et al., 1983; Parrish, 1984), which probably represent the beginning of the magmatic episode that culminated in Early Eocene time. The Eocene begins with a regionally developed basal conglomerate (Springbrook and Kettle River Formations) followed by the voluminous mafic alkaline Marron Formation. This volcanic sequence then evolved with time into a more felsic and calc-alkaline composition (Church, 1973). The higher parts of this Eocene basin are highly disrupted by syn-depositional normal faulting. The entire Eocene section appears to have been deposited in 4-10 Ma. This basin development and subsequent extensional deformation in the upper plate of the Okanagan Valley fault is coincident with intrusion, deformation and metamorphism of the rhomb porphyry in the lower plate, and development of extensive mylonites responsible for tectonic unroofing of the Okanagan Metamorphic and Plutonic Complex. A similar pattern of deformation, but with opposite sense of movement, has been documented for the Valhalla Dome to the east (Parrish et al., 1985; Carr, 1985). A highly extended Eocene section has also been documented at Midway (Monger, 1968), between the Okanagan and the Valhalla area.

The implication is that a large area of southern B.C. has undergone crustal extension (Parrish, 1985). The geochronometric evidence shows this to have taken place very rapidly beginning at approximately 51 Ma. This might possibly be tied to interaction of the North American plate and the Kula/Farallon plates offshore (Ewing, 1980). Plate motions and velocities for these plates (Engebretson et al., 1984) indicates that for most of Paleocene time the motion between North America and Kula/Farallon plates was at a low velocity with oblique, nearly strike slip, convergence. The Eocene is marked by very rapid plate velocities and more orthogonal convergence (Engebretson et al., 1984). This apparently set up an intense arc-back arc volcanic regime which may have brought about mantle upwelling. The initial mafic alkaline magmatism can be interpreted as mantle melting, signaling the onset of this aesthenospheric upwelling. As this thermal pulse moved upward into the crust the volcanism changed to a calc-alkaline, felsic composition. The deformation (extension) also appears to have followed the onset of volcanism and may be linked to the evolution of the arc or back arc environment. Tectonically little seems to have occured in the Okanagan region since the demise of this intense Eocene activity.

REFERENCES CITED

Allmendinger, R.W., Sharp, J.W., Von Tish, D., Serpa, L., Brown, L., Kaufman, S., Oliver, J., Smith, R.B., 1983, Cenozoic and Mesozoic structure of the eastern Basin and Range province, Utah, from COCORP seismic-reflection data: Geology v. 11, p. 532-536.

Anderson, J.L., and Rowley, M.C., 1981, Synkinematic intrusion of two mica and associated metaluminous granitoids, Whipple Mountains, California: Canadian Mineralogist v. 19, p 83-101.

Archibald, D.A., Krogh, T.E., Armstrong, R.L., Farrar, E., 1984, Geochronology and tectonic implication of magmatism and metamorphism; southern Kootenay Arc and neighbouring regions, southeastern British Columbia: Part II; Mid-Cretaceous to Eocene: Canadian Journal of Earth Sciences v. 21, p. 567-583.

Armstrong, R.L., 1968, Mantled gneiss domes in the Albion Range, southern Idaho: Geological Society of America Bulletin v. 79, p. 1295-1314.

Armstrong, R.L., 1972, Low-angle (denudation) faults, hinterland of the Sevier orogenic belt, eastern Nevada and western Utah: Geological Society of America Bulletin v. 83, p. 1729-1754.

Armstrong, R.L., 1974, Magmatism, orogenic timing, and orogenic diachronism in the Cordillera from Mexico to Canada: Nature v. 247, p. 348-351.

Armstrong, R.L., 1978, Cenozoic igneous history of the U.S. Cordillera from Latitude 42° to 49°: in Smith and Eaton, editors, Geological Society of America Memoir 152, p. 265-282.

Armstrong, R.L., 1982, Cordilleran metamorphic core complexes - from Arizona to southern Canada: Annual Review of Earth and Planetary Sciences v. 10, p. 129-154.

Armstrong, R.L., 1983, Cordilleran S- and I-type granites: Indicators of lithosphere thickness: Geological Associaion of Canada Annual meeting Program v. 8, p. A3.

Armstrong, R.L., 1985, Mesozoic-Early Cenozoic plutonism in the Canadian Cordillera - Distribution in time and space: Geological Society of America abstracts with programs v. 17, p. 338.

Armstrong R.L., and Petö, P., 1981, Eocene quartz-feldspar porphyry intrusions west of Okanagan Lake, southern B.C.; K-Ar and Sr isotopic composition: Northwest Geology v. 10, p. 13-19.

Armstrong, R.L., Taubeneck, W.H., and Hales, P.O., 1977, Rb-Sr and K-Ar geochronometry of Mesozoic granitic rocks and their Sr isotopic composition, Oregon, Washington, and Idaho: Geological Society of America Bulletin v. 88, p. 397-411.

Baadsgaard, H., Folinsbee, R.E., and Lipson, J., 1961, Potassium-Argon dates of biotites from Cordilleran granites: Geological Society of America Bulletin v. 72, p. 689-701.

Bardoux, Marc, 1985, Tertiary tectonic denudation of the hinterland of the Canadian Cordillera; initial results from Kelowna, B.C.: Geological Society of America abstracts with programs v. 17, p 339.

Barnes, W.C., and Ross, J.V., 1975, The Blind Creek limestone, Keremeos, British Columbia: Structure and regional tectonic significance: Canadian Journal of Earth Sciences v. 12, p. 1929-1933.

Bell, T.H., 1978, Progressive deformation and reorientation of fold axes in a ductile mylonite zone: the Woodroffe Thrust: Tectonophysics v. 44, p. 285.

Bell, T.H., and Etheridge, M.A., 1973, Microstructures of mylonites and their descriptive terminology: Lithos v. 6, p. 337-348.

Bell, T.H., and Hammond, R.L., 1984, On the internal geometry of mylonite zones: Journal of Geology v. 92, p. 667-686.

Berthe, D., and Brun, J.P., 1980, Evolution of folds during progressive shear in the South Armorican Shear Zone, France: Journal of Structural Geology v. 2, p. 127-133.

Best, M.G., Armstrong, R.L., Graustein, W.C., Embree, G.F., and Ahlborn, R.C., 1974, Mica granites of Kern Mountains pluton eastern White Pine County, Nevada; Re-mobilized basement of the Cordilleran miogeosyncline?: Geological Society of America Bulletin v. 85, p. 1277-1286.

Bostock, H.H., 1966, Feldspar and quartz phenocrysts in the Shingle Creek porphyry, B.C.: Geological Survey of Canada Bulletin 126, 70 p.

Bostock, H.S., 1940, Map of Hedley area: Geological Survey of Canada Map 341.

Bostock, H.S., 1941a, Okanagan Falls map-area: Geological Survey of Canada Map 627A.

Bostock, H.S., 1941b, Keremeos map area: Geological Survey of Canada, Map 628A.

Bradbury, H.J., and Nolen-Hoeksema, R.C., 1985, The Lepontine Alps as an evolving metamorphic core complex during A-type subduction: Evidence from heat flow, mineral cooling ages, and tectonic modeling: Tectonics v. 4, p. 187-211.

Brock, B.B., 1934, The metamorphism of the Shuswap Terrane of British Columbia: Journal of Geology v. 42, p. 673-699.

Brown, R.L., 1978, Structural evolution of the southeastern Canadian Cordillera: a new hypothesis: Tectonophysics v. 48, p. 133-151.

Brown, R.L., 1981, Metamorphic Complex of southeastern Canadian Cordillera and relationship to foreland thrusting: in Thrust and Nappe Tectonics, Geological Society London Paper 14.

Cairnes, C.E., 1937, Kettle River map area: Geological Survey of Canada, Map 37-21.

Cairnes, C.E., 1947, Kettle River map area, west half: Geological Survey of Canada, Map 538A.

Cannon, R.W., 1966, Geochronology and petrographic studies of the intrusive rocks of the Oliver area: B.A.Sc., U.B.C., 23 p.

Carmichael, I.S.E., Turner, F.J., and Verhoogen, J., 1974, Igneous Petrology: McGraw-Hill, 739 p.

Carr, Sharon, 1985, Ductile shearing and brittle faulting in Valhalla gneiss complex, southeastern British Columbia: in Current Research, Part A, Geological Survey of Canada, Paper 85-1A, p. 89-96.

Cawthorn, R.G., and Brown, P.A., 1976, A model for the formation and crystallization of C-normative calc-alkaline magmas through amphibole fractionation: Journal of Geology v. 84, p. 467-476.

Cawthorn, R.G., Strong, D.F., and Brown, P.A., 1976, Origin of C-normative intrusive and extrusive magmas: Nature v. 259, p. 102-104.

Chappell, B.W., and White, A.J.R., 1974, Two contrasting granite types: Pacific Geology v. 8, p. 173-174.

Cheney, E.S., 1980, Kettle Dome and related structures of northeast Washington: Geological Society of America Memoir 153, p. 463-483.

Christie, J.S., 1973, Geology of the Vaseaux Lake area: Ph.D. thesis U.B.C., 139 p.

Church, B.N., 1967, Geology of the White Lake Basin: Ph.D. thesis, U.B.C., 183 p.

Church, B.N., 1970, White Lake, in Geology Exploration and Mining in B.C., 1970: British Columbia Department of Mines and Petroleum Resources, p. 396-402.

Church, B.N., 1972, Lynx Lake, in Geology, Exploration and Mining in British Columbia, 1972: B.C. Ministry of Energy, Mines and Petroleum Resources, p. 386-396.

Church, B.N., 1973, Geology of the White Lake Basin, B.C. Ministry of Energy, Mines and Petroleum Resources, Bulletin 61, 120 p.

Church, B.N., 1975, Geology of the Hat Creek Coal Basin, B.C. Ministry of Energy, Mines and Petroleum Resources , Geology in B.C., 1975, p. G99-G118.

Church, B.N., 1977, Tertiary Stratigraphy in South-Central British Columbia, B.C. Ministry of Energy, Mines and Petroleum Resources, Geological Fieldwork, p. 7-11.

Church, B.N., 1978, Shackanite and Related Analcite-Bearing Lavas in British Columbia: Canadian Journal of Earth Sciences v. 15, p. 1669-1672.

Church, B.N., 1979a, Tertiary Stratigraphy and Resource Potential in South-Central British Columbia: B.C. Ministry of Energy, Mines and Petroleum Resources, Geological Fieldwork, 1978, Paper 79-1, p. 7-15.

Church, B.N., 1979b, Geology of the Penticton Tertiary Outlier (parts of 82E/4, 5): B.C. Ministry of Energy, Mines and Petroleum Resources, Preliminary Map 35 (revised).

Church, B.N., 1980a, Hat Creek Bocanne-Buchite: B.C. Ministry of Energy, Mines and Petroleum Resources, Geological Fieldwork, 1979, Paper 1980-1, p. 97-99.

Church, B.N., 1980b, Anomalous Uranium in the Summerland Caldera, B.C.: B.C. Ministry of Energy, Mines and Petroleum Resources, Geological Fieldwork, 1979, Paper 1980-1, p. 11-15.

Church, B.N., 1980c, Geology of the Terrace Mountain Tertiary Outlier (parts of 82L/4E, 5E), B.C. Ministry of Energy, Mines and Petroleum Resources, Preliminary Map 37 (revised).

Church, B.N., 1980d, Geology of the Kelowna Tertiary Outlier (West Half) (part of 82E/13): B.C. Ministry of Energy, Mines and Petroleum Resources, Preliminary Map 39.

Church, B.N., 1980e, Geology of the Rock Creek Tertiary Outlier (parts of 82E/3E, 2W): B.C. Ministry of Energy, Mines and Petroleum Resources, Preliminary Map 41.

Church, B.N., 1981a, Geology of the Kelowna Tertiary Outlier (East Half) (82E/14): B.C. Ministry of Energy, Mines and Petroleum Resources, Preliminary Map 45.

Church, B.N., 1981b, Lithology and Structural Setting of the Penticton Group - A Proposed New Tertiary Stratigraphic Unit in South-Central British Columbia, abstract, in The Last 100 Million Years of Geology and Mineral Deposits in the Canadian Cordillera, Geological Association of Canada, p. 14.

Church, B.N., 1982, Notes on the Penticton Group: A Progress Report on a New Stratigraphic Subdivision of the Tertiary, South-Central British Columbia: B.C. Ministry of Energy, Mines and Petroleum Resources, Geological Fieldwork, 1981, Paper 1982-1, p. 12-16.

Church, B.N., Ewing, T.E., and Hora, Z.D., 1983, Volcanology, Structure, Coal and Mineral Resources of Early Tertiary Outliers in South-Central British Columbia: Geologic Association of Canada, Field Trip Guidebook No. 1, 91 p.

Church, B.N., and Johnson, W.M., 1978, Uranium and Thorium in Tertiary Alkaline Volcanic Rocks in South-Central British Columbia: Western Miner v. 51, p. 33-34.

Coney, P.J., 1980, Cordilleran metamorphic core complexes: an overview. in: Cordilleran Metamorphic Core Complexes, Geological Society of America Memoir 153, p. 7-34.

Coney, P.J., and Harms, T., 1984, Cordilleran metamorphic core complexes: Cenozoic extensional relics of Mesozoic compression: Geology v. 12, p. 550-554.

Cox, K.G., Bell, J.D., and Pankhurst, P.J., 1979, The interpretation of igneous rocks: George Allen and Unwin, 450 p.

Crittenden, M., Coney, P.J., and Davis, G., 1980, Cordilleran metamorphic core complexes: Geological Society of America Memoir 153, 490 p.

Daly, R.A., 1906, Okanagan composite batholith of the Cascade Mountain system: Geological Society of America Bulletin v. 17, p. 329-376.

o

Daly, R.A., 1912, Geology of the North American Cordillera at the Forty-Ninth Parallel: Geological Survey of Canada Memoir 38, 3 v., 857 p.

Davis, G.H., 1983, Shear zone model for the origin of metamorphic core complexes: Geology v. 11, p. 342-347.

Davis, G.H., and Coney, P.J., 1979, Geologic development of Cordilleran metamorphic core complexes: Geology v. 7, p.120-124.

Dawson, G.M., 1877, Geologic Map of a portion of the southern interior of British Columbia: Geological Survey of Canada.

Deutsch, A., and Steiger, R.H., 1985, Hornblende K-Ar ages and the climax of Tertiary metamorphism in the Lepontine Alps (south-central Switzerland): an old problem reassesed: Earth and Planetary Science Letters v. 72, p. 175-189.

Eaton, G.P., 1982, The Basin and Range Province: Origin and Tectonic significance: Annual Reviews of Earth and Planetary Sciences v. 10, p. 409-440.

Engebretson, D.C., Cox, A., and Thompson, G.A., 1984, Correlation of plate motions with continental tectonics: Laramide to Basin-Range: Tectonics v. 3, p. 115-119.

Engels, J.C., Tabor, R.W., Miller, F.K., and Obradovich, J.D., 1976, Summary of K-Ar, Rb-Sr, and U-Pb, and Pb-α and fission track ages of rocks from Washington State prior to 1975 (exclusive of Columbia Plateau basalts): U.S. Geological Survey Misc. Field Studies Map MF-710, scale 1:1,000,000.

Ewing, T.E., 1980, Paleogene tectonic evolution of the Pacific Northwest: Journal of Geology v. 88, p. 619-638.

Ewing, T.E., 1981a, Petrology and geochemistry of the Kamloops Group volcanics, British Columbia: Canadian Journal of Earth Sciences v. 18, p. 1478-1491.

Ewing, T.E., 1981b, Regional stratigraphy and structural setting of the Kamloops Group, south-central British Columbia: Canadian Journal of Earth Sciences v. 18, p. 1464-1477.

Fox, K.F., Rinehart, C.D., and Engels, J.C., 1975, K-Ar Age of the Similkameen batholith and Kruger Alkalic Complex, Washington and British Columbia: Journal of Research, U.S. Geological Survey v. 3, p. 39-43.

Fox, K.F., Rinehart, C.D., Engels, J.C., 1977, Plutonism and orogeny in north-central Washington: U.S. Geological Survey Professional Paper 989, 27 p.

Fox, K.F., Rinehart, C.D., Engels, J.C., and Stern, T.W., 1976, Age of emplacement of the Okanogan gneiss dome, north-central Washington: Geological Society of America Bulletin v. 87, p. 1217-1224.

Frost, E.G., and Martin, D.L., editors, 1982, Mesozoic-Cenozoic tectonic evolution of the Colorado River trough region, California, Arizona and Nevada: Cordilleran Publishers, San Diego, CA.

Gabrielse, H., and Reesor, J.E., 1974, The nature and setting of granitic plutons in the central and eastern parts of the Canadian Cordillera: Pacific Geology v. 8, p. 109-138.

Goodge, J.W., and Hansen, V.L., 1983, Petrology and structure of rocks in the southwest portion of Okanogan Dome, north-central Washington: Northwest Geology v. 12, p. 13-24.

Harrison, T.M., 1981, The diffusion of ^{40}Ar in hornblende: Contributions to Mineralogy and Petrology v. 78, p. 324-331.

Harrison, T.M., and McDougall, I., 1980, Investigation of an intrusive contact, northwest Nelson, New Zealand-I. Thermal, chronological, and isotopic constraints: Geochimica et Cosmochimica Acta v.44, p. 1985-2003.

Harrison, T.M., and McDougall, I., 1982, The thermal significance of potassium feldspar K-Ar ages inferred from $^{40}Ar/^{39}Ar$ age spectrum results: Geochimica et Cosmochimica Acta v.46, p. 1811-1820.

Holtby, M.H., 1972, A study of vein-quartz in the Susie Mine, Oliver B.C.: U.B.C., B.Sc. thesis.

Hibbard, M.J., 1971, Evolution of a plutonic complex, Okanogan Range, Washington: Geological Society of America Bulletin v. 82, p. 3013-3047.

Hyndman, Donald W., A petrographic and chemical section through the northern Idaho batholith: Journal of Geology v. 92, p. 83-102.

Irvine, T.N., and Baragar, W.R.A., 1971, A guide to the chemical classification of the common volcanic rocks: Canadian Journal of Earth Sciences v. 8, p. 523-543.

Krauskopf, K.B., 1941, Intrusive rocks of the Okanogan Valley and the problem of their correlation: Journal of Geology v. 49, 1-53.

Kuno, H., 1968, Origin of Andesite and its bearing on the Island Arc structure: Bull. Volc. v. 32, p. 141-176.

Lammle, C.A.R., 1962, The dike system in the south drift of the Susie Mine, Oliver B.C.: U.B.C. B.Sc. thesis.

Lister, G.S., and Snoke, A.W., 1984, S-C Mylonites: Journal of Structural Geology v. 6, p. 617-638.

Little, H.W., 1961, Geologic Map of the Kettle River (west half) Map sheet: Geological Survey of Canada. Map 15-1961.

Mathews, W.H., 1964, Potassium-Argon Date Determination of Cenozoic Volcanic Rocks from British Columbia: Geological Society of America Bulletin v. 75, p. 465-468.

Mathews, W.H., 1981, Early Cenozoic resetting of potassium-argon dates in geothermal history of north Okanagan area, British Columbia: Canadian Journal of Earth Sciences v. 18, p. 1310-1319.

Mathews, W.H., 1983, Early Tertiary resetting of potassium-argon dates in the Kootenay Arc, southeastern British Columbia: Canadian Journal of Earth Sciences v. 20, p. 867-872.

Matsen, B., 1960, Geology of the Gypo Mine, Oliver B.C.: U.B.C. B.Sc. thesis.

Mattinson, J.M., 1972, Age of zircons from the Northern Cascade Mountains, Washington: Geological Society of America Bulletin v. 83, p. 3769–3784.

Mattinson, J.M., 1978, Age, Origin, and Thermal Histories of Some Plutonic Rocks From the Salinian Block of California: Contributions to Mineralogy and Petrology v. 67, p. 233–245.

McKenzie, Dan, 1978, Some remarks on the development of sedimentary basins: Earth and Planetary Science Letters v. 40, p. 25–32.

Medford, G.A., 1973, Geology and thermal history of an area near Okanagan Lake, southern B.C.: U.B.C. Ph.D. thesis.

Medford, G.A., 1975, K–Ar and fission track geochronometry of an Eocene thermal event in the Kettle River (west half) map area, southern British Columbia: Canadian Journal of Earth Sciences v. 12, p. 836–843.

Medford, G.A., Armstrong, Richard Lee, and Osatenko, M.J., 1983, Rb–Sr dating of Paleozoic(?), Mesozoic, and Cenozoic intrusive rocks, Okanagan Lake region, southern British Columbia, Canada: Canadian Journal of Earth Sciences v. 10, p. 1579–1585.

Milford, J., 1984, Geology of the Apex Mountain area: M.Sc. thesis U.B.C..

Miller, C.F., 1978, An early Mesozoic alkalic magmatic belt in western North America: in Mesozoic Paleogeography of the western United States: Pacific Section, Society of Economic Paleontologists and Mineralogists, p. 163–173.

Miller, C.F., and Bradfish, L.J., 1980, An inner Cordilleran belt of muscovite–bearing plutons: Geology v. 8, p. 412–416.

Miller, C.F., Stoddard, E.F., Bradfish, L.J., and Dollase, W.A., 1981, Composition of plutonic muscovite: Genetic implications: Canadian Mineralogist v. 19, p. 25–34.

Miller, D.M., 1983, Strain on a gneiss dome in Albion Mountains metamorphic core complex: American Journal of Science v. 238, p. 605–632.

Miller, E.L., Gans, P.B., and Garing, J., 1983, The Snake Range Decollement: An exhumed mid–Tertiary ductile–brittle transition: Tectonics v. 2, p. 239–263.

Miller, K.F., and Engels, J.C., 1975, Distribution and trends of discordant ages of the plutonic rocks of northeastern Washington and northern Idaho: Geological Society of America Bulletin v. 86, p. 517–528.

Monger, J.W.H., 1968, Early Tertiary stratified rocks Greenwood map–area, B.C.: Geological Survey of Canada Paper 67–42, 39 p.

Monger, J.W.H., 1977, Upper Paleozoic rocks of the western Canadian Cordillera and their bearing on Cordilleran evolution: Canadian Journal of Earth Sciences v. 14, p. 1832–1859.

Monger, J.W.H., and Price, R.A., 1979, Geodynamic evolution of the Canadian Cordillera – progress and problems: Canadian Journal of Earth Sciences v. 19, p. 770–791.

Monger, J.W.H., Price, R.A., and Tempelman-Kluit, D.J., 1982, Tectonic accretion and the origin of the two major metamorphic and plutonic welts in the Canadian Cordillera: Geology v. 10, p. 70-75.

Moore, D.P., 1970, Metasomatic alteration near the Gypo quartz deposit, Oliver B.C.: U.B.C. B.A.Sc. thesis.

Okulitch, A., 1969, Geology of Mount Kobau: Ph.D. thesis U.B.C., 141 p..

Okulitch, A., 1973, Age and correlation of the Kobau Group, Mt. Kobau, B.C.: Canadian Journal of Earth Sciences v. 10, p. 1508-1518.

Okulitch, A.V., 1984, The role of the Shuswap Metamorphic Complex in Cordilleran Tectonism: a review: Canadian Journal of Earth Sciences v. 21, p. 1171-1193.

Okulitch, A.V., Price, R.A., and Richards, T.A., 1977, Geology of the Southern Canadian Cordillera - Calgary to Vancouver; Field trip guidebook 8, edited by A.V. Okulitch; GAC, MAC, SEG Joint annual meeting, Vancouver, 1977, 135p.

Palmer, A.R., 1983, The Decade of North American Geology 1983 Geologic Time Scale: Geology v. 11, p. 503-504.

Parrish, R.R., 1979, Geochronology and tectonics of the northern Wolverine Complex, British Columbia: Canadian Journal of Earth Sciences v. 16, p. 1228-1238.

Parrish, R.R., 1981, Geology and regional tectonics of the Nemo Lakes Belt, northern Valhalla Range, British Columbia: Canadian Journal of Earth Sciences v. 18, p. 944-958.

Parrish, Randy, 1984, Slocan Lake fault: a low angle fault zone bounding the Valhalla gneiss complex, Nelson map area, southern British Columbia: Geological Survey of Canada Paper 84-1A, p. 323-330.

Parrish, R.R., 1985, Metamorphic Core Complexes of southern B.C.: Distinctions between extensional or compressional origins: Geological Society of America abstracts with programs v. 17, p. 399.

Parrish, R., and Wheeler, J.O., 1983, A U-Pb zircon age of the Kuskanax batholith, southeastern British Columbia: Canadian Journal of Earth Sciences v. 20, p. 1751-1756.

Parrish, R., Carr, S.D., and Brown, R.L., 1985, Valhalla gneiss complex, southeast British Columbia: 1984 Fieldwork: in Current Research Part A, Geological Survey of Canada Paper 85-1A, p. 81-87.

Parrish, Randy, Carr, Sharon, and Parkinson, David, 1985, Metamorphic Complexes and Extensional Tectonics, Southern Shuswap Complex, Southeastern British Columbia: in Field Guides to Geology and Mineral Deposits in the Southern Canadian Cordillera, Geological Society of America, Cordilleran Section meeting, May 1985.

Parrish, R.R., and Roddick, J.C., 1985, Geochronology and isotope geology for the geologist and explorationist: GAC Cordilleran Section short course number 4.

Peatfield, G.R., 1978, Geologic history and metallogeny of the 'Boundary District' southern British Columbia and northern Washington: Ph.D. Queens University, 250 p.

Petö, P., 1973, Petrochemical study of the Similkameen batholith, B.C.: Geological Society of America Bulletin v. 84, p. 3977-3984.

Petö, P., 1973a, K-Ar ages of igneous rocks from the area near Hedley, Southern B.C.: Discussion: Canadian Journal of Earth Sciences v. 10, p. 1357.

Petö, P., 1974, Plutonic evolution of the Canadian Cordillera: Geological Society of America Bulletin v. 85, p. 1269-1276.

Petö, P., 1979, On discerning magmatic populations in the batholith west of Okanagan Lake: Chemical Geology v. 26, p. 249-265.

Petö, P., and Armstrong, R.L., 1976, Strontium isotope study of the composite batholith between Princeton and Okanagan Lake: Canadian Journal of Earth Sciences v. 13, p. 1577-1583.

Price, R.A., 1979, Intracontinental ductile crustal spreading linking the Fraser River and northern Rocky Mountain Trench transform fault zones, south-central B.C. and northeast Washington: Geological Society of America abstracts v. 11, p. 499.

Price, R.A., 1985, Metamorphic Core Complexes of the first and second kind in the Cordillera of Southern Canada and Northern USA: Geological Society of America abstracts with programs v. 17, p. 401.

Price, R.A., Archibald, D., and Farrar, E., 1981, Eocene stretching and necking of the crust and tectonic unroofing of the Cordilleran metamorphic infrastructure southeast B.C. and adjacent Washington and Idaho: Geological Association of Canada abstracts with programs v. 6, p. A-47.

Read, P.B., and Okulitch, A.V., 1977, The Triassic unconformity of southcentral British Columbia: Canadian Journal of Earth Sciences v. 14, p. 606-638.

Rhodes, B.P., and Cheney, E.S., 1981, The low-angle Kettle River fault: The eastern contact of Kettle Dome, northeast Washington: Geology v. 9, p. 366-369.

Richards, G.C., 1968, Petrology of the Oliver Quartz Monzonite: U.B.C. B.Sc. thesis.

Rinehart, C.D., and Fox, K.F., 1972, Geology and Mineral deposits of Loomis Quadrangle, Okanogan County, Washington: Washington Division of Mines and Geology Bulletin no. 64.

Roddick, J.C., Farrar, E., and Procyshyn, E.L., 1972, Potassium-Argon ages of rocks from an area near Hedley, Southern B.C.: Canadian Journal of Earth Sciences v. 9, p. 1632-1639.

Ross, J.V., 1973, Mylonitic rocks and flattened garnets in the Southern Okanagan of B.C.: Canadian Journal of Earth Sciences v. 10, p. 1-17.

Ross, J.V., 1974, A Tertiary thermal event in south-central B.C.: Canadian Journal of Earth Sciences v. 11, p. 1116-1122.

Ross, J.V., 1981, A geodynamic model for some structures within and adjacent to the Okanagan Valley, southern B.C.: Canadian Journal of Earth Sciences v. 18, p.

1581-1598.

Ross, J.V., and Barnes, W.C., 1972, Evidence for the "Cariboоan Orogeny" in the southern Okanagan region of British Columbia: Canadian Journal of Earth Sciences v. 9, p. 1693-1702.

Ross, J.V., and Christie, J.S., 1979, Early recumbent folding in some westernmost exposures of the Shuswap Complex, Southern Okanagan, B.C.: Canadian Journal of Earth Sciences v. 16, p. 877-894.

Ryan, D.B., 1973, Geology and Rb-Sr geochronology of the Anarchist Mountain Area, south-central B.C.: U.B.C. Ph.D. thesis, 256 p.

Simpson, Carol, and Schmid, Stefan M., 1983, An evaluation of criteria to deduce the sense of movement in sheared rocks: Geological Society of America Bulletin v. 94, p. 1281-1288.

Sinclair, A.J., Moore, D., and Reinsbakken, A., 1983, Geology of Gypo quartz vein Oliver, British Columbia: B.C. Ministry of Energy, Mines and Petroleum Resources, p. 246-259.

Snook, J.R., 1965, Metamorphic and structural history of "Colville Batholith" gneisses, north-central Washington: Geological Society of America Bulletin v. 76, p. 759-776.

Steiger, R.H., and Jaget, E., 1977, Subcommission on Geochronology: Convention on the use of decay constants in geo- and cosmochronology: Earth and Planetary Science Letters v. 36, p. 359-362.

Stevens, R.D., Delabio, R.N., and Lachance, G.R., 1982, Age determinations and geologic studies: K-Ar Isotopic Ages, Report 16: Geological Survey of Canada Paper 82-2, 56 p..

Strekeisen A., 1976, To each plutonic rock its proper name: Earth Science Reviews v. 12, p 1-33.

Strong, D.F., 1979, The Mt. Peyton Batholith, Central Newfoundland: A Bimodal calc-alkaline suite: Journal of Petrology v. 20, p. 119.

Sturdevant, J.A., 1963, Petrography of Olalla Stock, Okanagan Mountains, B.C.: M.Sc. University of New Mexico, 84 p..

Templeman-Kluit, D.J., 1984, Meteoric water model for gold veins in a detached terrane: Geological Society of America abstracts with programs v. 16, p. 674.

Tuttle, O.F. and Bowen, N.L., 1958, Origin of Granite in the Light of Experimental Studies in the System $NaAlSi_3O_8-KAlSi_3O_8-SiO_2-H_2O$: Geological Society of America Memoir, no. 74.

Van der Heyden, P., Horsky, S., and Fletcher, K., 1982, XRF major element analysis on powder pellets: M.Sc. U.B.C., appendix 1.

Wagner, G.A., Reimer, G.M., and Jager, E., 1977, Cooling ages derived by apatite fission track, mica Rb-Sr, and K-Ar dating: the uplift and cooling history of the Central Alps: Memorie degli Instituti di Geologia e Mineralogia dell'Universita di Padova, XXX, p. 1-27.

Wanless, R.K., Stevens, R.D., Lachance, G.R., and Delabio, R.N., 1979, Age Determinations and Geological studies, K-Ar isotopic ages, Report 14: Geological Survey of Canada Paper 79-2, 67 p..

Waters, A.C., and Krauskopf, K., 1941, Protoclastic border of the Colville Batholith: Geological Society of America Bulletin v. 52, p. 1355-1418.

Wernicke, B., 1981, Low angle normal faults in the Basin and Range Province: nappe tectonics in an extending orogen: Nature v. 291, p. 645-648.

Wernicke, B., 1985, Uniform-sense normal simple shear of the continental lithosphere: Canadian Journal of Earth Sciences v. 22, p. 108-125.

Wernicke, B., and Burchfiel, B.C., 1982, Modes of extensional tectonics: Journal of Structural Geology v. 4, p. 105-115.

Wernicke, B., Spencer, J., Burchfiel, B.C., and Guth, P.L., 1982, Magnitude of Crustal extension in the southern Great Basin: Geology v. 10, p. 499.

Wernicke, B., Walker, J.D., and Beaufait, M.S., 1985, Structural discordance between Neogene detachments and frontal Sevier thrusts, central Mormon Mountains, southern Nevada: Tectonics v. 4, p. 213-246.

White, W.H., Harakal, J.E., and Carter, N.C., 1968, K-Ar Dates of some ore deposits in B.C.: Canadian Mining and Metallurgy Bulletin v. 61, p. 1326-1334.

White, S.H., Burrows, S.E., Carreras, J., Shaw, N.D. and Humphreys, F.J., 1980, On mylonites in ductile shear zones: Journal of Structural Geology v. 2, p. 175-187.

Williams, I.S., Compston, W., Black, L.P., Ireland, T.R., and Foster, J.J., 1984, Unsupported radiogenic Pb in zircon: a cause of anomalously high Pb-Pb, U-Pb and Th-Pb ages: Contribution to Mineralogy and Petrology v. 88, p. 322-327.

Zeitler, P., 1985, Cooling history of the northwest Himalaya, Pakistan: Tectonics v. 4, p. 127-151.

APPENDIX A - WHOLE ROCK SAMPLE LOCALITIES AND DESCRIPTIONS

Sample #	Description	Latitude and Longitude
Diorite samples (Jd):		
207	biotite-hornblende diorite	49°13.3'N, 119°34.2'W
178	biotite-hornblende diorite	49° 119° 'W
261.1	hornblende-biotite diorite	49°14.2'N, 119°35.0'W
261.2	hornblende diorite	49°14.2'N, 119°35.0'W
140	biotite-hornblende diorite	49°13.55'N, 119°35.4'W
Porphyritic biotite granite samples (Jpgr):		
275.1	porphyritic biotite granite	49°12.2'N, 119°31.2'W
275.2	porphyritic biotite granite	49°12.2'N, 119°31.2'W
245.2	hornblende-biotie granodiorite	49°11.5'N, 119°35.0'W
227	porphyritic biotite granite	49°12.4'N, 119°35.4'W
205	porphyritic biotite granite	49°13.1'N, 119°34.7'W
203	porphyritic biotite granite	49°13.1'N, 119°34.8'W
71	porphyritic biotite granite (altered)	49°13.2N, 119°35.0'W
Garnet-Muscovite granite samples (Jgr):		
234	garnet-muscovite granite	49°11.75'N, 119°33.8'W
209.1	garnet-muscovite granite	49°13.1'N, 119°34.3'W
209.2	garnet-muscovite granite	49°13.1'N, 119°34.3'W
263	garnet-muscovite granite	49°12.5'N, 119°34.4'W
182	garnet-muscovite granite	49°13.3'N, 119°37.4'W
9	garnet-muscovite granite	49°13.2'N, 119°37.35'W

Whole rock data was derived from XRF analyses of pressed powder pellets using an automated Phillips X-ray spectrometer in the Oceanography Department of U.B.C.

Results are oxidized, anhydrous, and normalized to 100 percent totals. Trace element analyses of the same pellets were done using the same equipment. Major and tracre element concentrations are based on comparison with U.S.G.S. and other widely analysed igneous rock standards. Mass absorption coefficients are calculated from major element compositions.

APPENDIX B - U-PB ANALYTICAL PROCEDURE AND DATA

Mineral Separation

Zircon concentrates were separated from 20–40 kg samples using standard Wilfley table, heavy liquid, and magnetic techniques. The procedure is summarized below.

1. samples were broken into fist-sized pieces at the collecting site, and stored in separate pails for shipment. Only the freshest available material with the cleanest surfaces was collected.
2. the surfaces of the sample were wire-brushed and all loose matter was removed using a high-pressure air nozzle.
3. samples were reduced to very fine sand size or smaller using a jaw crusher and a disk mill. The crushing equipment was completely dismantled and cleaned, and all crushing surfaces wire-brushed and blown clean between samples.
4. the heavy mineral concentrate was separated from the sample using a Wilfley table. The concentrates were washed with acetone and then dried.
5. metal filings and magnetite were removed using a strong hand magnet.
6. the light minerals were removed using tetrabromoethane (S.G.=2.89).
7. the samples were washed in warm 6N HCl for 15 minutes to remove iron oxide coatings on the grains.
8. samples were passed through methylene iodide (S.G.=3.32) to remove apatite and other impurities.
9. the final heavy mineral concentrates were washed for 15 minutes in warm 8N HNO_3 and then for 15 minutes in warm 6N HCl to remove sulfides and any remaining iron oxide coatings.
10. samples were cleaned using a Franz magnetic separator (25° forward tilt, 2° side tilt, 1.7 amps magnet current).

This procedure usually produced a 99% pure zircon separate.

Preparation of Fractions and Sample Dissolution

Desired magnetic fractions were separated using the Franz. Each of these samples was then separated into a coarse (100–200 mesh) and fine (200–325 mesh) fraction. Several samples yielded very coarse (70–100 mesh) fractions.

Individual fractions were then weighed and hand-picked to greater than 90% purity under a binocular microscope. These hand-picked fractions were carefully weighed, then put into pre-cleaned Teflon dissolution capsules, given a final acid wash (15 minutes in 7N HNO_3, 15 minutes 6N HCl, 15 minutes 2B H_2O on a hot plate at 120°C). After pipetting off the rinse water, 0.75 to 1.0 ml of concentrated 2B HF was added to the samples along with 3–4 drops of concentrated 2B HNO_3. The capsules were then sealed in steel jackets, and placed in a 200°–210°C oven for one week. In all cases dissolution was complete in 7 days.

After one week, the samples were removed from the oven, and capsules opened. The contents (HF plus fluorides) were evaporated to dryness overnight on a 120° hotplate. The capsules were then placed back in the ovens at 200°–210°C overnight, after adding 0.5 ml of 3.1 N HCl. They were then removed and the sample was aliquoted, one half of the 3.1N HCl solution to be analysed for the isotopic composition (IC), the other half to be mixed with a $^{208}Pb/^{235}U$ spike for determination of U and Pb concentrations using isotope dilution (ID). The IC and ID splits were carefully weighed and the ID placed on the hotplate overnight to equilibrate the spike and sample. Then both IC and ID were ready for column chemistry.

Ion Exchange Column Chemistry

All chemical processing of samples was carried out in a laminar flow hood. Separation of the U and Pb from the dissolved samples was carried out using 0.5 and 0.15 ml Teflon columns. These were stored in 8N HNO_3 between use. They were removed from storage, rinsed in 2B H_2O, then loaded with pre–cleaned anion exchange resin, (Dowex AG1–X8, 100–200 mesh chloride form, in 2B H_2O). The resin was then washed as follows.

1. 2 column volumes (c.v.) 1X H_2O
2. 2 c.v. 6N HCl
3. 2 c.v. 2B H_2O
4. 2 c.v. 6N HCl
5. 2 c.v. 2B H_2O

The resin was then equilibrated with 3–4 c.v. of 3.1N HCl. The samples (dissolved in 3.1N HCl) were then carefully pipetted onto the columns and allowed to drip through. The sample was then washed and Pb and U collected as follows.

1. add 1 drop 3.1N HCl and allow to drip through
2. repeat step (1) five times
3. add 100 lambda 3.1N HCl
4. add 150 lambda 3.1N HCl
5. take off Pb with 6 c.v. of 6N HCl
6. take off U with 6 c.v. of 2B H_2O

After the Pb and U have been taken off the columns, the resin is removed and the columns are rinsed in 1X H_2O and stored in 8N HNO_3. The resin is discarded.

Cleaning of Dissolution Capsules and Beakers

Teflon dissolution capsules and beakers were cleaned after use as follows:

1. wash in warm soapy water; rinse in 1X H_2O.
2. 2 days in warm aqua regia; "
3. 2 days in warm 8N HNO_3; "
4. 2 days in warm 6N HCl; "
5. 2 days in cold 1N HBr; "
6. 2 days in warm 1X H_2O; "
7. remove, drain, and store in 1X H_2O in a clean plastic container.

Reagants and Blanks

1X H_2O was obtained from a pyrex-vycor still in K. Fletcher's lab, or from a quartz still in K. Scott's lab. Using 1X H_2O, 2B H_2O was prepared by a sub-boiling teflon bottle still described by Mattinson (1970). All other reagents were purified starting with reagent grade stock. 1X HCl and HNO_3 were obtained by distillation in pyrex; 2B HCl, HNO_3, and HF were then prepared by sub-boiling still.

Total procedural blanks, run with every batch of zircons processed, range from 0.1 ng to 1.0 ng Pb, and generally were 0.5 ng or less.

Mass Spectrometry

U and Pb isotopic ratios were measured on a V.G. Isomass 54 R which has data aquisition digitized and automated using a H.P. 85 computer. Pb was loaded using the phosphoric acid-silica gel method on a single rhenium filament, U was run as an oxide using tantalum oxide-nitric acid-phosphoric acid method on a single rhenium filament. U was also loaded using the phosphoric acid-silica gel method and found to be more stable and gave longer runs. Precision on all measured ratios were normally better than 0.1%, and commonly better than 0.05%. Pb and U ratios were corrected for instrumental mass fractionation on the basis of replicate analyses of National Bureau of Standards SRM-981, and 983 for Pb and U-500 for U.

Data reduction and error calculation

U-Pb date errors (2σ) are obtained by individually propagating all calibration and analytical uncertainties through the entire date calculation program and summing all the individual contributions to the total variance. Data reduction and automation are done on a dedicated Hewlett-Packard HP-85 computer.

U decay constants and isotope ratios are:

$^{238}U\lambda = 0.155125 \times 10^{-9}\ a^{-1}$

$^{235}U\lambda = 0.98485 \times 10^{-9}\ a^{-1}$

$^{238}U/^{235}U = 137.88$

All published dates cited in the text have been recalculated, if necessary, to conform to these constants.

(NTS 82 E/5)

U-Pb

☐ Mineral analysis
☐ Concordia interpretation
☐ Mineral or rock isochron

Sample Number(s) and Reference(s)
Lab No: DP156

Ref: Christie, 1973 PhD.
Ross + christie, 1978 CJES

Record No:
Suite No:
Sample Name:

gneissic sill of Vaseaux Lake

decay constant

☐ old: 0.1537/0.9722/0.0499/137.8
☑ new: 0.155125/0.98485/0.049475/137.88
☐ other:
☐ not reported

Upper Intercept 2σ error
Computed ☐
Assumed ☐ ± Ma

Lower Intercept 2σ error
Computed ☐
Assumed ☐ ± Ma

$^{238}U-^{206}Pb$ date ± Ma

$^{235}U-^{207}Pb$ date ± Ma

$^{207}Pb/^{206}Pb$ date ± Ma

$^{232}Th-^{208}Pb$ date ± Ma

Number of Points: n= 4

Latitude: Longitude: (X° Y' Z" or X° Y.Y')
(49 ° 18 ' 00 " N, 119 ° 31 ' 30 " W (±); Elevation: 1250 ft.

UMT Zone ____ ______E______N; Province: B.C.

Sec.____, T.____, R.____; ______ Co., State ______

(NTS ______) Penticton Map Area (1:250,000)

Location: ½ Km NE of Vaseaux Lake at base of cliffs above gravel rd.
Source Type:
Rock Types: leucocratic plag-qtz-k-spar mylonitic gneissic sill
Geologic Unit: gneissic sill of Vaseaux Lake
Geologic Setting: intrudes Vaseaux Fm Paragneisses
Material Analysed: Zircon

Comment on Analyses:

Interpretation:

Collected by: D. Parkinson
Dated by: D. Parkinson

Date of listing:

Sample Name or Number: gneissic sill of Vaseaux Lake

Sheet [ ]

Split-Mineral	ppm U	ppm Pb	206	207	208	204	Meas. 206/204	Mole % Blank Pb	Rad. Pb / Rad+ComPb	Common Pb Age
Fine Mag 37.4mg	1474	20.5	100	4.8808	3.0853	0.0002	38,426	0.2%	1.000	98

	206Pb/238U ratio ±		207Pb/235U ratio ±		207Pb/206Pb ratio ±		206Pb/238U date ±		207Pb/235U date ±		207Pb/206Pb date ±		R
200-325m	0.01496	±0.00008	0.1006	±0.0005	0.04878	±0.00008	95.7	±1.0	97.3	±1.0	137.3	+8.2 -8.2	0.93

Split-Mineral	ppm U	ppm Pb	206	207	208	204	Meas. 206/204	Mole % Blank Pb	Rad. Pb / Rad+ComPb	Common Pb Age
Fine NonMag 0.3mg	3594	49.4	100	4.8454	1.7174	0.0085	2005	2.5%	0.994	95

	206Pb/238U ratio ±		207Pb/235U ratio ±		207Pb/206Pb ratio ±		206Pb/238U date ±		207Pb/235U date ±		207Pb/206Pb date ±		R
200-325m	0.01497	±0.00010	0.0974	±0.0010	0.04721	±0.00037	95.8	±1.2	94.4	±1.8	59.7	+37.6 -38.0	0.89

Split-Mineral	ppm U	ppm Pb	206	207	208	204	Meas. 206/204	Mole % Blank Pb	Rad. Pb / Rad+ComPb	Common Pb Age
Coarse NonMag 38.5mg	1272	17.4	100	4.8855	1.7445	0.0006	20,105	0.3%	1.00	98

	206Pb/238U ratio ±		207Pb/235U ratio ±		207Pb/206Pb ratio ±		206Pb/238U date ±		207Pb/235U date ±		207Pb/206Pb date ±		R
100-200m	0.01495	±0.00008	0.1005	±0.0005	0.04877	±0.00006	95.6	±1.0	97.3	±1.0	136.9	+5.8 -5.8	0.97

Split-Mineral	ppm U	ppm Pb	206	207	208	204	Meas. 206/204	Mole % Blank Pb	Rad. Pb / Rad+ComPb	Common Pb Age
Very Coarse 3.9mg	1620	22.6	100	4.9296	1.8944	0.0028	17,459	0.3%	0.998	140

	206Pb/238U ratio ±		207Pb/235U ratio ±		207Pb/206Pb ratio ±		206Pb/238U date ±		207Pb/235U date ±		207Pb/206Pb date ±		R
70-100m	0.01520	±0.00009	0.1024	±0.0006	0.04888	±0.00013	97.2	±1.0	99.0	±1.2	142.3	+12.6 -12.8	0.93

Split-Mineral	ppm U	ppm Pb	206	207	208	204	Meas. 206/204	Mole % Blank Pb	Rad. Pb / Rad+ComPb	Common Pb Age

206Pb/238U ratio ±	207Pb/235U ratio ±	207Pb/206Pb ratio ±	206Pb/238U date ±	207Pb/235U date ±	207Pb/206Pb date ±	R
±	±	±	±	±	±	

Statement of Uncertainties: errors are 2σ for dates; 1σ for isotopic ratios.

Isotopic composition of blank: [ ] S-K Modern Pb (6/4:18.7, 7/4:15.63, 8/4:38.63) or [✓] Other (6/4:17.75 7/4:15.57 8/4:37.00)
Isotopic composition of common Pb based on S-K growth curve: 6/4=11.152, 7/4=12.998, 8/4=31.23 at 3.7Ga with 238U/204Pb=9.74, 232Th/204Pb=37.19; decay constants 0.155125, 0.98485, 137.88; or [ ] Other (6/4: 7/4: 8/4:)

(NTS 82 E/5)

U-Pb

- ☐ Mineral analysis
- ☐ Concordia interpretation
- ☐ Mineral or rock isochron

Sample Number(s) and Reference(s)

Lab No: DP 179

Ref: Little, Map 15-1961

Record No:

Suite No:

Sample Name:

gneiss of Skaha Lake

decay constant

- ☐ old: 0.1537/0.9722/0.0499/137.8
- ☑ new: 0.155125/0.98485/0.049475/137.88
- ☐ other:
- ☐ not reported

Upper Intercept — 2σ error
Computed ☐
Assumed ☐ ± Ma

Lower Intercept — 2σ error
Computed ☐
Assumed ☐ ± Ma

$^{238}U-^{206}Pb$ date ± Ma

$^{235}U-^{207}Pb$ date ± Ma

$^{207}Pb/^{206}Pb$ date ± Ma

$^{232}Th-^{208}Pb$ date ± Ma

Number of Points: n= 2

Latitude: Longitude: (X^o Y' Z" or X^o Y.Y')

(49 °24 '35 " N, 119 °34 '05 " W (±); Elevation: 1110'

UMT Zone ____ ____ E ____ N; Province: B.C.

Sec.____, T.____, R.____; ____ Co., State ____

(NTS ____) Penticton Map Area (1:250,000)

Location: 5.1 Km South of Penticton - on Road - East shore Skaha Lake

Source Type: roadcut

Rock Types: gneissic Hb granodiorite

Geologic Unit: gneiss of Skaha Lake

Geologic Setting: intrudes Vaseaux Fm equivalents (Little, 1961)

Material Analysed: Zircon

Comment on Analyses:

Interpretation:

Collected by: D. Parkinson

Dated by: D. Parkinson

Date of listing:

Sample Name or Number: *gneiss of Skaha Lake*

Sheet ☐

Split-Mineral	ppm U	ppm Pb	206	207	208	204	Meas. $\frac{206}{204}$	Mole % Blank Pb	Rad. Pb / Rad+ComPb	Common Pb Age
Fine Mag 34.2mg	308	4.7	100	4.9393	10.0325	0.0064	5,885	0.6%	0.996	98

	$\frac{206\,Pb}{238\,U}$ ratio ±		$\frac{207\,Pb}{235\,U}$ ratio ±		$\frac{207\,Pb}{206\,Pb}$ ratio ±		$\frac{206\,Pb}{238\,U}$ date ±		$\frac{207\,Pb}{235\,U}$ date ±		$\frac{207\,Pb}{206\,Pb}$ date ±		R
200-325m	0.01544	±0.00009	0.1031	±0.0006	0.04846	±0.00014	98.7	±1.0	99.7	±1.2	121.6	+13.2 −13.2	0.93

Split-Mineral	ppm U	ppm Pb	206	207	208	204	Meas. $\frac{206}{204}$	Mole % Blank Pb	Rad. Pb / Rad+ComPb	Common Pb Age
Coarse NonMag 33.0mg	381	6.12	100	4.9574	9.4778	0.0064	4233	0.9%	0.996	105

	$\frac{206\,Pb}{238\,U}$ ratio ±		$\frac{207\,Pb}{235\,U}$ ratio ±		$\frac{207\,Pb}{206\,Pb}$ ratio ±		$\frac{206\,Pb}{238\,U}$ date ±		$\frac{207\,Pb}{235\,U}$ date ±		$\frac{207\,Pb}{206\,Pb}$ date ±		R
100-200m	0.1630	±0.00009	0.1093	±0.0007	0.04863	±0.00016	104.3	±1.2	105.4	±1.2	130.1	+15.8 −16	0.92

Split-Mineral	ppm U	ppm Pb	206	207	208	204	Meas. $\frac{206}{204}$	Mole % Blank Pb	Rad. Pb / Rad+ComPb	Common Pb Age

$\frac{206\,Pb}{238\,U}$ ratio ±	$\frac{207\,Pb}{235\,U}$ ratio ±	$\frac{207\,Pb}{206\,Pb}$ ratio ±	$\frac{206\,Pb}{238\,U}$ date ±	$\frac{207\,Pb}{235\,U}$ date ±	$\frac{207\,Pb}{206\,Pb}$ date ±	R
±	±	±	±	±	±	

Split-Mineral	ppm U	ppm Pb	206	207	208	204	Meas. $\frac{206}{204}$	Mole % Blank Pb	Rad. Pb / Rad+ComPb	Common Pb Age

$\frac{206\,Pb}{238\,U}$ ratio ±	$\frac{207\,Pb}{235\,U}$ ratio ±	$\frac{207\,Pb}{206\,Pb}$ ratio ±	$\frac{206\,Pb}{238\,U}$ date ±	$\frac{207\,Pb}{235\,U}$ date ±	$\frac{207\,Pb}{206\,Pb}$ date ±	R
±	±	±	±	±	±	

Split-Mineral	ppm U	ppm Pb	206	207	208	204	Meas. $\frac{206}{204}$	Mole % Blank Pb	Rad. Pb / Rad+ComPb	Common Pb Age

$\frac{206\,Pb}{238\,U}$ ratio ±	$\frac{207\,Pb}{235\,U}$ ratio ±	$\frac{207\,Pb}{206\,Pb}$ ratio ±	$\frac{206\,Pb}{238\,U}$ date ±	$\frac{207\,Pb}{235\,U}$ date ±	$\frac{207\,Pb}{206\,Pb}$ date ±	R
±	±	±	±	±	±	

Statement of Uncertainties: *errors are 2σ for dates; 1σ for isotopic ratios*

Isotopic composition of blank: ☐ S-K Modern Pb (6/4:18.7, 7/4:15.63, 8/4:38.63) or ☑ Other (6/4:17.75 7/4:15.57 8/4:37.06)
Isotopic composition of common Pb based on S-K growth curve: 6/4=11.152, 7/4=12.998, 8/4=31.23 at 3.7Ga with 238U/204Pb=9.74, 232Th/204Pb=37.19; decay constants 0.155125, 0.98485, 137.88; or ☐ Other (6/4: 7/4: 8/4:)

(NTS 82 E)

U-Pb

☐ Mineral analysis
☐ Concordia interpretation
☐ Mineral or rock isochron

Sample Number(s) and Reference(s)
Lab No: DP300
Ref:
Record No:
Suite No:
Sample Name:
Rhomb Porphyry

decay constant

☐ old: 0.1537/0.9722/0.0499/137.8
☐ new: 0.155125/0.98485/0.049475/137.88
☐ other:
☐ not reported

Upper Intercept 2σ error
Computed ☐
Assumed ☐ ± Ma

Lower Intercept 2σ error
Computed ☐
Assumed ☐ ± Ma

$^{238}U-^{206}Pb$ date ± Ma

$^{235}U-^{207}Pb$ date ± Ma

$^{207}Pb/^{206}Pb$ date ± Ma

$^{232}Th-^{208}Pb$ date ± Ma

Number of Points: n= 2

Latitude: Longitude: (X° Y' Z" or X° Y.Y')
(49 ° 15.25' " N, 119 ° 33 ' 0 " W (±); Elevation: 1400 ft

UMT Zone E N; Province: B.C.

Sec. , T. ,R. ; Co., State

(NTS) Penticton Map Area (1:250,000)

Location: N end of Covert Farms, 50m up from end of fields
Source Type: outcrop
Rock Types: Anorthoclase-pyroxene porphyry; foliated lineated + metamorphosed
Geologic Unit: Rhomb Porphyry dike
Geologic Setting: Intrudes Vaseaux Fm. paragneisses and leucogneiss sill
Material Analysed: Zircon

Comment on Analyses:

Interpretation:

Collected by: D. Parkinson
Dated by: D. Parkinson
Date of listing:

Sample Name or Number: *Rhomb Porphyry*

Sheet ☐

Split-Mineral	ppm U	ppm Pb	206	207	208	204	Meas. 206/204	Mole % Blank Pb	Rad. Pb / Rad+ComPb	Common Pb Age
Fine 1.6 mg	1100	9.5	100	5.8566	18.0336	0.0658	799	4.3%	0.961	50

200-325m

206 Pb/238 U ratio ±		207 Pb/235 U ratio ±		207 Pb/206 Pb ratio ±		206 Pb/238 U date ±		207 Pb/235 U date ±		207 Pb/206 Pb date ±		R
0.00802	±0.00005	0.0540	±0.0004	0.04888	±0.00026	51.5	± 0.6	53.4	± 0.8	142.2	+24.8 −25	0.9%

Split-Mineral	ppm U	ppm Pb	206	207	208	204	Meas. 206/204	Mole % Blank Pb	Rad. Pb / Rad+ComPb	Common Pb Age
Coarse 1.4 mg	1923	16.1	100	5.6498	15.7190	0.0661	617	6.6%	0.960	50

100-200m

206 Pb/238 U ratio ±		207 Pb/235 U ratio ±		207 Pb/206 Pb ratio ±		206 Pb/238 U date ±		207 Pb/235 U date ±		207 Pb/206 Pb date ±		R
0.00793	±0.00005	0.0511	±0.0009	0.04675	±0.0008	50.9	± 0.6	50.6	± 1.8	36.7	+40 −40	0.8

Split-Mineral	ppm U	ppm Pb	206	207	208	204	Meas. 206/204	Mole % Blank Pb	Rad. Pb / Rad+ComPb	Common Pb Age

206 Pb/238 U ratio ±	207 Pb/235 U ratio ±	207 Pb/206 Pb ratio ±	206 Pb/238 U date ±	207 Pb/235 U date ±	207 Pb/206 Pb date ±	R
±	±	±	±	±	±	

Split-Mineral	ppm U	ppm Pb	206	207	208	204	Meas. 206/204	Mole % Blank Pb	Rad. Pb / Rad+ComPb	Common Pb Age

206 Pb/238 U ratio ±	207 Pb/235 U ratio ±	207 Pb/206 Pb ratio ±	206 Pb/238 U date ±	207 Pb/235 U date ±	207 Pb/206 Pb date ±	R
±	±	±	±	±	±	

Split-Mineral	ppm U	ppm Pb	206	207	208	204	Meas. 206/204	Mole % Blank Pb	Rad. Pb / Rad+ComPb	Common Pb Age

206 Pb/238 U ratio ±	207 Pb/235 U ratio ±	207 Pb/206 Pb ratio ±	206 Pb/238 U date ±	207 Pb/235 U date ±	207 Pb/206 Pb date ±	R
±	±	±	±	±	±	

Statement of Uncertainties: *errors are 2σ for dates; 1σ for isotopic ratios*

Isotopic composition of blank: ☐ S-K Modern Pb (6/4:18.7, 7/4:15.63, 8/4:38.63) or ☑ Other (6/4:17.75 7/4:15.57 8/4:37.00)
Isotopic composition of common Pb based on S-K growth curve: 6/4=11.152, 7/4=12.998, 8/4=31.23 at 3.7Ga with 238U/204Pb=9.74, 232Th/204Pb=37.19; decay constants 0.155125, 0.98485, 137.88; or ☐ Other (6/4: 7/4: 8/4:)

(NTS 82E)

U-Pb

- [x] Mineral analysis
- [ ] Concordia interpretation
- [ ] Mineral or rock isochron

Sample Number(s) and Reference(s)
Lab No: Olalla

Ref: Sturdevant, 1963

Record No:
Suite No:
Sample Name:

Olalla

decay constant

- [ ] old: 0.1537/0.9722/0.0499/137.8
- [x] new: 0.155125/0.98485/0.049475/137.88
- [ ] other:
- [ ] not reported

Upper Intercept 2σ error
Computed ☐
Assumed ☐ ± Ma

Lower Intercept 2σ error
Computed ☐
Assumed ☐ ± Ma

$^{238}U-^{206}Pb$ date ± Ma

$^{235}U-^{207}Pb$ date ± Ma

$^{207}Pb/^{206}Pb$ date ± Ma

$^{232}Th-^{208}Pb$ date ± Ma

Number of Points: n= 1

Latitude: Longitude: (X° Y' Z" or X° Y.Y')
(49 ° 16 ' 0 " N, 119 ° 49.5 " W (±); Elevation: 1800 ft

UMT Zone ____ ____E____N; Province: B.C.

Sec.____, T.____, R.____; ____ Co., State ____

(NTS ____) Penticton Map Area (1:250,000)

Location: town of Olalla, from roadcut just south of town
Source Type: outcrop
Rock Types: Mafic syenite complex
Geologic Unit: Olalla Syenite
Geologic Setting: intrudes Apex Mountain Group
Material Analysed: Zircon

Comment on Analyses:

Interpretation:

Collected by: R.L. Armstrong
Dated by: D. Parkinson

Date of listing:

Sample Name or Number: *Olalla* Sheet ☐

Split-Mineral	ppm U	ppm Pb	206	207	208	204	Meas. 206/204	Mole % Blank Pb	Rad. Pb / Rad+ComPb	Common Pb Age
Fine 6.7mg 200-325m	1341	51.2	100	5.1738	46.3786	0.0060	9279	0.4%	0.997	200

206 Pb/238 U ratio ±	207 Pb/235 U ratio ±	207 Pb/206 Pb ratio ±	206 Pb/238 U date ±	207 Pb/235 U date ±	207 Pb/206 Pb date ±	R
0.02921 ±0.00016	0.2049 ±0.0011	0.05086 ±0.00007	185.6 ±2.0	189.2 ±1.8	234.6 +6.2 −6.2	0%

Split-Mineral	ppm U	ppm Pb	206	207	208	204	Meas. 206/204	Mole % Blank Pb	Rad. Pb / Rad+ComPb	Common Pb Age

206 Pb/238 U ratio ±	207 Pb/235 U ratio ±	207 Pb/206 Pb ratio ±	206 Pb/238 U date ±	207 Pb/235 U date ±	207 Pb/206 Pb date ±	R
±	±	±	±	±	±	

Split-Mineral	ppm U	ppm Pb	206	207	208	204	Meas. 206/204	Mole % Blank Pb	Rad. Pb / Rad+ComPb	Common Pb Age

206 Pb/238 U ratio ±	207 Pb/235 U ratio ±	207 Pb/206 Pb ratio ±	206 Pb/238 U date ±	207 Pb/235 U date ±	207 Pb/206 Pb date ±	R
±	±	±	±	±	±	

Split-Mineral	ppm U	ppm Pb	206	207	208	204	Meas. 206/204	Mole % Blank Pb	Rad. Pb / Rad+ComPb	Common Pb Age

206 Pb/238 U ratio ±	207 Pb/235 U ratio ±	207 Pb/206 Pb ratio ±	206 Pb/238 U date ±	207 Pb/235 U date ±	207 Pb/206 Pb date ±	R
±	±	±	±	±	±	

Split-Mineral	ppm U	ppm Pb	206	207	208	204	Meas. 206/204	Mole % Blank Pb	Rad. Pb / Rad+ComPb	Common Pb Age

206 Pb/238 U ratio ±	207 Pb/235 U ratio ±	207 Pb/206 Pb ratio ±	206 Pb/238 U date ±	207 Pb/235 U date ±	207 Pb/206 Pb date ±	R
±	±	±	±	±	±	

Statement of Uncertainties: *Errors are 2σ for dates; 1σ for isotopic ratios*

Isotopic composition of blank: ☐ S-K Modern Pb (6/4:18.7, 7/4:15.63, 8/4:38.63) or ☑ Other (6/4:17.75 7/4:15.57 8/4:37.00)
Isotopic composition of common Pb based on S-K growth curve: 6/4=11.152, 7/4=12.998, 8/4=31.23 at 3.7Ga with 238U/204Pb=9.74, 232Th/204Pb=37.19; decay constants 0.155125, 0.98485, 137.88; or ☐ Other (6/4: 7/4: 8/4:)

(NTS 82 E/4)

U-Pb

☐ Mineral analysis
☐ Concordia interpretation
☐ Mineral or rock isochron

Sample Number(s) and Reference(s)
Lab No: DP 246

Ref: Fox et al. 1977

Record No:
Suite No:
Sample Name:

Similkameen batholith

decay constant

☐ old: 0.1537/0.9722/0.0499/137.8
☑ new: 0.155125/0.98485/0.049475/137.88
☐ other:
☐ not reported

Upper Intercept — 2σ error
Computed ☐
Assumed ☐ ± Ma

Lower Intercept — 2σ error
Computed ☐
Assumed ☐ ± Ma

$^{238}U-^{206}Pb$ date ± Ma

$^{235}U-^{207}Pb$ date ± Ma

$^{207}Pb/^{206}Pb$ date ± Ma

$^{232}Th-^{208}Pb$ date ± Ma

Number of Points: n= 2

Latitude: Longitude: (X° Y' Z" or X° Y.Y')
(49° 02' 00" N, 119° 41' 45" W (±); Elevation:

UMT Zone ____ ____E ____N; Province: B.C.

Sec.____, T.____, R.____; ____ Co., State ____

(NTS ____) Penticton Map Area (1:250,000)

Location: 4 Km north of US-Canada border on Hwy 3; 21 Km SE of Keremeo
Source Type: Boulders blasted from road cut.
Rock Types: Hb Granodiorite
Geologic Unit: Similkameen batholith
Geologic Setting: intrudes Kobau Formation
Material Analysed: Zircon

Comment on Analyses:

Interpretation:

Collected by: D. Parkinson
Dated by: D. Parkinson
Date of listing:

Sample Name or Number: *Similkameen batholith* Sheet ☐

Split-Mineral	ppm U	ppm Pb	206	207	208	204	Meas. 206/204	Mole % Blank Pb	Rad. Pb/Rad+ComPb	Common Pb Age
Fine Mag. 36.4 mg	632.9	17.3	100	5.4754	13.7505	0.0338	2554.5	0.3%	0.979	170

	206 Pb/238 U ratio ±	207 Pb/235 U ratio ±	207 Pb/206 Pb ratio ±	206 Pb/238 U date ±	207 Pb/235 U date ±	207 Pb/206 Pb date ±	R
200-325m	0.02650 ±0.00015	0.1819 ±0.0011	0.04979 ±0.00014	168.6 ± 1.8	169.7 ± 1.8	185.3 +13.4 −13.6	0.93

Split-Mineral	ppm U	ppm Pb	206	207	208	204	Meas. 206/204	Mole % Blank Pb	Rad. Pb/Rad+ComPb	Common Pb Age
Crs Non Mag 35.2 mg	488	13.6	100	5.9722	13.4675	0.0700	1,000	1.1%	0.957	169

	206 Pb/238 U ratio ±	207 Pb/235 U ratio ±	207 Pb/206 Pb ratio ±	206 Pb/238 U date ±	207 Pb/235 U date ±	207 Pb/206 Pb date ±	R
100-200m	0.02671 ±0.00015	0.1821 ±0.0011	0.04944 ±0.00018	169.9 ± 1.8	169.8 ± 2.0	168.6 +17 −17	0.91

Split-Mineral	ppm U	ppm Pb	206	207	208	204	Meas. 206/204	Mole % Blank Pb	Rad. Pb/Rad+ComPb	Common Pb Age

206 Pb/238 U ratio ±	207 Pb/235 U ratio ±	207 Pb/206 Pb ratio ±	206 Pb/238 U date ±	207 Pb/235 U date ±	207 Pb/206 Pb date ±	R
±	±	±	±	±	±	

Split-Mineral	ppm U	ppm Pb	206	207	208	204	Meas. 206/204	Mole % Blank Pb	Rad. Pb/Rad+ComPb	Common Pb Age

206 Pb/238 U ratio ±	207 Pb/235 U ratio ±	207 Pb/206 Pb ratio ±	206 Pb/238 U date ±	207 Pb/235 U date ±	207 Pb/206 Pb date ±	R
±	±	±	±	±	±	

Split-Mineral	ppm U	ppm Pb	206	207	208	204	Meas. 206/204	Mole % Blank Pb	Rad. Pb/Rad+ComPb	Common Pb Age

206 Pb/238 U ratio ±	207 Pb/235 U ratio ±	207 Pb/206 Pb ratio ±	206 Pb/238 U date ±	207 Pb/235 U date ±	207 Pb/206 Pb date ±	R
±	±	±	±	±	±	

Statement of Uncertainties: *errors are 2σ for dates; 1σ for isotopic ratios*

Isotopic composition of blank: ☐ S-K Modern Pb (6/4:18.7, 7/4:15.63, 8/4:38.63) or ☑ Other (6/4:17.75 7/4:15.57 8/4:37.00)
Isotopic composition of common Pb based on S-K growth curve: 6/4=11.152, 7/4=12.998, 8/4=31.23 at 3.7Ga with 238U/204Pb=9.74, 232Th/204Pb=37.19; decay constants 0.155125, 0.98485, 137.88; or ☐ Other (6/4: 7/4: 8/4:)

(NTS 82E/5)

U-Pb

- [x] Mineral analysis
- [ ] Concordia interpretation
- [ ] Mineral or rock isochron

Sample Number(s) and Reference(s)

Lab No: DP90

Ref: Christie, 1973 PhD
Ross & Christie, 1978 CJES

Record No:

Suite No:

Sample Name:

leucogneiss

decay constant

- [ ] old: 0.1537/0.9722/0.0499/137.8
- [x] new: 0.155125/0.98485/0.049475/137.88
- [ ] other:
- [ ] not reported

Upper Intercept 2σ error
Computed ☐
Assumed ☐ ± Ma

Lower Intercept 2σ error
Computed ☐
Assumed ☐ ± Ma

$^{238}U-^{206}Pb$ date ± Ma

$^{235}U-^{207}Pb$ date ± Ma

$^{207}Pb/^{206}Pb$ date ± Ma

$^{232}Th-^{208}Pb$ date ± Ma

Number of Points: n= 5

Latitude: Longitude: (X° Y' Z" or X° Y.Y')
(49 ° 18 ' 30 " N, 119 ° 30 ' 10 " W (±); Elevation: 2250 ft

UMT Zone ____ ____ E ____ N; Province: B.C.

Sec.____, T.____, R.____; ____ Co., State ____

(NTS ____) Penticton Map Area (1:250,000)

Location: 2.3 Km NE of N end of Vaseaux Lake; 1.4 Km S (on rd.) of Shuttleworth Creek Logging Rd.

Source Type: outcrop

Rock Types: biotite granite

Geologic Unit: Unit A of Christie (1973); leucogneiss in Parkinson (1985)

Geologic Setting: intrudes Vaseaux Fm.

Material Analysed: Zircon

Comment on Analyses:

Interpretation:

Collected by: D. Parkinson & R.L. Armstrong

Dated by: D. Parkinson

Date of listing:

Sample Name or Number: *leucogneiss*

Sheet [ ]

Split-Mineral	ppm U	ppm Pb	206	207	208	204	Meas. 206/204	Mole % Blank Pb	Rad. Pb / Rad+ComPb	Common Pb Age
Fine Mag 31.6mg 200-325m	1111	18.5	100	5.3178	4.4765	0.0032	11,877	0.3%	0.998	160

206 Pb/238 U ratio ±		207 Pb/235 U ratio ±		207 Pb/206 Pb ratio ±		206 Pb/238 U date ±		207 Pb/235 U date ±		207 Pb/206 Pb date ±		R
0.01766	±0.00010	0.1284	±0.0007	0.05271	±0.00007	112.9	±1.2	122.6	±1.2	316.3	+6.4 −6.4	0.96

Split-Mineral	ppm U	ppm Pb	206	207	208	204	Meas. 206/204	Mole % Blank Pb	Rad. Pb / Rad+ComPb	Common Pb Age
Fine Mag (H.D) 14.9mg 200-325m	1132	18.8	100	5.4198	4.3973	0.0017	21,819	0.3%	0.999	300

206 Pb/238 U ratio ±		207 Pb/235 U ratio ±		207 Pb/206 Pb ratio ±		206 Pb/238 U date ±		207 Pb/235 U date ±		207 Pb/206 Pb date ±		R
0.01763	±0.00010	0.1311	±0.0007	0.05394	±0.00007	112.6	±1.2	125.1	±1.2	368.6	+6.0 −6.0	0.97

Split-Mineral	ppm U	ppm Pb	206	207	208	204	Meas. 206/204	Mole % Blank Pb	Rad. Pb / Rad+ComPb	Common Pb Age
Fine NonMag 16.4mg 200-325m	1080	18.33	100	5.3411	4.5535	0.0032	12,864	0.4%	0.998	240

206 Pb/238 U ratio ±		207 Pb/235 U ratio ±		207 Pb/206 Pb ratio ±		206 Pb/238 U date ±		207 Pb/235 U date ±		207 Pb/206 Pb date ±		R
0.01796	±0.00010	0.1311	±0.0007	0.05294	±0.00007	114.7	±1.2	125.1	±1.2	326.1	+5.8 −5.8	0.97

Split-Mineral	ppm U	ppm Pb	206	207	208	204	Meas. 206/204	Mole % Blank Pb	Rad. Pb / Rad+ComPb	Common Pb Age
Coarse NonMag 16.4mg 100-200m	954	17.4	100	5.5007	5.0930	0.0032	11,107	0.3%	0.995	200

206 Pb/238 U ratio ±		207 Pb/235 U ratio ±		207 Pb/206 Pb ratio ±		206 Pb/238 U date ±		207 Pb/235 U date ±		207 Pb/206 Pb date ±		R
0.01913	±0.00011	0.1439	±0.0008	0.05453	±0.00007	122.2	±1.4	136.5	±1.4	393.1	+5.6 −5.6	0.97

Split-Mineral	ppm U	ppm Pb	206	207	208	204	Meas. 206/204	Mole % Blank Pb	Rad. Pb / Rad+ComPb	Common Pb Age
Very Coarse 9.5mg 70-100m	845	15.5	100	5.1965	7.6540	0.0091	6774	0.5%	0.994	300

206 Pb/238 U ratio ±		207 Pb/235 U ratio ±		207 Pb/206 Pb ratio ±		206 Pb/238 U date ±		207 Pb/235 U date ±		207 Pb/206 Pb date ±		R
0.01890	±0.00011	0.1319	±0.0007	0.05063	±0.00008	120.7	±1.4	125.8	±1.2	223.8	+6.8 −7.0	0.96

Statement of Uncertainties: *Errors are 2σ for dates; 1σ for isotopic ratios*

Isotopic composition of blank: [ ] S-K Modern Pb (6/4:18.7, 7/4:15.63, 8/4:38.63) or [✓] Other (6/4:17.75 7/4:15.57 8/4:37.00)
Isotopic composition of common Pb based on S-K growth curve: 6/4=11.152, 7/4=12.998, 8/4=31.23 at 3.7Ga with 238U/204Pb=9.74, 232Th/204Pb=37.19; decay constants 0.155125, 0.98485, 137.88; or [ ] Other (6/4: 7/4: 8/4:)

(NTS 82 E/3)

U-Pb

- [x] Mineral analysis
- [ ] Concordia interpretation
- [ ] Mineral or rock isochron

Sample Number(s) and Reference(s)

Lab No: DP95

Ref: Ryan, 1973 PhD Thesis

Unit VIII

Record No:

Suite No:

Sample Name:

Anarchist Mtn. granite

decay constant

- [ ] old: 0.1537/0.9722/0.0499/137.8
- [x] new: 0.155125/0.98485/0.049475/137.88
- [ ] other:
- [ ] not reported

Upper Intercept 2σ error
Computed ☐
Assumed ☐ ± Ma

Lower Intercept 2σ error
Computed ☐
Assumed ☐ ± Ma

$^{238}U-^{206}Pb$ date ± Ma

$^{235}U-^{207}Pb$ date ± Ma

$^{207}Pb/^{206}Pb$ date ± Ma

$^{232}Th-^{208}Pb$ date ± Ma

Number of Points: n= 2

Latitude: Longitude: (X° Y' Z" or X° Y.Y')

(49 ° 03 ' 30 " N, 119 ° 21 ' " W (±); Elevation: 4200 ft.

UMT Zone ____ E ____ N; Province: B.C.

Sec.____, T.____, R.____; ____ Co., State ____

(NTS ____) Penticton Map Area (1:250,000)

Location: Anarchist Mtn area – ~8 Km ENE of Osoyoos; 28 Km NW of Anarchist Mtn.

Source Type: outcrop

Rock Types: garnet-biotite granite

Geologic Unit: Unit VIII of Ryan (1973); granite of Anarchist Mtn in Parkin (198

Geologic Setting: intrudes Anarchist Group.

Material Analysed: Zircon

Comment on Analyses:

Interpretation:

Collected by: D. Parkinson & R.L. Armstrong

Dated by: D. Parkinson

Date of listing:

Sample Name or Number: *Anarchist Mtn. granite*

Sheet ☐

Split-Mineral	ppm U	ppm Pb	206	207	208	204	Meas. 206/204	Mole % Blank Pb	Rad. Pb/Rad+ComPb	Common Pb Age
Fine Mag 31.9 mg	7852	185	100	4.9749	4.2912	0.0015	36,116	0.1%	0.999	160

200-325m

206 Pb/238 U ratio ±	207 Pb/235 U ratio ±	207 Pb/206 Pb ratio ±	206 Pb/238 U date ±	207 Pb/235 U date ±	207 Pb/206 Pb date ±	R
0.02509 ±0.00014	0.1713 ±0.0009	0.04953 ±0.00006	159.7 ± 1.8	160.6 ± 1.6	172.9 +5.6 −5.8	0.97

Split-Mineral	ppm U	ppm Pb	206	207	208	204	Meas. 206/204	Mole % Blank Pb	Rad. Pb/Rad+ComPb	Common Pb Age
Coarse NonMag 39.0 mg	3983	94.6	100	4.9660	4.2654	0.0003	34,856	0.1%	1.00	161

100-200m

206 Pb/238 U ratio ±	207 Pb/235 U ratio ±	207 Pb/206 Pb ratio ±	206 Pb/238 U date ±	207 Pb/235 U date ±	207 Pb/206 Pb date ±	R
0.02528 ±0.00014	0.1729 ±0.0009	0.04961 ±0.00005	160.9 ± 1.8	162.0 ± 1.6	176.9 +4.8 −4.8	0.97

Split-Mineral	ppm U	ppm Pb	206	207	208	204	Meas. 206/204	Mole % Blank Pb	Rad. Pb/Rad+ComPb	Common Pb Age

206 Pb/238 U ratio ±	207 Pb/235 U ratio ±	207 Pb/206 Pb ratio ±	206 Pb/238 U date ±	207 Pb/235 U date ±	207 Pb/206 Pb date ±	R
±	±	±	±	±	±	

Split-Mineral	ppm U	ppm Pb	206	207	208	204	Meas. 206/204	Mole % Blank Pb	Rad. Pb/Rad+ComPb	Common Pb Age

206 Pb/238 U ratio ±	207 Pb/235 U ratio ±	207 Pb/206 Pb ratio ±	206 Pb/238 U date ±	207 Pb/235 U date ±	207 Pb/206 Pb date ±	R
±	±	±	±	±	±	

Split-Mineral	ppm U	ppm Pb	206	207	208	204	Meas. 206/204	Mole % Blank Pb	Rad. Pb/Rad+ComPb	Common Pb Age

206 Pb/238 U ratio ±	207 Pb/235 U ratio ±	207 Pb/206 Pb ratio ±	206 Pb/238 U date ±	207 Pb/235 U date ±	207 Pb/206 Pb date ±	R
±	±	±	±	±	±	

Statement of Uncertainties: *Errors are 2σ for dates; 1σ for isotopic ratios*

Isotopic composition of blank: ☐ S-K Modern Pb (6/4:18.7, 7/4:15.63, 8/4:38.63) or ☑ Other (6/4:17.75 7/4:15.57 8/4:37.00)
Isotopic composition of common Pb based on S-K growth curve: 6/4=11.152, 7/4=12.998, 8/4=31.23 at 3.7Ga with 238U/204Pb=9.74, 232Th/204Pb=37.19; decay constants 0.155125, 0.98485, 137.88; or ☐ Other (6/4: 7/4: 8/4:)

(NTS 82 E/3)

U-Pb

- ☐ Mineral analysis
- ☐ Concordia interpretation
- ☐ Mineral or rock isochron

Sample Number(s) and Reference(s)

Lab No: Osoyoos

Ref: Ryan, 1973 PhD Thesis U.B.C.

Record No:

Suite No:

Sample Name:

Osoyoos gneiss

decay constant

- ☐ old: 0.1537/0.9722/0.0499/137.8
- ☑ new: 0.155125/0.98485/0.049475/137.88
- ☐ other:
- ☐ not reported

Upper Intercept 2σ error
Computed ☐
Assumed ☐ ± Ma

Lower Intercept 2σ error
Computed ☐
Assumed ☐ ± Ma

$^{238}U-^{206}Pb$ date ± Ma

$^{235}U-^{207}Pb$ date ± Ma

$^{207}Pb/^{206}Pb$ date ± Ma

$^{232}Th-^{208}Pb$ date ± Ma

Number of Points: n= 3

Latitude: Longitude: (X° Y' Z" or X° Y.Y')
(49 ° 02' 10 " N, 119 ° 25' 10 " W (±); Elevation:

UMT Zone E N; Province: B.C.

Sec. , T. ,R. ; Co., State

(NTS) Penticton Map Area (1:250,000)

Location: 3 km downhill from lookout on Hwy. 3, east of Osoyoos

Source Type: road cut

Rock Types: gneissic granodiorite

Geologic Unit: Unit V of Ryan (1973); gneiss of Osoyoos in Parkinson (1985)

Geologic Setting: intrudes Anarchist Group.

Material Analysed: Zircon

Comment on Analyses:

Interpretation:

Collected by: R. L. Armstrong

Dated by: D. Parkinson

Date of listing:

Sample Name or Number: *Osoyoos gneiss* Sheet [ ]

Split-Mineral	ppm U	ppm Pb	206	207	208	204	Meas. 206/204	Mole % Blank Pb	Rad. Pb / Rad+ComPb	Common Pb Age
Fine Mag. 37.6 mg (200-325m)	464	14.18	100	5.0794	7.6381	0.0016	19,421	0.2%	0.999	201

206 Pb/238 U ratio ±	207 Pb/235 U ratio ±	207 Pb/206 Pb ratio ±	206 Pb/238 U date ±	207 Pb/235 U date ±	207 Pb/206 Pb date ±	R
0.03155 ±0.00017	0.2199 ±0.0012	0.05056 ±0.00009	200.2 ±2.2	201.8 ±2.0	220.7 ±8.4	0.95

Split-Mineral	ppm U	ppm Pb	206	207	208	204	Meas. 206/204	Mole % Blank Pb	Rad. Pb / Rad+ComPb	Common Pb Age
Fine NonMag 0.6 mg (200-325m)	891	27.79	100	5.2043	8.6363	0.0105	5383.5	0.7%	0.993	235

206 Pb/238 U ratio ±	207 Pb/235 U ratio ±	207 Pb/206 Pb ratio ±	206 Pb/238 U date ±	207 Pb/235 U date ±	207 Pb/206 Pb date ±	R
0.03178 ±0.00018	0.2213 ±0.0016	0.05050 ±0.00025	201.7 ±2.2	203.0 ±2.8	218.2 ±22.6	0.91

Split-Mineral	ppm U	ppm Pb	206	207	208	204	Meas. 206/204	Mole % Blank Pb	Rad. Pb / Rad+ComPb	Common Pb Age
Crs NonMag 27.5 mg (100-200m)	476	14.5	100	5.0651	7.1205	0.0005	19,468	0.3%	1.00	201

206 Pb/238 U ratio ±	207 Pb/235 U ratio ±	207 Pb/206 Pb ratio ±	206 Pb/238 U date ±	207 Pb/235 U date ±	207 Pb/206 Pb date ±	R
0.03159 ±0.00017	0.2203 ±0.0012	0.05058 ±0.00006	200.5 ±2.2	202.2 ±2.0	221.9 ±6.0	0.97

Split-Mineral	ppm U	ppm Pb	206	207	208	204	Meas. 206/204	Mole % Blank Pb	Rad. Pb / Rad+ComPb	Common Pb Age

206 Pb/238 U ratio ±	207 Pb/235 U ratio ±	207 Pb/206 Pb ratio ±	206 Pb/238 U date ±	207 Pb/235 U date ±	207 Pb/206 Pb date ±	R
±	±	±	±	±	±	

Split-Mineral	ppm U	ppm Pb	206	207	208	204	Meas. 206/204	Mole % Blank Pb	Rad. Pb / Rad+ComPb	Common Pb Age

206 Pb/238 U ratio ±	207 Pb/235 U ratio ±	207 Pb/206 Pb ratio ±	206 Pb/238 U date ±	207 Pb/235 U date ±	207 Pb/206 Pb date ±	R
±	±	±	±	±	±	

Statement of Uncertainties: errors are 2σ for dates; 1σ for isotopic ratios.

Isotopic composition of blank: [ ] S-K Modern Pb (6/4:18.7, 7/4:15.63, 8/4:38.63) or [✓] Other (6/4:17.75 7/4:15.57 8/4:37.00)
Isotopic composition of common Pb based on S-K growth curve: 6/4=11.152, 7/4=12.998, 8/4=31.23 at 3.7Ga with 238U/204Pb=9.74, 232Th/204Pb=37.19; decay constants 0.155125, 0.98485, 137.88; or [ ] Other (6/4: 7/4: 8/4:)

APPENDIX C - RB/SR ANALYTICAL TECHNIQUES

Rb and Sr concentrations were determined by replicate analysis of pressed powder pellets using X-ray fluorescence. U.S. Geological Survey rock standards were used for calibration; mass absorption coefficients were obtained from Mo K-alpha Compton scattering measurements. Rb/Sr ratios have a precision of 2% (1 sigma) and concentrations a precision of 5% (1 sigma). Sr isotopic composition was measured on unspiked samples prepared using standard ion exchange techniques. The mass spectrometer, a V.G. Isomass 54 R, has data aquisition digitized and automated using a H.P. 85 computer. Experimental data have been normalized to a $^{86}Sr/^{88}Sr$ ratio of 0.1194 and adjusted so that the NBS standard $SrCO_3$ (SRM 987) gives a $^{87}Sr/^{86}Sr$ ratio of 0.71020 ± 2 and the Eimer and Amend Sr a ratio of 0.70800 ± 2. The precision of a single $^{87}Sr/^{86}Sr$ ratio is better than 0.00010 (1 sigma). Rb-Sr dates are based on a Rb decay constant of $1.42 \times 10^{-11} y^{-1}$. The regressions are calculated according to the technique of York (1967).